

UCLA

UCLA Electronic Theses and Dissertations

Title

High-throughput cell screening tools to enhance yields of cell bioproducts

Permalink

<https://escholarship.org/uc/item/5gd2207v>

Author

van Zee, Mark

Publication Date

2022

Peer reviewed|Thesis/dissertation

UNIVERSITY OF CALIFORNIA

Los Angeles

High-throughput cell screening tools
to enhance yields of cell bioproducts

A dissertation submitted in partial satisfaction of the
requirements for the degree Doctor of Philosophy
in Bioengineering

by

Mark van Zee

2022

© Copyright by

Mark van Zee

2022

ABSTRACT OF THE DISSERTATION

High-throughput cell screening tools
to enhance yields of cell bioproducts

by

Mark van Zee

Doctor of Philosophy in Bioengineering

University of California, Los Angeles, 2022

Professor Dino Di Carlo, Chair

With the current climate change situation, it is more necessary than ever to generate sustainable infrastructure. Unfortunately, we are unable to produce the materials necessary for such infrastructure at high enough yields. This is largely because of our lack of high-throughput cell screening tools that can select cells based on their behavior in production-relevant (rather than lab) environments. So, we have developed PicoShells, microparticles with a hollow inner cavity where cells are encapsulated and a porous outer shell that allows for direct interaction with the external environment. PicoShells can be placed directly into production environments and therefore may be produce high-yielding cell populations that maintain their phenotypes in production settings.

The dissertation of Mark van Zee is approved.

Aaron S. Meyer

Paul S. Weiss

Timothy J. Deming

Dino Di Carlo, Committee Chair

University of California Los Angeles

2022

DEDICATION

To all my experimental algae, yeast, hybridomas, CHO cells, and bacteria, thank you for giving up your lives in pursuit of this PhD

To the Los Angeles Dodgers, thank you for finally winning a World Series while I am alive

To Kerry and Mike, thank you for delivering my packages and I am sorry for the delays

To all my students, thank you for all the help and I am sorry for what I put you through

To Star Wars, I hope you start getting good again after I graduate

To Marvel, thank you for being better than Star Wars

To Vish and Rose, thank you for cleaning up after me

To Sophia, your Instagram is better than my sister's

To my sister, you are ugly

To Vivek, sorry

TABLE OF CONTENTS

Chapter 1. High-throughput cell screening tool to enhance bioproduct yields.....	1
1.1 Motivations and background.....	1
1.2 Initial gel microdrop.....	5
1.3 Attempts to expand gel microdrop.....	8
1.4 Motivations behind PicoShells.....	11
1.5 References.....	14
Chapter 2. High-throughput sorting of cells based on growth and division using PicoShells.....	17
2.1 Introduction.....	18
2.2 Results.....	23
2.2.1 Fabrication of PicoShells.....	23
2.2.2 Enhanced growth in PicoShells vs droplets.....	25
2.2.3 Sorting of <i>Chlorella</i> based on accumulated growth.....	29
2.2.4 Selection and re-growth of a hyper-performing <i>Chlorella</i> sub-population.....	32
2.3 Discussion.....	34
2.3.1 Advantages of PicoShells.....	34
2.3.2 Potential for chemically degradable PicoShells.....	36
2.3.3 Limitations on throughput.....	38
2.3.4 Potential future applications.....	40
2.4 Materials and Methods.....	42
2.4.1 Bulk culture of cells.....	42
2.4.2 PicoShell Fabrication.....	43
2.4.3 PicoShell versus droplet emulsion growth comparison.....	44
2.4.4 Staining of Intracellular Lipids.....	47

2.4.5 Incubation and flow cytometric sorting of PicoShells.....	48
2.4.6 Release of cells and re-culture of selected populations.....	48
2.4.7 Chemically-induced degradation of PicoShells.....	49
2.4.8 Environmental effects studies.....	50
2.5 References.....	52
Chapter 3. Retention of released cell materials and future directions.....	59
3.1 Optimizing PicoShell pore size to retain protein and genetic material.....	59
3.2 Protein engineering using PicoShells.....	61
3.2.1 Introduction.....	61
3.2.2. Results.....	66
3.2.3. Discussion and future directions.....	69
3.2.4. Methods.....	71
3.3 References.....	76
Appendix A.....	81
Appendix B.....	92
Appendix C.....	114

ACKNOWLEDGMENTS

Chapter 3 is adapted from: van Zee M., de Rutte J., Rumyan R., Williamson C., Burnes T., Radakovits R., Sonico Eugenio A., Badih S., Lee S., Lee D., Archang M., and Di Carlo D. High-throughput selection of cells based on accumulated growth and division using PicoShell particles. *Proceedings of the National Academy of Sciences*, 19(4), 2022. [Doi.org/10.1002/adfm.201900071](https://doi.org/10.1002/adfm.201900071). J.D., M.v.Z., and D.D conceived and designed initial PicoShell systems and protocols. J.D. designed the fabrication workflow for PicoShells and performed dextran diffusion experiments. J.D., M.v.Z., and M.A fabricated PicoShells. M.v.Z. and R.Ru. developed algae growth assay protocols, performed experiments, and analyzed data. M.v.Z. and C.W. developed yeast growth assay protocols, performed experiments, and analyzed data. T.B. and M.v.Z. performed algae growth comparison assays and analyzed data. A.S., D.L. S.B., and M.v.Z. performed yeast growth comparison assays and analyzed data. M.v.Z. and R.Ru. designed and performed flow sorting studies. M.v.Z. designed and performed the full *Chlorella* selection assay and analyzed data. S.L. took confocal images of the PicoShells. R.Ra. provided valuable microalgae insights and expertise. M.v.Z. and D.D. wrote the manuscript with inputs from all authors. M.v.Z prepared figures. D.D. supervised the study.

VITA

Education

B.S. in Biochemistry from University of California, Los Angeles

B.A. in Physics from University of California, Los Angeles

Publications

van Zee, M., de Rutte J., Rumyan R., Willaimson C., Burnes T., Radakovits R., Sonico Eugenio A., Badih S., Lee S., Lee D.H., Archang M., and Di Carlo D. High-throughput selection of cells based on accumulated growth and division using PicoShell Particles. *Proceedings of the National Academy of Sciences*. 119(5), (2022).

van Zee M., Li M., Riche C., Tofig B., Gallaher S., Merchant S., Damoiseaux R., Goda K., and Di Carlo D. Gelatin Microdroplet Platform for High-Throughput Sorting of Hyperproducing Single-Cell-Derived Microalgal Clones. *Small* 14(44), 1803315 (2018).

Li M., **van Zee M.**, Goda K., and Di Carlo D. Size-based sorting of hydrogel droplets using inertial microfluidics. *Lab on a Chip* 18(17), 2575-2582 (2018).

de Rutte J., Dimatteo R., Archang M. A., **van Zee M.**, Koo D., Lee S., Sharrow A. C., Krohl P. J., Mellody M. P., Zhu S., Eichenbaum J., Kizerwetter M., Udani S., Ha K., Bertozzi A. L., Spangler J. B., Damoiseaux R., and Di Carlo D. Massively parallel encapsulation of single cells with structured microparticles and secretion-based flow sorting. *bioRxiv* (2020).

Ng S., Williamson C., **van Zee M.**, Di Carlo D., and Santa Maria S.R. Enabling clonal analysis of yeast in outer space by encapsulation and desiccation in hollow microparticles. (*Submitted*).

Munoz H.E., Riche C.T., Kong J.E., **van Zee M.**, Garner O., Ozcan A., and Di Carlo D. Fractal LAMP: Label-free analysis of fractal precipitate for digital loop-mediated isothermal nucleic acid amplification. *ACS sensors* 5(2), 385-394 (2020).

Orfanos S., Jude J., Deeney B., Cao G., Rastogi D., **van Zee M.**, Pushkarsky I., Munoz H.E., Damoiseaux R., Di Carlo D., and Panettieri R.A. Obesity increases airway smooth muscle responses to contractile agonists. *American Physiological Society* 315(5), L673-L681 (2018).

Chapter 1. The need to develop a high-throughput cell screening tool to enhance bioproduct yields

1.1 Motivations and background

Production and design of sustainable bioproducts may play a major role in the development of a environmentally sustainable society. Despite the fact that there have been many well-defined and needed technologies that have needed to be developed for several decades (e.g. atmospheric carbon capture systems, naturally-degradable plastics, renewable energy sources, tools that replenish nitrogen in soil, technologies that separate NaCl from seawater, etc), there has been little to no progress in the development of such tools. The lack of progress and innovation in this area is largely to do with the types of fundamental materials that are attempting to be used to develop such systems. Currently, most of the infrastructure is built using materials derived from silicon, petroleum, metals, and other Earth-derived substances. While innovations enabling us to manipulate such materials has led to tremendous amounts of innovation over the last couple centuries with the development of transportation vehicles, electricity grids, microwaves, plastics, computers, etc, we have reached the limitations of what these materials are capable of doing. As a result, most of the innovation over the last couple decades have been mainly digital rather than physical.

Unfortunately, the lack of innovation in the physical space has led to serious negative impacts on the environment. For example, our reliance on the burning of petroleum-based fuels to power society without developing a mechanism to remove the released atmospheric carbon has led to a general warming of the Earth that is resulting in serious, irreparable damage to the environment¹. Our inability to develop plastic-substitutes that can be degraded is damaging the oceans and killing

a lot of the wildlife that lives in it². In order for society to develop tools that can solve such problems, engineers are required to make changes at the atomic or molecular scale of the underlying materials used to develop such technologies that is simply not possible using traditional methods (i.e. heating/cooling, applying pressure, chemical mixing, etc).

. Fortunately, biological systems have the machinery to make such molecular and atomic changes necessary to design these desired materials. All biological cells have enzymes, proteins, and biochemical pathways that enable them to make atomic- and molecular-level changes to the substances around them that enable them to perform highly complex functions and behaviors. In addition, sequencing and gene editing tools have enabled us to program these biological systems to make the changes that we desire. CHO cells can be programmed to produce humanized antibodies that are highly specific to a desired target and can be used as a therapeutic³. Microalgae can be programmed to produce high-energy lipids that can be used as fuel sources⁴. Bacteria can be programmed to produce protein biosensors that can fluoresce in response to ions (Ca^{2+} , Mg^+ , etc), toxins, or other chemicals^{5,6}. Cell-free enzymatic systems can be designed to convert atmospheric carbon into glucose⁷. The cells themselves can even serve and behave as highly dynamic materials rather than just as a producer of them. For example, T-cells can be modified to be drug therapies that can be a substitute for traditional synthetic and recombinant protein drugs⁸. Bacteria can be designed to secrete concrete-like material such that they have form re-growable and self-sustaining bricks⁹.

While the methods to design useful and relevant bioproducts have reached a point where they are ready to have a large impact on society, such biomaterials have yet to be widely adopted because of our lack of ability to scale such materials. Generally, once a biomaterial (i.e. polymer, protein therapeutic, lipid, etc) has been designed, a cell population, generally comprised of CHO

cells, microalgae, yeast, or bacteria, is genetically modified to produce that biomaterial via transformation, transfection, and other gene editing methods. Afterwards, the cell population is optimized to produce higher yields of the desired bioproduct within large scale bioreactors. To achieve this, engineers often perform a series of gene edits, have higher producing strains overtake a population in small-scale bioreactors (<1L), and repeat until a strain or multiple strains are produced that can produce high yields in larger scale bioreactors (>1000L).

Unfortunately, there are several issues with traditional methods of scaling. First, engineers and scientists do not understand cell biology enough to rationally design a way that repeatably produces desired phenotypic properties in cells. While direct genetic modification is useful when attempting to have a cell produce or express a desired bioproduct, it rarely works when trying to change entire cell behavior (growth rate, secretion rate, etc). This is largely because these behaviors do not rely on any single gene. Rather, cell behavior depends on many different interacting epigenetic, genetic, and environmental factors that are simply too difficult for any biologist or group of biologists to fully understand. Second, a biologist that optimizes for the enhancement of one desired phenotypic property, only to un-intendedly cause negative and undesired effects in other desired phenotypic properties. For example, approaches that have been explored to enhance bioproduct production by a cell often does so by reducing cell growth, resulting in a net neutral or even negative impact on the overall yield of the cell population¹⁰. Third, the traditional method of having high-producers overtake a population in small-scale and then large-scale bioreactors can take several months to occur¹¹. Fourth, this bulk method doesn't enable engineers to explore the full heterogeneity of cells that can produce these higher yields. As a result, these bulk methods often produce populations with un-intended and un-desired phenotypic properties. For example, microalgae intended to produce biofuels that overtake a population within

a small-scale bioreactor often do so by increasing their chlorophyll size. This increased chlorophyll size results in un-desired shading effects in outdoor cultivation farms where microalgae closest to the surface shade the microalgae are farther depths, reducing the yields of these deeper microalgae. As a result of these issues, scaling of these biomaterials costs at least \$50 million and can take 3-5 years, something that is simply not practical for wide-spread adoption¹².

To increase yields of desired biomaterials, it is necessary to develop a cell screening technology that enables the following:

1. Selection of single cells and clonal colonies so that researchers can directly select for desired phenotypic traits and remove any un-desired ones
2. Applies an evolutionary selection pressure on clonal colonies based on coupled growth and bioproduct production rates, where the bioproduct is either retained intracellularly or secreted
3. Can achieve throughputs of 1,000,000+ cells or clonal colonies per screen so that the full genetic diversity can be explored

Traditional single cell and clonal colony selection methods have involved the use of 96- or 384-microtiter plates and image processing systems¹³. While it is possible to select for cells based on coupled growth and bioproduct production rates using this method, throughputs are realistically limited to ~10,000 cells/screen, even with advanced automated robotic handling systems. More recently, there have been microfluidic systems developed to perform that enable the selection of single cells and/or clonal colonies based on more specific phenotypic properties and/or at higher throughputs. For example, Berkeley Lights has developed an optofluidics workflow that can make

very precise selection of cells based on phenotypic traits. However, while this system can reach throughputs of 20,000 – 50,000 cells/screen, which is higher than what is achievable with microtiter plates, it's still not enough to explore the full genetic diversity of directed cellular evolution assays. Other new microfluidic systems such as nanowell arrays¹⁴ and microfluidic droplet systems¹⁵ can achieve the 1,000,000+ cells/screen throughputs necessary for evolutionary workflows. These systems have also been successfully used to select cells based on growth¹⁶, secretion¹⁷, and/or intracellular bioproduct accumulation rates¹⁸. However, the practical issue with using these microfluidic tools for solution exchange so that fluorescent stains can enter the microfluidic compartment and later be washed out. Generally, these assays rely on the localization of pre-encapsulated stains on a single bead or cell such that there can be a difference in the readout between a positive and negative hit. While this works when selecting cells based on secretions that bind to a particular target or presence of a bioproduct in a single cell, this does not work when selecting clonal colonies based on coupled growth and bioproduct production properties. In these assays, the clonal colonies and/or secretions will not localize at a single point but will be spread out throughout the volume of the compartment. As a result, the fluorescence readout between positive and negative hits will be same. So, it is necessary to develop a similar microfluidic technology where unbound stains can be readily removed from the compartment so that positive and negative hits can be distinguished from one another.

1.2 Initial gel microdrop work

As an undergraduate student, I worked under the guidance of Dr. Carson Riche and Dr. Ming Li to develop a gel microdrop workflow designed to select microalgae based on coupled growth and lipid accumulation rates that resulted in a co-first authorship for a paper published in *Small*:

“A Gelatin Microdroplet Platform for High-Throughput Sorting of Hyperproducing Single-Cell-Derived Microalgal Clones”¹⁹. At this time, there were publications describing the use of gel microdrops to perform high-throughput sorting of cells²⁰. In these workflows, cells were encapsulated into microfluidic droplets along with reversibly-gellable hydrogel (in particular, agarose), incubated to allow for growth/secretion, cooled to solidify the hydrogel, transferred from oil to aqueous solution, stained, sorted using a fluorescence-activated cell sorter (FACS), and heated to melt the hydrogel and release selected cells. Since the hydrogel is porous, this workflow is better for evolution assays designed to enhance production of clonal colonies since unbound stains can be readily washed away and give better fluorescent readouts for our desired application.

To further explore this system, we developed a gel microdrop workflow where we selected microalgae clonal colonies based on coupled growth and lipid production (Figure 1). In particular, we successfully sorted out and released *Euglena gracilis* colonies with higher amounts of chlorophyll (which we determined roughly correlated to the number of cells per gel microdrop) and lipid. We also developed two innovations over previous workflows. First, we substituted agarose with gelatin as our hydrogel material. When we initially started working with agarose, we found that the melting point of low melting point agarose (~45 – 50°C) was higher than the maximum temperature that our cells *E. gracilis* and *Chlamydomonas reinhardtii* can survive at (~37 – 40°C). Gelatin was capable of melting at lower temperatures (~35 – 40°C) and therefore was able to be used for this application. Second, we developed a much easier way to transfer the hydrogels from oil to aqueous solution. Previous methods centrifuged or filtered the PicoShells, which was incredibly inefficient and resulted in oil droplets that stayed within the sample and greatly diminished the sorting efficiency during FACS. Other methods used hexanes to remove oil, which is highly toxic and would kill encapsulated cells. We found that we can more efficiently and

quickly remove oil by washing the emulsified gel microdrops with the de-emulsifying reagent 1h,1h,8h-Perfluoro-1-octanol (PFO) that very effectively removed all the oil without causing significant damage to the encapsulated cells.

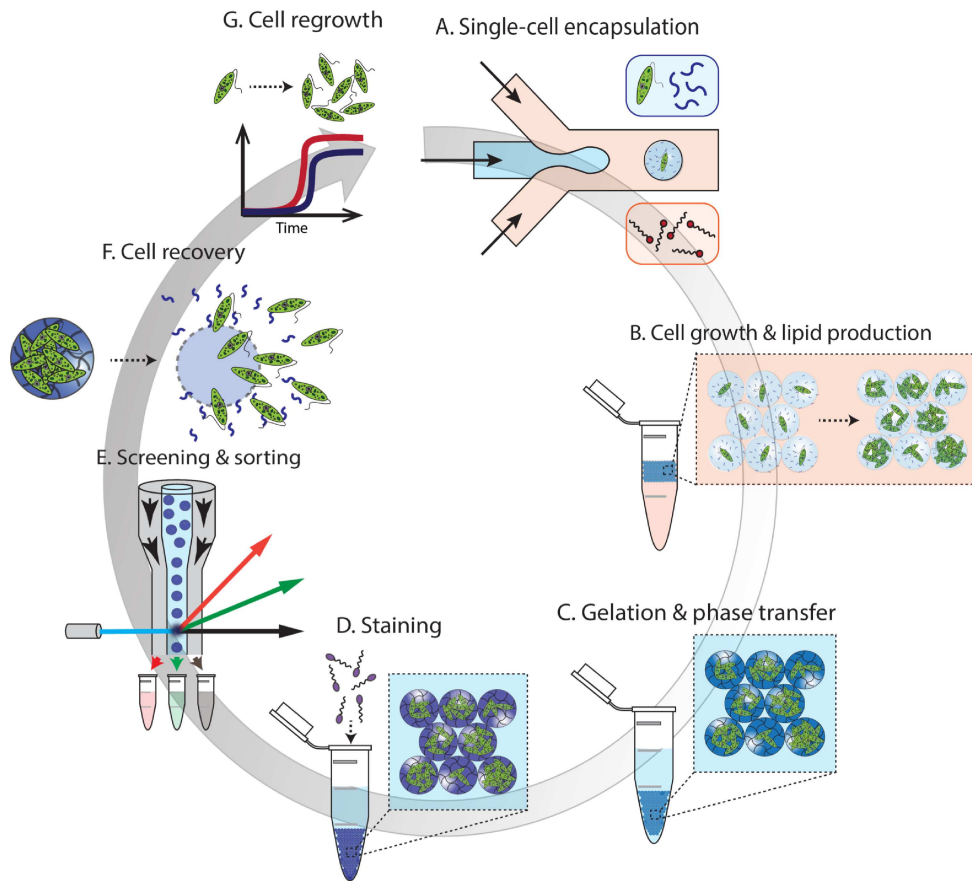


Figure 1-1. Gel microdrop workflow. a) Encapsulation of single microalgal cells within monodisperse gelatin microgel compartments using microfluidic techniques. b) Growth and metabolite (e.g. chlorophyll and lipids) production of individual microalgal colonies derived from single cells within the gelatin microgel droplets. c) Following gelation, transfer of cell-laden microdroplets from oil into an aqueous solution. d) Staining of specific metabolites in microgel beads. d) Staining of specific metabolites in microgel beads. e) Flow cytometric screening and sorting of microgel compartments containing hyperproductive microalgal cells. f) Recovery of cells from the microgel beds by melting. g) Following release, cells can be regrown, or reintroduced into another selection cycle.

1.3 Attempts to expand gel microdrop technology

During the beginning of my PhD, we sought to expand upon this gel microdrop workflow. In particular, we aimed to further optimize the proof-of-concept workflow developed during my undergrad to perform a full evolution assay with microalgae and to enable the system to perform secretion assays. Interestingly, we found that gelatin could not be used for secretion assays because the charges on gelatin results in non-specific binding to the cells matrix (Figure A1). However, we found that this non-specific binding did not occur in agarose due to the reduced amount of charges in a carbohydrate matrix (Figure A2). So, we decided to re-optimize the system to be used with agarose and aimed to find new ways to break down the hydrogel post-sort (e.g. via agarase or mechanical breakdown). We initially aimed to capture cell secretions with anti-IgG or protein A coated microbeads but found that the capture sites would be saturated after 2-4h of secretions (Figures A3 and A4). So, we developed a workflow to add conjugate capture sites directly to the agarose matrix such that we can we have more capture sites within the gel matrix. We were successfully able to conjugate biotin groups to the agarose matrix by activating the hydroxyl groups of agarose with de-tert-butyl-dicarbonate and adding a carboxylic acid-linked biotin to the system such that a stable ester is formed and the biotin remains bound to the agarose matrix (Figure A5). We also found that the ability for agarose-conjugated biotin to bind to streptavidin is greatly enhanced by increasing the chain length size between the biotin and carboxylic acid functional groups (Figure A6). Interestingly, we also found that conjugating biotin to the agarose matrix reduced the melting point to be lowered below 37°C such that it can be melted as temperatures that do not induce cell death, unlike un-modified low-melting point agarose (Figure A7). We also demonstrated that we can use biotin-streptavidin affinity binding to bind protein A that can capture

fluorescent IgG antibodies (Figure A8). We were also able to encapsulate CHO cells into protein A functionalized gel microdrops and were able to capture cell secretions (Figure A9).

Unfortunately, there were several practical issues that arose when we started pushing the gel microdrop forward. First, there was a lot of crosstalk between the gel microdrops that made it difficult for us to localize positive hits from negative ones (Figure A9). Second, it was very difficult to remove all the toxic chemicals required for the conjugation reaction such that the cells would often die. Lastly and most importantly, cells tended to pre-maturely degrade the hydrogel matrix during growth studies (Figure A10 and A11). While we were unable to obtain any conclusive data or evidence why this occurs, we hypothesize that cells naturally release enzymes that degrade motifs found in proteins and carbohydrates, including those found in gelatin and agarose²¹. As a result, the hydrogel would often fall apart before we would get to sorting and was incredibly difficult to make work consistently. So, we concluded that while gel microdrop is okay for short term studies (<4h) as has been explored in other studies, it is not compatible for evolution workflows designed to increase bioproduct yields and when cells are required to grow within the compartments for longer than 4h.

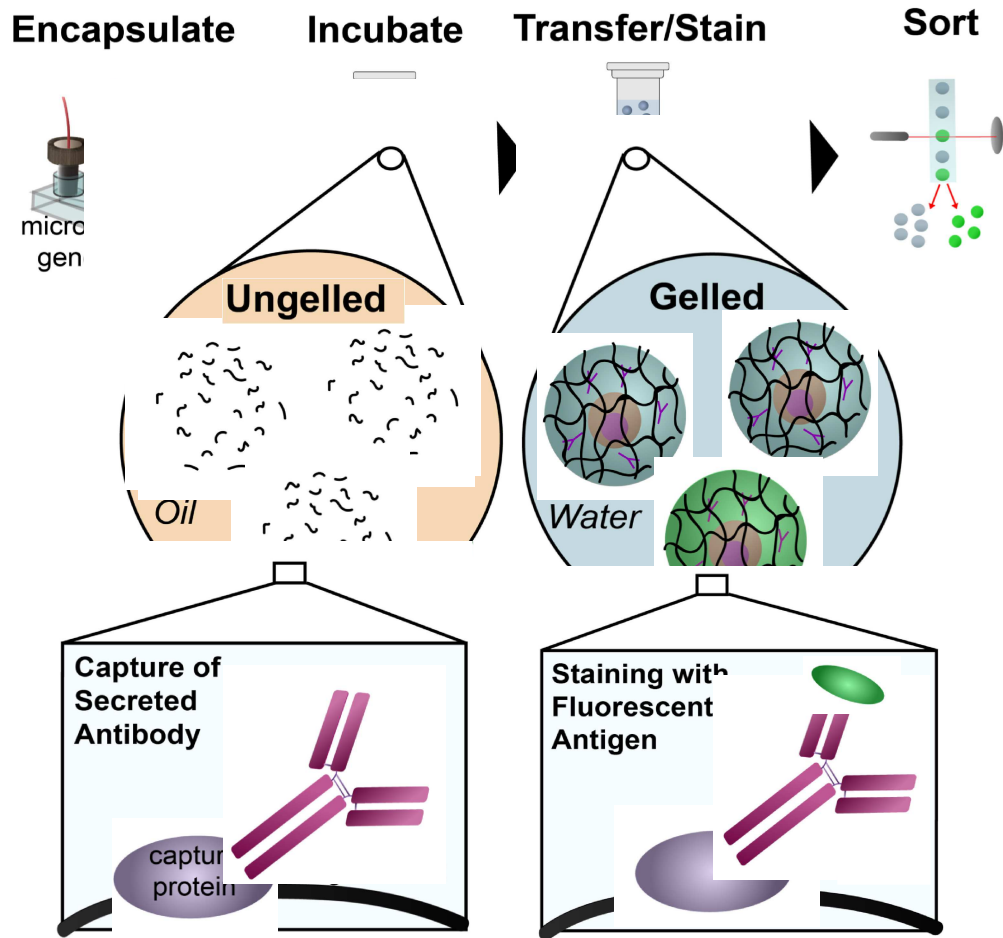


Figure 1-2. Gel microdrop secretion workflow. Secreting cells are first encapsulated into water-in-oil emulsions containing an un-gelled hydrogel using a microdroplet generator. Cells are incubated in the water-in-oil emulsions where they are allowed to secrete antibodies that are captured by capture proteins conjugated to the hydrogel matrix. Following incubation, the hydrogel is gelled via cooling and the gel microdrops are transferred from oil to aqueous solution where they are mixed with a fluorescently labeled antigen. Gel microdrops containing cells that secrete the desired antibody and fluorescently stained and un-bound antigen is washed away. The gel microdrops are placed into a fluorescent-activated cell sorter (FACS) where fluorescently labeled microdrops are selected from the population. The selected gel microdrops are then melted via heating to release cells for further processing.

1.4 Motivations behind PicoShells

While there were several practical issues with the gel microdrop workflow, we also determined that there were several fundamental issues with the model itself and that we would have not succeeded even if we solved the practical issues. Specifically, the cells are incubated in an environment that is very different than what they would be exposed to in a production setting (e.g. a bioreactor or outdoor cultivation farm). This issue is a major reason why improving yields by selecting clonal colonies with microtiter plates and microfluidic systems has largely been unsuccessful. While engineers are able to generate cell populations that produce high yields in a laboratory setting, these populations often lose the desired phenotypic traits when placed into production environments. In the case of the gel microdrop system, encapsulated cells are grown up in water-in-oil emulsions which alters gas exchange and limits nutrient diffusion, both of which would be continuously regulated in a production setting. Also, cells are co-encapsulated with a large concentration of un-gelled hydrogel material that would not normally be present. In addition, cell-cell communication factors play a large role in the behavior of cells, something that is greatly reduced within gel microdrops (and other microfluidic systems). Lastly, encapsulated cells are not exposed to temperature, pH, and light gradients/factors that are normally present in large-scale systems.

So, we aimed to develop a cell screening system with the updated criteria:

1. Selection of single cells and clonal colonies so that researchers can directly select for desired phenotypic traits and remove any un-desired ones

2. Applies an evolutionary selection pressure on clonal colonies based on coupled growth and bioproduct production rates, where the bioproduct is either retained intracellularly or secreted
3. Can achieve throughputs of 1,000,000+ cells or clonal colonies per screen so that the full genetic diversity can be explored
4. **Has cells incubated and characterized in environments that replicate the factors experienced in a production setting**

Our efforts eventually led to the development of PicoShells, a new cell-screening platform that is specifically designed to meet all the criteria necessary to enhance bioproduct yields. PicoShells are spherical, hydrogel microparticles that range from 35 to 100 μ m in diameter, that can be produced at a rate of 2000-3000 PicoShells/s and have the following key features:

1. A hollow inner cavity where cells can be encapsulated in
2. A porous outer shell
3. The ability to be stable and freely suspendable in an aqueous environment
4. Is compatible with FACS

The hollow inner cavity is an advancement over gel microdrop technology since cells are no longer exposed to a hydrogel material during incubation. The porous outer shell is an advancement over gel microdrop and microfluidic technologies because nutrients can be continuously replenished, cell-cell communication factors can readily be exchanged between compartments and with un-encapsulated cells, and enclosed cells can be directly exposed to stimuli from the external

environment. The ability to be stable and freely suspendable in an aqueous environment is an advancement over microtiter plates and microfluidic systems because enclosed cells can be placed directly into a production environment such as a bioreactor rather than needing to attempt to simulate it in the laboratory setting. Compatibility with FACS is an advancement over microtiter plates and many microfluidic systems because PicoShells can be sorted at rates of 100 – 5000 events/s. The outer shell of the PicoShell matrix can also be modified to retain secretions and/or genetic material via the addition of capture groups or modulating the matrix pore size, as is discussed more thoroughly in Chapter 3. With PicoShells, we believe we have successfully developed a workflow that enables the high-throughput selection of cells based on their ability to enhance production yields of desired bioproducts and biomaterials.

1.5 References

1. Cline W. The Impact of Global Warming of Agriculture: Comment. *The American Economic Review*. 86(5), 1309-1311 (1996).
2. Heinze C., Meyer S., Goris N., Anderson L., Steinfeldt R., Chang N., Le Quere C., and Bakker D.C.E. The ocean carbon sink – impacts, vulnerabilities, and challenges. *ESD Reviews*. 6(1), 327-358 (2015).
3. Grillberger L., Kreil T.R., Nasr S., and Reiter M. Emerging trends in plasma-free manufacturing of recombinant protein therapeutics expressed in mammalian cells. *Biotechnology Journal*. 4(2), 186-201 (2009).
4. Ghasemi Y., Rasoul-Amini S., Naseri A.T., Montazeri-Najafabady N., Mobasher A., and Dabbagh F. *Applied Biochemistry and Microbiology*. 48, 126-144 (2012).
5. Pinton P., Rimessi A., Romagnoli A., Prandini A., and Rizzuto R. Biosensors for the Detection of Calcim and pH. *Methods in Cell Biology*. 80, 297-325 (2007).
6. Giuliano K. and Taylor D.L. Fluorescent-protein biosensors: New tools for drug discovery. *Cell Press*. 16(3), 135-140 (1998).
7. Cai T., Sun H., Qiao J., Zhu L., Zhang F., Zhang J., Tang Z., Wei X., Yang J., Yuan Q., Wang W., Yang X., Chu H., Wang Q., You C., Ma H., Sun Y., Li Y., Li C., Hiang H., Wang Q., and Ma Y. Cell-free chemoenzymatic starch synthesis from carbon dioxide. *Science*. 373, 1523-1527 (2021).
8. Almasbak H., Aarvak T., and Vemuri M.C. CAR T Cell Therapy: A Game Changer in Cancer Treatment. *Journal of Immunology Research* (2016).

9. Heveran C. M., Williams S., Qiu J., Cook S., Cameron J., and Srubar W. Biomineralization and Successive Regeneration of Engineered Living Building Materials. *Matter* 2(2), 481-494 (2020).
10. Formenti L. R., Norregaard A., Bolic A., Hernandez D. Q., Hagemann T., Heins A.L., Larsson H., Mears L., Mauricio-Iglesias M., Kruhne U., and Gernaey K. Challenges in industrial fermentation technology research. *Biotechnology Journal* 9(6) 727-738 (2014).
11. Hsu Y. L. and Wu W.T. A novel approach for scaling-up a fermentation system. *Biochemical Engineering Journal*. 11(2) 123-130 (2002).
12. Zymergen. (2022). Prospectus.
13. Uber D., Jaklevic J., Theil E., and Lishanskaya A. Application of Robotics and Image Processing to Automated Colony Picking and Arraying. *Biotechniques* (1990).
14. Choi J. Advanced in single cell technologies in immunology. *Biotechniques* 69(3) (2020).
15. Griffiths A. and Tawfik D.S. Miniaturising the laboratory in emulsion droplets. *Cell Press* 24(9), 395-402 (2006).
16. Li M., van Zee M., Goda K., and Di Carlo D. Size-based sorting of hydrogel droplets using inertial microfluidics. *Lab on a Chip* 18, 2575-2582 (2018).
17. Mazutis L., Gilbert J., Ung W. L., Weitz D., Griffiths A., and Heyman J. A. Single-cell analysis and sorting using droplet-based microfluidics. *Nature protocols* 8, 870-891 (2013).
18. Yu Z., Giesler K., Leontidou T., Young R. E. B., Vonlanthen S. e>, Purton S., Abell C., Smith A. G. Droplet-based microfluidic screening and sorting of microalgal populations for strain engineering applications. *Algal Research* 56 (2021).

19. Li M., van Zee M., Riche C. T., Tofig B., Gallaher S., Merchant S. S., Damoiseaux R., Goda K., and Di Carlo D. A Gelatin Microdroplet Platform for High-Throughput Sorting of Hyperproducing Single-Cell-Derived Microalgal Clones. *Small* 14(44) (2018).
20. Weaver J. C. McGrath P., and Adams S. Gel microdrop technology for rapid isolation of rare and high producer cells. *Nature Medicine* 3(5), 583-585 (1997).
21. Luxmi R., Blaby-Haas C., Kumar D., Rauniyar N., King S. M., Mains R. E., and Eipper B. A. Proteases Shape the *Chlamydomonas* Secretome: Comparison to Classical Neuropeptide Processing Machinery. *Proteomes* 6(4), 36 (2018).

Chapter 2. High-throughput selection of cells based on accumulated growth and division using PicoShells

Production of high-energy lipids by microalgae may provide a sustainable, renewable energy source that can help tackle climate change. However, microalgae engineered to produce more lipids usually grow slowly, leading to reduced overall yields. Unfortunately, tools that enable the selection of cells based on growth while maintaining high biomass production, such as well-plates, water-in-oil droplet emulsions, and nanowell arrays do not provide production-relevant environments that cells experience in scaled-up cultures (e.g. bioreactors or outdoor cultivation farms). As a result, strains that are developed in the lab often do not exhibit the same beneficial phenotypic behavior when transferred to industrial production. Here we introduce PicoShells that enable >100,000 individual cells to be compartmentalized, cultured in production-relevant environments, and selected based on desired phenotypic traits using standard flow cytometers. PicoShells are picoliter-scale hydrogel particles with a hollow inner cavity where cells are encapsulated and a porous outer shell that allows for continuous solution exchange with the external environment. PicoShells may also be placed directly into environments that are not possible with previous cell-screening technologies such as shaking flasks and bioreactors. We experimentally demonstrate that *Chlorella* sp., *Saccharomyces cerevisiae*, and Chinese Hamster Ovary cells grow to significantly larger colony sizes in PicoShells than in water-in-oil droplet emulsions ($P < 0.05$). We have also demonstrated that PicoShells containing faster dividing and growing *Chlorella* clonal colonies can be selected using a fluorescence-activated cell sorter and

re-grown. Using the PicoShell process, we select a *Chlorella* population that accumulates chlorophyll 8% faster than does an un-selected population.

2.1 Introduction

With the heightened interest in cell-derived bioproducts (e.g. high-energy lipids, recombinant proteins, antibody therapies, and nutraceuticals) and cell therapies (chimeric antigen receptor T-cell and stem cell therapies), the selection of desired cells based on their phenotypic properties has become increasingly important. In particular, the selection of microalgae strains for use as factories that convert light into biofuels has a long history because of their potential to be used as a carbon-neutral energy source. Specifically, high-energy lipids such as triacylglycerols (TAG) extracted from microalgae strains can be processed into biodiesel that can serve as an alternative energy source to power transportation^{1,2}. CO₂ emissions from the burning of biodiesel can later be fixed by microalgae and used to produce more high-energy lipids, creating a carbon-neutral mechanism to power today's economy³. Microalgae are preferred over terrestrial plants because they have much faster biomass accumulation rates and particular strains won't compete for resources that are important for agriculture⁴. Specifically, algae will occupy less land and certain strains can survive within recycled waste or seawater, eliminating potential competition for fresh water. In order to scale the microalgae industry to a point where microalgal-derived biofuels can be used ubiquitously, it is important to identify novel algae populations with enhanced biomass and lipid accumulation rates⁵. However, algal populations that are selected to overaccumulate high-energy lipids often have reduced cell division rates⁶, making it necessary to develop

technologies that can select algae populations based on their coupled division rate and lipid production.

Unfortunately, high-throughput screening tools for selection based on growth and bioproduct accumulation have not been readily available for scientists engineering cell strains. Fluorescence activated cell sorting (FACS) methods to select microalgal strains are only capable of selecting based on lipid content and not growth rate. This is because FACS traditionally has measured single cells at a single time point, rather than assaying colonies that are growing over time. Growth-based selection has been limited to low-throughput techniques such as using microtiter plates⁷ or small-scale bioreactors.

Microwell⁸, microcapillary⁹, droplet^{10,11}, and gel microdrop technologies^{12,13} are capable of compartmentalizing single cells into nanoliter-sized compartments and allowing cells to grow into small clonal colonies for selection but do have some key limitations. The microfluidic approaches can have automated high-throughput selection mechanisms that make it possible to screen populations greater than 100,000 colonies or single cells per screen. Unfortunately, these microfluidic compartments have physical or chemical barriers that inhibit transport between the compartment and the external environment. In consequence, enclosed cells may deplete nutrients within the compartment, can accumulate secreted cytotoxic elements, change the pH of the environment, and may have reduced ability to communicate with other cells via secreted factors. So, these high-throughput screening technologies may not be suitable for long-term (e.g. > 24 hour) growth assays, yielding selection pressures that are not aligned with final growth environments. This is because over these time scales, the compartments do not provide an environment that is physiologically similar to what is expected in scaled production cultures. As a result, selected cells may not behave the same way when scaled up for real-world applications as

they did when cultured within these nanoliter-sized compartments. This behavior has been recently observed for yeast cells, where the size of the droplet affects overall cell morphology following culture¹⁴. Scientists often need to perform further experiments and do additional genetic manipulation of selected strains to adapt them to scaled-up industrial cultures, a process that can take several months or years and without guaranteed success. Nanopen technology¹⁵ does have nanoliter-sized compartments that can have their solution replaced without dislodging the cells; however, it requires light-based manipulation of cells to isolate desired colonies that has a limited throughput of ~10,000 cells/screen.

To address these issues, we have developed a hollow shell microparticle platform (PicoShells), which enables compartmentalization of growing colonies, continuous media exchange, phenotypic screening and sorting via FACS, and viable downstream recovery. The PicoShell particles are ~90µm in diameter, consist of a solid outer shell made of polymerized (poly-ethylene glycol) PEG, and have a hollow inner cavity where microalgae can be encapsulated and cultured. More importantly, the solid PEG matrix is porous, allowing the PicoShells to be refreshed by external media, which would enable transport of nutrients into the compartment and facilitate potential communication between cells in nearby compartments or in surrounding media. We have also demonstrated that PicoShells can be placed into unique environments that have not been previously possible such as a stirring solution within a 100mL beaker. Cell-containing PicoShells should therefore be compatible with culture in various bioreactors or other relevant environments, providing a production-similar environment for enclosed cells that is not possible to attain with any other nanoliter-scale compartments. As a result of these features, strains developed using PicoShells may be expected to exhibit their desired phenotypes in relevant scaled up cultures, promising to save cell-line developers months or years of additional labor to reach a

similar point. These PicoShell particles can be loaded with single cells such that those cells grow over a multi-day period to form clonal colonies. Additionally, the pores in the outer hydrogel shell allow for encapsulated cells to be stained with common fluorescent tags such as BODIPY and live/dead stains. Since these particles are stable in aqueous solution, they can be screened and sorted using standard FACS instruments, allowing colony-containing PicoShells to be sorted at throughputs >300 particles/s. Cells can be released from PicoShells via mechanical or chemical mechanisms, retaining viability such that selected cells can be re-cultured, further scaled, analyzed, and perhaps re-sorted (Figure 2-1).

Here, we compare growth of colonies in PicoShells with microfluidic droplet-in-oil approaches and demonstrate a proof-of-concept workflow for the selection of hyper-performing microalgae populations. In particular, we show the accumulated growth of microalgae, yeast, and adherent CHO cell colonies is higher in PicoShells than in water-in-oil droplet emulsions. Also, we demonstrate that particles containing faster growing algae colonies can be selected using FACS, that selected colonies can be released, and that the selected population can maintain a higher rate of accumulation of chlorophyll than the un-selected population upon re-culture. We anticipate the PicoShell platform can play a key role in the selection of hyper-producing microalgae strains that translate to scaled-up culture environments as well as various other producer cell lines for a range of bio-products.

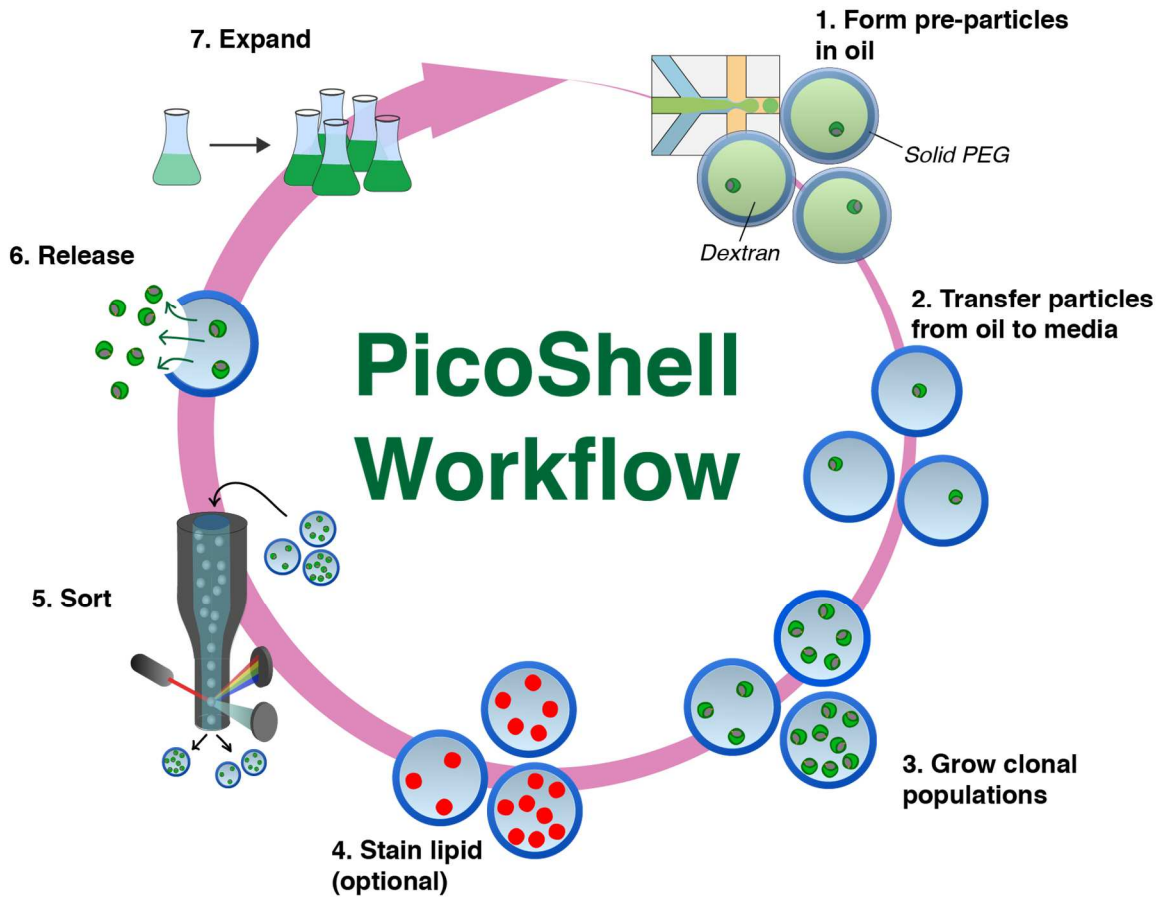


Figure 2-1. Workflow to enrich microalgae using PicoShell particles. (1) PicoShells are formed using droplet microfluidics, an aqueous-two phase system, and polymer chemistry. Particles are initially formed within an aqueous droplet surrounded by oil. Microalgae are within the dextran phase, which is surrounded by a solidifying PEG matrix. (2) Soon after particle formation, the particles are transferred into the algae's native media. Pores in the solid outer shell allow for dextran to leak out and for continuous solution exchange. (3) Microalgae can divide within particles over multiple days to form clonal populations. (4) Pores in the solid matrix allow algal lipids to be fluorescently labeled. (5) High-performing populations can be sorted using FACS with scatter and/or fluorescence readouts. (6) Sorted particles can be broken down mechanically or by adding chemical reagents that degrade the PicoShell's solid matrix, allowing associated cells to be released. (7) Released cells remain viable and can be re-cultured for further analysis and/or sorting.

2.2. Results

2.2.1 Fabrication of PicoShells

PicoShell particles are made using a combination of microfluidic droplet technology^{16,17,18}, aqueous two-phase systems (ATPS)^{19,20} and PEG polymer chemistry²¹ (Figure B1). When mixed together at certain concentrations, a PEG-rich and dextran-rich phase can form, with a degree of phase separation that is tunable by adjusting the relative concentrations of the PEG and dextran components^{22,23}. Coalescence of the PEG-rich phase at different concentrations of PEG and dextran can lead to particles of unique shapes, owing to the unique interfacial tensions of the three-phase system (PEG-rich, dextran-rich, and oil phase)^{24,25}. To determine the concentrations of PEG and dextran required to obtain PicoShell particles, we first obtained the binodal curve with the particular PEG and dextran used, a plot that defines the boundary between a completely mixed and phase separated aqueous two-phase solution. The binodal is dependent on the molecular weights and chemical functionality of the materials (Figure B2). We found that regions close to the binodal but above and to the right of the boundary led to the formation of concentric phases. When droplets contain PEG/dextran concentrations within 1-2% into the phase separation region above and to the right of the binodal, the dextran orients in the center of the droplet with PEG uniformly surrounding the dextran at the aqueous-oil interface. Complete stable phase separation occurs within ~20s following droplet formation. Crosslinking the PEG phase at these concentrations results in PEG hydrogel shells, i.e. PicoShell particles, that can remain stable when transferred out of oil and into aqueous solution (DPBS, media, etc.). The molecular weight of the dextran is chosen such that it can diffuse out of the enclosed shell particle following the phase transfer (Figure B3). The

mechanism to form such hollow shell or capsule particles using the methods we describe has been adapted from previous work^{26,27}.

We identified a cell-compatible cross-linking chemistry to form PicoShell particles. While we can use UV-dependent chemistries to crosslink porous hydrogel particles of similar geometries²⁸, we chose a different approach as UV-light and free radicals generated are likely to genetically or phenotypically affect cells being encapsulated, potentially introducing negative impacts on the assay/selection²⁹. We incorporated a biocompatible pH-induced crosslinking chemistry where gelation occurs within physiologically-compatible pH ranges (pH ~6-8)³⁰. However, pH-induced crosslinking introduces new challenges as the mixing time of crosslinker and functionalized PEG within droplets along with solidification affects the final particle morphology, even at the same PEG/dextran concentrations (Figure B4). If the crosslinking reaction time is too short, the PEG and dextran phases do not have enough time to fully phase separate, usually resulting in a non-uniform outer shell and/or un-desired crosslinking density in the cavity. In contrast, if the crosslinking reaction time is too long, the shift in the binodal resulting from the increasing molecular weight of the PEG phase as it starts to polymerize causes the formation of bowl-shaped particles instead. To obtain the ideal particle shape, we adjusted the crosslinking time by modulating the pH of the formed droplet. We found that repeatable, uniform shells could be formed by generating emulsions with in-droplet concentrations of 11% (w/w) 10kDa dextran, 5% (w/w) 10kDa 4-arm PEG maleimide (PEG-MAL), and 1.54mg/mL dithiothreitol (DTT) crosslinker at pH 6.25. All reagents were dissolved at a pH of 6.25. With this combination of reagents, we are able to form uniform particles (Figure B5) with an outer diameter of 91 μm and shell thickness of 13 μm (CV of 1.7% and 6.9% respectively) at a particle generation rate of 720 PicoShells/s.

2.2.2 Enhanced growth in PicoShells vs droplets

We found that encapsulated cells (*Chlorella* sp., *Saccharomyces cerevisiae*, and adherent CHO cells) grow more rapidly and to higher final densities in PicoShells than in microfluidic droplets in oil (Figures 2-2c, 2-2d, and 2-2e). We found that cells tend to grow and settle to the bottom of the PicoShell rather than be suspended in the core (Figure S6).

Cells from were encapsulated into PicoShells and droplets. *Chlorella* growth was tracked every 12h over a 72h period and *S. cerevisiae* was tracked every 6h over a 36h period. The number of cells in each PicoShell and droplet was estimated by dividing the cell mean area within each compartment by the average area of a single cell in each population respectively. Since the cells become very dense at longer time frames, it is difficult to verify how accurate this measurement is. So, ‘Estimated count’ is designed to provide a rough quantification of the differences in the cell numbers between PicoShells and droplets rather than providing an precise measurements of cell count. Interestingly, we found that *Chlorella* grow rapidly in PicoShells starting with the formation of a first generation of daughter cells following 12h of incubation but did not grow when encapsulated in microfluidic droplets even over a 72h period (Figure 2-2c). *Chlorella* were encapsulated and incubated in autotrophic media, presumably making cells more susceptible gas transport. *Chlorella* were found to double every 12.2 hours and reached a carrying capacity within the 155 pL hollow cavity of a PicoShell of an estimated 250 cells (Figure 2-2c). In parallel, we found that *Saccharomyces cerevisiae* grow both in PicoShells and in water-in-oil droplet emulsions (Figure 2-2d). However, while the growth rate of the yeast in both types of compartments were not statistically different before the first 18 hours of culture ($P = 0.28$ at 12h),

the growth rate of droplet-encapsulated yeast became significantly slower than PicoShell-encapsulated yeast at later times ($P < 0.001$ at times $> 18\text{h}$). The average number of yeast cells in PicoShells is dramatically increased between 24 and 48 hrs after encapsulation to an estimated 2900 cells/PicoShell, $\sim 20\text{X}$ higher than the carrying capacity in droplets (estimated to be ~ 150 cells/droplet). We also found that adherent CHO cells can grow within PicoShells and not within droplets (Figure 2-2e). CHO cells have a reduced growth rate for the first 24h (doubling time = 178h) and grow with a doubling time of 18h per doubling starting at 24h after encapsulation. CHO cells reach a carrying capacity of an estimated ~ 100 cells/PicoShell 96h after encapsulation. It is important to note that droplets containing CHO cells were capped with mineral oil to reduce the evaporation of droplets during the study (Figure B7). While this may have resulted in the lack of growth by CHO cells in this assay, we ran a side-by-side study with yeast grown in droplets capped with and without mineral oil and did not find any significant difference in the growth rate over a 48h period (Figure B8).

Differences in growth in PicoShells may be due to transport of nutrients and cytotoxic factors, and/or increased cell-cell communication (Figure 2-2b). The reduction in the growth rate of droplet-encapsulated yeast is likely due to the depletion of essential nutrients and/or accumulation cytotoxic cellular waste. All nutrients present in both media types were below 200Da. Such nutrients are expected to be freely exchanged through the outer membrane of the PicoShells given the molecular weights below $\sim 40\text{kDa}$ (Figure B3). This result is in agreement with the enhanced growth rate of *E.coli* observed when encapsulated in capsule particles compared with droplets in oil²⁷. To further explore these effects, we introduced a leucine-dependent yeast cell strain into PicoShells and transferred them into media with and without leucine after encapsulation. Yeast in PicoShells transferred to medium that contains leucine resulted in a statistically significant

increase ($P < 0.001$) in the number of cell divisions over a 12h period when compared to a leucine-free medium (Figure B9). This indicates that nutrients like the amino acid leucine can transport across the PicoShells during incubation. We have also demonstrated that cell-cell communication factors have an effect on the behavior of cells within PicoShells by incubating encapsulated yeast in a solution with yeast cells at a concentration of 100 million cells/mL and another solution without yeast cells. We observed a statistically significant difference in the number of cell divisions over a 12h period (Figure B10). Interestingly, we observed a reduced division rate when PicoShells are placed in a solution with a large background of yeast cells in stationary phase in the external environment despite replenishing the nutrients just prior to the start of the study. Supposedly, the quorum sensing factors secreted by the yeast in the external solution were those normally secreted during stationary phase to inhibit growth³⁰.

Intriguingly, we also observed that *S.cerevisiae* and CHO cells do not stop dividing once they fully occupy the volume of the inner cavity of the particle and additional cells actually causes the particle to stretch, increasing the overall diameter (Figure B11 and B12). The diameter of the PicoShells can actually expand from an initial diameter of $\sim 90\mu\text{m}$ to a maximum size of $\sim 500\mu\text{m}$ after 4 days at which point the particle ruptures and releases the encapsulated cells. This phenomenon was not observed for encapsulated *Chlorella* colonies. Instead, the microalgae were observed to stop dividing when the colony reaches the particle boundary.

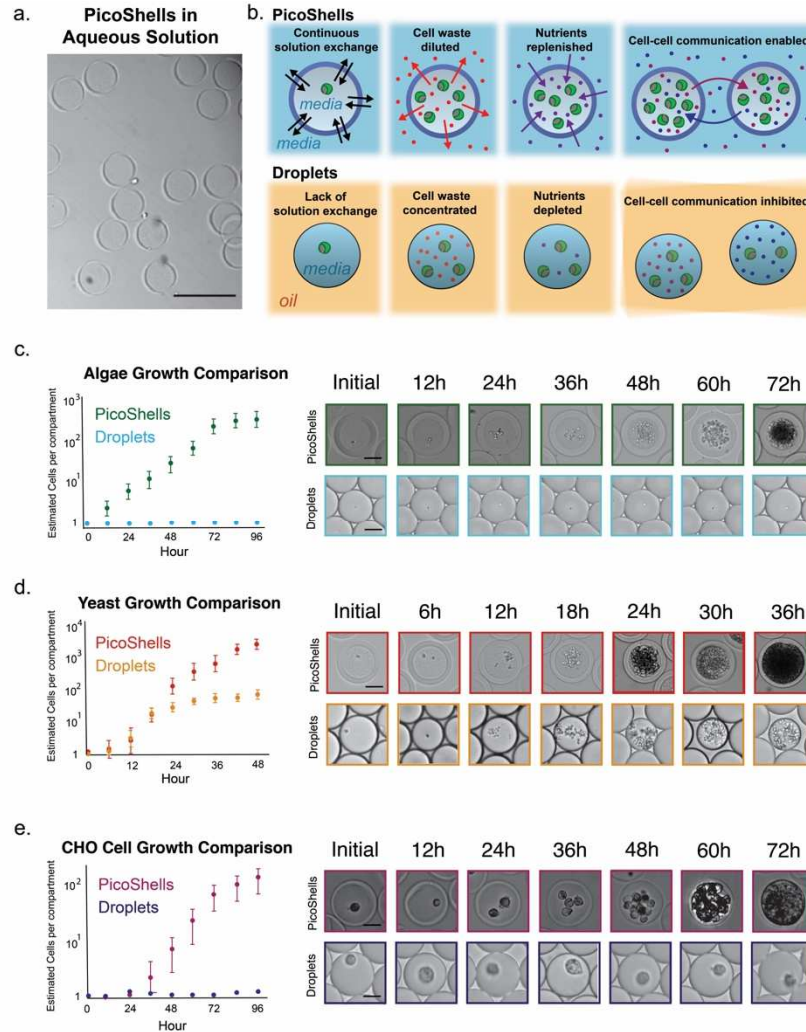


Figure 2. Growth comparison between PicoShells and emulsion droplets. (a) PicoShells are solid spherical particles that contain a hollow inner cavity and a porous outer shell. Scale bar = 200 μm . (b) PicoShells allow for continuous solution exchange with the external environment such that cell waste can be diluted, nutrients replenished, and cell-cell communication factors can pass between adjacent PicoShells (c) *Chlorella* were encapsulated into PicoShells and droplets to compare the estimated division rates in each compartment. Results show that the microalgae do not grow in droplets but grow readily in the particles. 5000-6000 cell-containing PicoShells/droplets were counted for each time point. Error bars represent the standard deviation in the number of cells per PicoShell at each time point. Scale bars = 50 μm (d) *S. cerevisiae* were also encapsulated into PicoShells and droplets to compare growth rates. The yeast initially grow at the same rate in both compartments but growth eventually slows down in droplets. 5000-6000 cell-containing PicoShells/droplets were counted for each time point. Error bars represent the standard deviation in the number of cells per PicoShell at each time point. Scale bars = 50 μm . (e) Adherent CHO DP12 cells were also encapsulated into PicoShells and droplets to compare growth rates. CHO cells do not grow within droplets but grow readily in PicoShells. 400-500 cell-containing PicoShells/droplets were counted for each time point. Error bars represent the standard deviation in the number of cells per PicoShell at each time point. Scale bars = 50 μm .

2.2.3. *Sorting of Chlorella based on accumulated growth*

Chlorella colonies seeded and cultured in PicoShells were selected based on the accumulated growth of cells using a FACS instrument. We used the colony's chlorophyll autofluorescence, appearing in the Cy5 channel (ex:620, em:647), as a metric for growth and production of biological materials (Figure 2-3a). Generally, colonies containing greater numbers of cells also contain higher amounts of chlorophyll, generating higher Cy5 fluorescence readouts, as we have demonstrated in a previous study¹². We demonstrated that lipids could also be stained through the PicoShells by mixing BODIPY with the colony-containing particles (Figure 2-3b). However, to simplify the study design to focus on improving the engineering aspects of the workflow, we only sorted clonal colonies based on overall accumulation of chlorophyll and not lipid productivity. We encapsulated *Chlorella* at an average loading density, lambda of 0.1, which resulted in 91.7% of cell-containing particles with no more than a single cell.

Following culture for 48 hours, PicoShells containing *Chlorella* colonies were sorted using the On-Chip Sort at an average event rate of 100-200 events/sec. We observed three distinct populations in the forward scatter height [FSC(H)] vs side scatter height [SSC(H)] plot: one from colony-containing particles, one from empty particles, and one from debris (Figure 2-3c). The debris population was confirmed to be from particulates naturally present in *Chlorella* media. If the media is filtered, a greatly reduced fraction of debris events is observed (Figure B13). As expected, ~14.3% of detected particles contain cells which correlates with the target loading fraction of 10%. In agreement with contrast observed in brightfield microscopy, PicoShells that contain microalgal colonies generally have increased forward and side scatter intensities. We verified that most of the colony-containing particles are within this high FSC/SSC gate by

demonstrating that events in this gate also contained the highest Cy5 fluorescence (i.e. chlorophyll autofluorescence). A selected sample based on this gate had 94.0% purity of colony containing PicoShells (Figure B14).

Using the On-Chip Sort we selected out PicoShell particles with the fastest growing colonies by gating on chlorophyll autofluorescence. When we selected particles from different regions of the Cy5 distribution of colony-containing particles, we observed differing numbers of microalgae in the sorted colonies (Figure 2-3d). PicoShells gated on the lowest 50% in the Cy5 channel and within the high scatter gate possessed on average 9.2 ± 3.7 cells. This was statistically different from colonies recovered when gating the highest 50% (19.5 ± 7.1 cells, $P < 0.0001$) and highest 15% (27.0 ± 7.2 cells) (Figure 2-3e). Before sorting, colony-containing PicoShells contained on average 13.0 ± 7.7 cells. Overall, higher Cy5 fluorescence intensities corresponded to particles with a greater number of cells and given our loading conditions favoring single cell-derived colonies, it is likely these particles contained microalgae sub-populations that have faster doubling times and/or increased production of chlorophyll (Figure 2-3e).

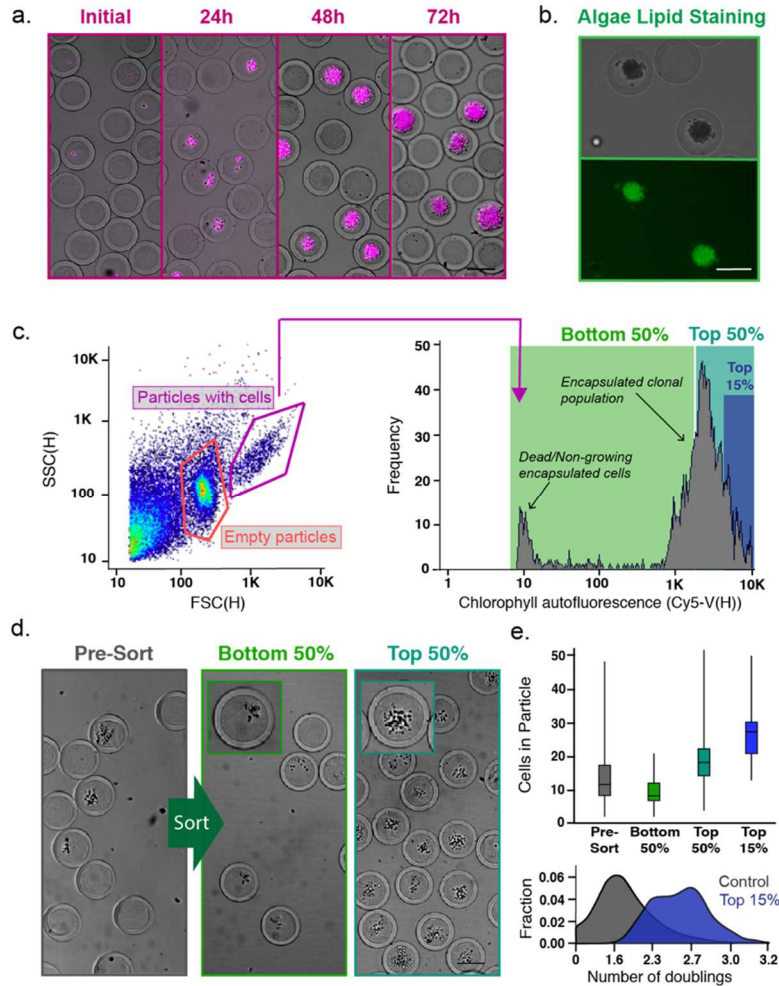


Figure 2-3. Screening and sorting characterization of microalgae-containing PicoShells. (a) PicoShells were loaded with *Chlorella* at $\lambda = 0.1$ and allowed to grow for 48h. The growth of *Chlorella* can be characterized via the chlorophyll autofluorescence that appears in the Cy5 channel. (b) The lipids in encapsulated *Chlorella* cells were stained with the addition of BODIPY 505/515. Localization of the stain were observed in the FITC channel. (c) After allowing *Chlorella* to divide in PicoShells, the particles were screened using an On-Chip Biotechnologies Cell Sorter. Particles that contain colonies and cells can be distinguished from empty particles using scatter readouts. Colony-containing particles produce an observable Cy5 fluorescence distribution via the colony's chlorophyll autofluorescence. (d) The colony-containing particles that produced the lowest 50%, highest 50%, and highest 15% Cy5 fluorescence readouts were sorted with 94.0% purity and 72.7% yield. 400 particles were sorted in each sample. (e) Selection of colony-containing PicoShells from different regions of the Cy5 distribution corresponds to particles containing different numbers of algal cells, with particles with higher Cy5 fluorescence readouts containing more cells than those with lower Cy5 fluorescent readouts. Particles sorted from the higher end of the Cy5 distribution contain colonies that have undergone more doublings and have divided more during the incubation period. Middle line within each of the boxes in the box and whisker plot represent the average number of cells in the particle, the top and bottom of each box represent the first and third quartiles respectively, and the top and bottom of the error bars represent the maximum and minimum values respectively. 350-400 PicoShells were counted in each sample. Scale bars = 50 μ m.

2.2.4. Selection and re-growth of a hyper-performing *Chlorella* sub-population

We used the workflow to select *Chlorella* colonies based on Cy5 fluorescence, released colonies from the particles, re-cultured, and verified after re-culture that the selected sub-population divides and accumulates chlorophyll faster than an un-selected population (Figure 2-4a). For these studies we minimized PicoShells with more than one cell initially loaded by using $\lambda = 0.05$, resulting in 3.2% of all particles containing colonies and ~98.3% of cell-loaded particles containing no more than one cell. Following 48h of growth in PicoShells immersed in *Chlorella* native media, we sorted colony-containing PicoShells gated to have the highest 11.1% of Cy5 fluorescence (425 events were selected from a population of 3839 colony-containing particles) (Figure S13).

Selected colonies were released from PicoShells by applying mechanical shearing stress onto the particles, causing them to rupture. PicoShells were disrupted with mechanical shear and released cells were re-cultured in a flask (Figure 2-4b). We compared the division rate of the selected sub-population during re-culture to an un-selected population by seeding each population at the same concentrations and tracking their cell concentrations over a 4-day period (Figure 2-4c). We observed that the selected sub-population had an ~8% faster growth rate than the un-selected population (doubling times of 10.2h and 11.2h respectively, $P < 0.01$) for the first 48h of growth after seeding. This resulted in a 40% difference in the cell concentrations 48h after seeding that can be visibly seen in the culture flask (Figure 2-4d). We also measured the total chlorophyll autofluorescence within well-mixed aliquots from each culture at this time point (Figure 2-4e), observing a 27.6% increase in chlorophyll autofluorescence for the selected sub-population. As

expected, the differences in cell number and overall chlorophyll accumulation between the two populations diminished after 48h as the cultures reach carrying capacity.

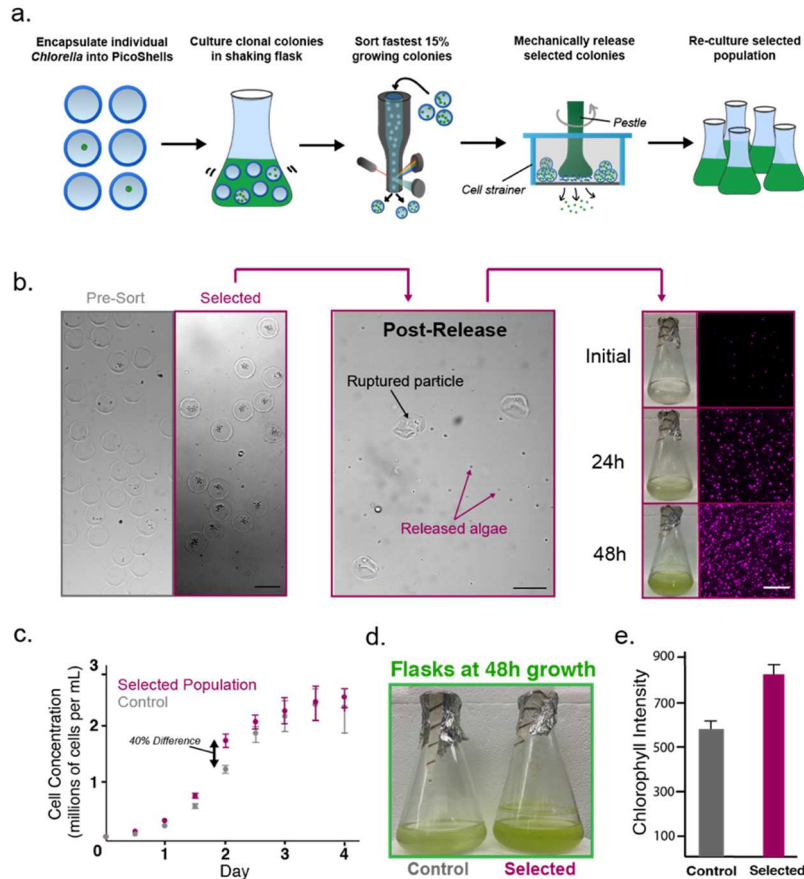


Figure 2-4. Selection of a hyperperforming *Chlorella* sub-population based on division rate (a) Single *Chlorella* were encapsulated into PicoShells and incubated under standard culturing conditions in a shaking flask to allow cells to produce greater numbers of cells. Colony-containing PicoShells from the top 15% of the Cy5 fluorescence distribution were selected by FACS and mechanically released from particles. Released cells were then re-cultured for further analysis. (b) From a particle population of 121,213 particles (3839 containing colonies), 425 particles were selected. Selected particles were ruptured on top of a cell strainer, causing selected algae to be released into fresh culture media. This sample was re-grown in an Erlenmeyer flask under standard culturing conditions for several days. (c) The selected population and an un-selected population were seeded in separate flasks at the same concentration and their cell concentrations were tracked for 4 days. The selected population had an 8% faster growth rate (10.2h doubling times) than the un-selected population (11.2h doubling time) for the first 48h after seeding before slowing down as the culture reached carrying capacity. Error bars represent the standard deviation in the cell concentration at each time point between samples. (d) The largest difference in cell concentration was observed at 48h after seeding (~40% difference in cell concentration), a difference that can be visibly seen in the green color of the cultures. (e) The difference in division rate was verified by measuring the chlorophyll density of each sample with a well plate reader at 48h after seeding. The selected population was measured to have a 27.6% higher chlorophyll density ($P < 0.05$). Error bars represent the standard deviation between the different wells used to measure the chlorophyll fluorescence at the 48h time point. 10 wells were measured for each sample. Scale bars = 100 μ m.

2.3. Discussion

2.3.1. *Advantages of PicoShells*

Several key aspects of the PicoShell workflow suggest it can aid in the selection/evolution of cells and cell-based products including: (1) Cell behavior and growth is significantly enhanced in PicoShells compared to water-in-oil droplet emulsions. (2) PicoShells containing desired cells/colonies can be selected using commercial fluorescence activated cell sorters. (3) Selected cells/colonies can be successfully released from the PicoShells and re-cultured. (4) Selected populations maintained a high-growth phenotype post-process at least for several generations. Importantly, PicoShells can be placed and remain stable in more production-relevant environments (e.g. a shaking culture flask, bioreactor, outdoor cultivation farms) that are not feasible with other high-throughput selection technologies (e.g. droplet technology, microwells, etc) (Figure B11). The porous outer shell enables solution exchange with the external environment, likely allowing replenishment of nutrients, diffusive transport and dilution of cytotoxic cellular waste, access to quorum sensing factors from external cells/colonies, and exposure to natural concentration, temperature, light, or physical gradients in the culture environment. As a result, PicoShell technology may provide a novel high-throughput screening tool that enables cell line developers and researchers to select cells based on their behavior in production-relevant environments, making it much more likely that selected populations will exhibit the desired phenotypic properties when scaled up for real-world applications.

Transport across PicoShells is likely responsible for distinct growth phenotypes for encapsulated cells compared to droplets in oil. Previous studies demonstrated that droplet size affects the division of cells in microfluidic droplets surrounded by oil³¹. Another recent study has

demonstrated that yeast cells cultured in large flasks, large droplets, and small droplets differed morphologically¹⁴. There may be several reasons for this phenomenon. For example, smaller droplets have less nutrients which could be depleted more rapidly when cells are placed within droplets and begin to grow and divide. Similar effects are expected with sealed nanowell arrays. With PicoShells, we have demonstrated that nutrients, such as the amino acid leucine, present in solution outside of the shell affects the growth and division of cells within (Figure B6). Based on this data, we conclude that leucine is able to transport across into the internal environment of the PicoShell, and we postulate other factors and nutrients will be able to transport as well. In addition, it is well understood that cells release elements to the external environment that change its pH. For example, CHO cells release lactate that lowers the pH of the external media³³ and yeast release alcohol that increases the pH of the external media³⁴. Charged species that modulate pH are expected to not easily transport out of droplets in oil or through solid barriers of nanowell arrays. Lastly, it is probable that proteins or other small molecules that are used for cell communication cannot pass through the walls of nanowell arrays or easily partition and transport through the oil phase of water-in-oil droplet emulsions. Since the outer shell of PicoShells are porous and have a molecular weight cutoff above 70kDa, it is likely that these factors can pass through the outer matrix. This is supported by our data demonstrating that the presence of cells in the external solution can affect the growth behavior of cells within the cavity of the PicoShells (Figure B4). In addition, inclusion of a solid surface of adherent cell lines to attach to in PicoShells likely enhances the growth properties of adherent CHO cells in PicoShells compared to in droplets. It is important to note that the lack of adherent CHO cell growth in droplets that we observed may have resulted from the lack of gas exchange through the mineral oil cap we placed on top of the droplets intended to reduce evaporation. However, we have demonstrated that *S. cerevisiae* do not have different

growth properties within droplets capped or not capped with mineral oil in Figure B10. In addition, a study has shown that most gases can diffuse through mineral oil³⁵. At the same time, it is possible that the mineral oil slows down the diffusion of relevant gases in a way that results in the lack of adherent CHO cell growth in droplets capped with mineral oil.

Growth of other algae species in droplets has been previously shown^{11,12, 36, 37}, making it intriguing why *Chlorella* in particular does not survive when encapsulated into water-in-oil droplet emulsions. While it is unclear exactly why this particular phenomenon occurs, we believe that the lack of cell survival is related to the restricted gas exchange across the oil barrier. This particular species is grown in autotrophic media and is very sensitive to gaseous CO₂ concentrations. We have observed that bulk cultures of this particular species cannot grow when not cultured in an incubator that regulates CO₂ or not cultured with media that is not supplemented with sodium bicarbonate³⁸. While previous studies have shown that gases can generally pass through fluorinated oil^{39, 40}, this diffusion may be limited or altered to an extent that sensitive species are greatly affected unlike more robust cell types (*Chlamydomonas reinhardtii*, *Euglena gracilis*, etc). Regardless of the root cause for the lack of growth in droplets, the results demonstrate that the environments in PicoShells and droplets are different enough that we can observe a noticeable effect on cell behavior, a result that is substantiated by the improved growth properties of *S. cerevisiae* in PicoShells.

2.3.2. Potential for chemically degradable PicoShells

We have explored multiple mechanisms to chemically release cells from PicoShells by including chemically-degradable motifs in the outer PEG shell. Currently, we can consistently fabricate PicoShells crosslinked with PEG-MAL and DTT. These are compatible with multiple

cell types, including *Chlorella*, *S. cerevisiae*, and *Euglena gracilis* (Figure B15). PicoShells crosslinked with PEG-MAL and DTT can be broken down with the addition of sodium periodate (NaIO_4) due to presence of a diol in DTT. Unfortunately, NaIO_4 can be toxic⁴¹ and likely kills or has large negative impacts on many cell types. Previously, we have made hydrogel particles with degradable peptide crosslinkers²⁰, and similar incorporation of degradable crosslinkers could enable enzymatic or chemical degradation of particles to release selected cells/colonies. As an initial proof of concept of this approach, we developed PicoShells that contain di-sulfide linkages that can be degraded via the addition of DTT or TCEP. *S. cerevisiae* encapsulated in these particles, remain viable, grow, and can be chemically released (Figure B16). Unfortunately, a chemical precursor we use to form these particles (4-arm PEG-Ortho-Pyridyldisulfide) is toxic to *Chlorella* (Figure B17), suggesting that the chemical formulation of the PicoShell should be matched to the cell type. We have also encapsulated and grown *Chlamydomonas reinhardtii* in PicoShells crosslinked with matrix-metalloprotease (MMP)-degradable-peptides (Figure S18) that can be degraded with the addition of trypsin. Unfortunately, *C. reinhardtii* (and likely other cell types) naturally secrete MMPs that often pre-maturely break down the particles⁴².

While the mechanical mechanism of release we demonstrate works well for releasing bulk populations of selected particles, it is likely difficult to adapt the process to separately release individual colonies (e.g. a single particle in a single well). Such single particle isolation is important if a researcher wishes to explore the different strategies for hyper-performance and the various underlying genetic mechanisms that result in such phenotypes. While it may be possible to engineer tools to mechanically break down a single particle, release of cells using these tools may be complicated and inefficient. In addition, there are studies that indicate shear stress can negatively impact cells. For example, while shear stress may not induce cell death, such stress on

microalgae or yeast may cause a decreased growth rate^{43,44}. Shear stress can even reduce the expression of a recombinant protein in CHO cells⁴⁵. Hence, it may be necessary to fully develop PicoShells that are chemically degradable and compatible with several cell types. Although we have engineered di-sulfide crosslinked PicoShells that are compatible for yeast applications, we have also shown that it is difficult to discover chemistries that enable chemical degradation and maintain cell viability for more sensitive cell types.

2.3.3. Limitations on throughput

We have also found that there is a tendency for crosslinked material to stick to the walls near the droplet generation junction, causing a disruption in the flow (Figure B19). Since we use pH-induced gelation and the gellable materials (PEG-MAL and DTT) come into close proximity briefly before droplet generation, gelled material often forms at the junction, inducing jetting and disruption of particle formation approximately 15 minutes after initial particle formation. As a result, the device needs to be replaced each time particle formation is halted, reducing the overall number of PicoShells that can be manufactured to 370,000 particles per device.

The jetting of reagents due to pre-mature formation of gelled material that sticks to the walls of the droplet generator limits the overall throughput of PicoShell generation. One potential way to address this is to use a co-axial device geometry to reduce the amount of gelled material that sticks to the walls of the device⁴⁶. Use of UV-induced crosslinking mechanisms can also address this problem since gelation would occur downstream of droplet generation^{29, 47, 48} unlike pH-induced mechanisms where mixing of reagents immediately prior to droplet generation often results in gelled material forming in the droplet-generation junction over time that disrupts the overall flow. UV-crosslinking could also enable PicoShell manufacturing approaches with higher

throughput⁴⁹. However, use of UV-induced crosslinking likely creates issues for particular cellular applications, as previously discussed. At the same time, UV-induced crosslinking may be used for workflows involving resilient cell types (e.g. bacteria) or workflows where cells are mutagenized prior to selection, and UV-induced mutations would be potentially beneficial. A summary of the different types of PicoShells that can we can currently fabricate and their advantages and disadvantages is shown in Table 2-1.

Table 2-1. Summary of Current PicoShell Variations.

	Fabrication throughput (PicoShells/hr)	Chemical release mechanism	Primary advantage	Primary disadvantage
DTT-crosslinked with UV	2.5 million	Sodium periodate	High fabrication throughput	Unclear how UV affects cells
DTT-crosslinked via pH	1.3 million	Sodium periodate	Compatible with most cell types	Limited to mechanical degradation to viably release cells
Peptide-crosslinked via pH	1.3 million	MMPs or Trypsin	Cells can be chemically released	Cells may pre- maturely release themselves via enzyme secretions
Disulfide- crosslinked via pH	1.3 million	MMPs or Trypsin	Cells can be chemically released	Only compatible with robust cell types such as bacteria and yeast

2.3.4. Potential future applications

Despite these solvable limitations, the experimental evidence we have presented shows that PicoShell technology has significant advantages. The workflow can be potentially used for directed evolution of cell populations⁵⁰ where mutagenized cells are placed under selection pressures to generate novel strains, based on unique selection criteria that are time-dependent (e.g. growth and production of pigments), at the colony level (multi-cellular construct formation), or require solution exchange steps (lipid staining, ELISA-based assays). For example, the technology may be used to produce microalgae strains that overperform in lipid accumulation rates without significantly reducing their rate of growth for biofuel applications. The technology may also be used to generate novel yeast strains that maintain high growth rate at higher ethanol concentrations, potentially enhancing the overall production of ethanol biofuels^{51,52}, plastics⁵³, materials⁵⁴, and alcoholic beverages⁵⁵.

Additionally, PicoShells have now enabled the ability to select single cells and/or clonal colonies based on their behavior in environments that have not been previously possible. For example, we have demonstrated that *S. cerevisiae* can grow in a bioreactor that has cells external to the PicoShells, with constant stirring, and temperature controls (Figure S20). Such a culture environment is not possible to achieve with other nanoliter-scale screening technologies, indicating the PicoShells may enable unique assays and applications that have previously been impossible. Given that PicoShells remain stable within our custom bioreactor and can be re-isolated, it is probable that PicoShells can be placed into other commercial bioreactors, outdoor cultivation farms, and other unique environments and later isolated for screening and/or selection.

The outer shell's PEG material is also able to be modified, enabling the technology to be potentially used for relevant mammalian cell applications. For example, affinity motifs such as antibodies and peptides can be added to the solid matrix that can capture cellular secretions²⁹. Antibody-conjugated PicoShells may be used to produce hyper-secreting and hyper-growing CHO cell populations based on their behavior in bioreactors for scaled production of protein therapeutics. The pore size of the particles may also be modulated by changing the MW of PEG used to crosslink the solid phase⁵⁶ or by including non-functionalized PEG⁵⁷, gelatin⁵⁸, or hyaluronic acid⁵⁹ in the PEG phase. Adherence motifs such as RGD peptides, fibronectin, or poly-L-lysine (PLL) may be also added to the outer PEG matrix so that stem cells, adherent CHO cells, or other adherent cell types have a solid surface to adhere to, further expanding the potential applications of the PicoShell workflow.

In summary, we have shown that PicoShells may enable cell line developers to develop novel cell populations based on their behavior in production environments. Unlike previously developed high-throughput screening tools, individual cells may be compartmentalized, placed into relevant environments such as bioreactors, exposed to natural stimuli, and selected based on their time-dependent behavior and growth in such environments via widely used flow cytometers. As a result, the technology has the exciting potential to rapidly accelerate the development of cell-derived bioproducts such as biodiesel, materials, cell-derived agriculture, nutrient supplements, and protein therapeutics.

2.4. Materials and Methods

2.4.1 Bulk culture of cells

Chlorella cells (CCMP1124 from National Center for Marine Algae and Microbiota) used in the study were provided by Synthetic Genomics, Inc. *Chlorella* populations were cultured in 500mL Erlenmeyer flasks containing seawater based medium with added vitamins, trace metals, nitrate, phosphate, and sodium bicarbonate (SM-NO₃ medium)⁶⁰. SM-NO₃ medium was also supplemented with penicillin-streptomycin (P/S, Thermo Fisher Scientific, 15140122). *Chlamydomonas reinhardtii* (STR CC-4568) and *Euglena gracilis* Z (NIES-48) procured from Microbial Culture Collection at National Institute for Environmental Studies (NIES) Japan were cultured in 500mL using Tris-acetate-phosphate medium⁶⁰ and Koren-Hunter (KH) medium at a pH of 5.5⁶² respectively. Flasks containing algae cultures were shaken continuously at 120RPM with constant 150 μ E light at room temperature. Algae cultures were kept at a concentration of 2-10 million cells/mL. Strains of *Saccharomyces Cerevisiae* were obtained from Sigma-Aldrich (STR YSC1). The yeasts were grown in yeast extract (1%, w/v) peptone (2%, w/v) glucose (2%, w/v) (YPD) media supplemented with 50mg/L ampicillin (Sigma-Aldrich, 69534). The strains were grown in 250 mL Erlenmeyer flasks containing 100 mL of YPD, under aerobic conditions at 30°C with agitation (300 rpm). Yeast cultures were kept at a concentration of 10-100 million cells/mL. Adherent CHO DP-12 cells (ATCC CRL-12445) were cultured in media containing DMEM (Invitrogen) supplemented with 10%FBS, 1% P/S, 0.002 mg/mL recombinant human insulin (Sigma), 0.1% Trace Elements A (Fisher Scientific), 0.1% Trace Elements B (Fisher Scientific), and 200nM Methotrexate (MTX, SIGMA). CHO DP-12 cells were also cultured in T75 flasks with vented caps that were placed into incubators at 37°C and 5% CO₂. CHODP12 cells

were passaged and diluted at a 1:20 ratio using 3mL 0.05% Trypsin-EDTA (Thermo Fisher Scientific) once cells reached 70-90% confluency within the flask (~every 3-4 days).

2.4.2. *PicoShell Fabrication*

Mechanically-degradable particles demonstrated throughout the majority of the study were fabricated forming uniform water-in-oil droplet emulsions containing in-droplet concentrations of 5% (w/w) 10kDa 4-arm PEG-maleimide (4-arm PEG-MAL, Laysan Bio), 11% (w/w) 10kDa dextran (Sigma Aldrich, D9260), and 1.54mg/mL dithiothreitol (DTT, Sigma Aldrich, 10197777001). Reagents were dissolved into SM-NO₃ medium, YB, TAP, or KH medium for the encapsulation of *Chlorella*, *S. cerevisiae*, *C. reinhardtii*, or *E. gracilis* respectively (each at a pH of 6.25). Novec™ 7500 Engineered fluid (3M™, 297730-92-9) with 0.5% Pico-Surf™ (Sphere Fluidics, C024) acting as surfactant was used as the continuous, oil phase. Droplet emulsions were formed using a 4-inlet microfluidic channel fabricated with polydimethylsiloxane (PDMS) using standard soft-lithography techniques⁶³. Reagents were loaded into separate syringes and pushed through the PDMS droplet generator using syringe pumps (Harvard Apparatus, MA, USA). In order to reduce the effects of functionalized PEG and crosslinker on cell growth during encapsulation in PicoShells, cells were suspended in the dextran phase such that the cells only interact with the PEG and DTT reagents for a short period of time. In-droplet concentrations of 3.25% (w/w) 20kDa 4-arm PEG Ortho-Pyridyldisulfide (4-arm PEG-OPSS, Creative PEGWorks, PSB-459), 10% (w/w) 10kDa dextran, and 0.80mg/mL DTT were used to form di-sulfide linked PicoShells. In-droplet concentrations of 5% (w/w) 10kDa 4-arm PEG-MAL, 11% (w/w) 10kDa dextran, and 14.1mg/mL di-cysteine modified Matrix Metallo-protease (MMP) (Ac-

GCRDGPQGIWGQDDRCG-NH₂) (Genscript) peptide substrate were used to form MMP-degradable PicoShells.

Following droplet generation, emulsions were stored at room temperature for 1h to allow PicoShells to fully solidify. The PicoShells were de-emulsified by adding Pico-Break™ (Sphere Fluidics, C081) at a 1:1 volume ratio on top of the PicoShells. Once Pico-Break had passed through all the PicoShells, the particles were transferred into aqueous solution (DPBS or cell media) containing 10μM N-ethylmaleimide (NEM, Sigma-Aldrich, E3876) at a pH of 6.5. The PicoShells were kept in NEM solution for 0.5h to allow NEM to react to any free thiols on the particles to reduce clumping. PicoShells were then passed through a 100μM cell strainer to remove any oversized or clumped particles and a 40μM cell strainer to remove any free cells or small debris before being transferred into cell media to be used for the particular assay.

2.4.3. *PicoShell versus droplet emulsion growth comparison*

Chlorella and *S. cerevisiae* from were separately encapsulated into mechanically-degradable PicoShells and microfluidically-generated droplets in oil of approximately the same volume (155pL) using the same droplet generator. PicoShells and droplets containing *Chlorella* were incubated in Eppendorf tubes with constant 150μE light at room temperature (no shaking). Compartments containing *S. cerevisiae* were incubated in Eppendorf tubes at 30°C (no shaking). Both PicoShells and droplets were not shaken since droplets tend to de-emulsify when shaken at speeds >100RPM. PicoShells and droplets were imaged using an inverted microscope in BF and Cy5 (ex: 620nm, em: 676nm) fluorescence at equal time intervals over a multi-day period to track the growth of cells in their respective compartments over time.

The same droplet generator design was used for both PicoShell fabrication and droplet generation for in-droplet growth assays (Figure B21). The devices were fabricated from polydimethylsiloxane (PDMS, Ellsworth Adhesives) with a 1:10 curing agent to base ratio that were plasma bonded to a glass microscope slide (VWR). Holes for the inlets were punched using a 1.5mm biopsy punch (Miltex®). Reagents were loaded into 1mL BD Luer-Lok syringes (Fisher Scientific) and were attached to the inlets of the device using flexible plastic tubing with a 0.02 in I.D. and 0.06 in O.D. (Tygon), 25Ga luer stubs (Fisher Scientific), and 0.02 in x 1/32 in PEEK™ tubing (to connect Tygon tubing to the luer stubs, IDEX Corporation). Syringes were loaded with the reagents required for PEG-MAL PicoShell generation in the appropriate media and at concentrations that generate in-droplet concentrations of PEG, dextran, and DTT detailed previously. Cells were placed into the dextran phase at a concentration of 2 million cells/mL. The dextran solution was connected into the middle bottom inlet (orientation based on Figure S21). DTT and PEG solutions were connected to the left and right inlets (these inlets are interchangeable). For droplet generation in oil, three syringes were all loaded with the appropriate cell media and the syringe connected to the middle bottom inlet was loaded with a cell concentration of 2 million cells/mL. For both PicoShell fabrication and droplet generation, Novec™ 7500 with 0.5% PicoSurf was loaded into a 5mL BD Luer-Lok syringe (Fisher Scientific) and connected to the top middle inlet the same way the 1mL syringes were connected. Reagents were injected into the device using 3 separate Standard Infuse/Withdraw PHD 22/2000 Syringe Pumps from Harvard Apparatus (PEG/DTT or media with cells were loaded onto the same syringe pump respectively). Cell containing solution for both PicoShell fabrication and droplet generation were injected into the device at a flow rate of 4μL/min. Aqueous solutions without cells (PEG/DTT solutions for PicoShell fabrication) were each injected at a flow rate of 2μL/min. Oil was injected into the device

at a flow rate of 40 μ L/min. PicoShells or droplets were flowed out to a 15mL conical tube using flexible plastic tubing with a 0.02 in I.D. and 0.06 in O.D. for collection. PicoShells were phase transferred using previously discussed methods.

PicoShells for *Chlorella* and *S. cerevisiae* growth experiments were placed into 4 mL of their respective medias at a concentration of 100,000 PicoShells/mL within a 5 mL Eppendorf Tubes (Fisher Scientific). Rather than using the standard caps to seal each tube, the caps were removed and the top was sealed using a cut piece of sterile KimwipesTM (Fisher Scientific). This enables a seal of the tube while still allowing gas exchange. The tubes were placed into an incubator with the appropriate temperature and lighting conditions for each cell type that were detailed in the “Bulk Culture of Cells” section.

PicoShells for CHODP12 growth experiments were placed into 8 mL of CHODP12 culture media (detailed previously) at a concentration of 100,000 PicoShells/mL within a T25 cell culture flask with vented cap (Fisher Scientific). The PicoShell-containing flask was placed into an incubator with the appropriate culture conditions detailed earlier (temperature, humidity, etc).

For all cell types, cell-containing 500 μ L volumes of droplets were placed into a 5 mL Eppendorf tube with 2.5 mL Novec 7500TM with 0.5% PicoSurf (1:5 ratio of droplets to oil). Droplets containing adherent CHO cells were covered with 1 mL of light mineral oil (Sigma Aldrich) to reduce evaporation of droplets within an incubator at 37°C. Mineral oil was not used for *Chlorella sp.* and *S. cerevisiae* droplet vs. PicoShells growth comparison studies. However, we also made a separate sample of *S. cerevisiae* containing droplets that was capped with mineral oil so that we can observe potential effects that covering droplets with mineral has on the growth of encapsulated cells. Multiple studies have covered cell-containing droplets to reduce evaporation^{64, 65}. The Caps of each tube were removed and the top was sealed using a cut piece of sterile KimwipesTM (Fisher

Scientific). Each tube was placed in an incubator with the appropriate culture conditions for each cell type.

A MATLAB code was used to count cells in PicoShells and droplets throughout the study. MATLAB's FindCircles function was used to find PicoShells/droplets in the brightfield channel (referred to here as 'compartment region'). A fluorescence overlay of the images was used to find the cells (Cy5 for microalgae and FITC for yeast) within each of these compartment regions and the area for each cell cluster was obtained using blob analysis. The number of cells was calculated by taking the area of each blob and dividing it by the 2D area of each cell within the compartment region. For later timepoints, the cell cluster became thick enough where a simple area calculation for each blob did not give the actual number of cells. To solve this, a secondary blob analysis was done on these high-density areas and this added volume of cells was approximated to be a total of 2 times the amount of the low density areas. This approximation was visually verified by testing the code on specific counted particles. Since CHODP12 cells do not provide a natural autofluorescence, these samples were counted manually. Several test clusters were used to verify that the number of cells computed by the code was not significantly different ($P > 0.05$) compared to visual counting (Figure S22).

2.4.4. Staining of Intracellular Lipids

Following a 48h culture of *Chlorella* in PicoShells, intracellular lipids were stained with BODIPY^{505/515}. Stock BODIPY^{505/515} was prepared by dissolving 4, -Difluoro-1,3,5,7-Tetramethyl-4-Bora-3a,4a-Diaza-s-Indacene (Life Technologies, D3921) powder into dimethyl sulfoxide (DMSO) at a concentration of 2.5mg/mL and then diluted to 2.5 μ g/mL using SM-NO3 media. Colony-containing PicoShells were placed at a concentration of 2×10^6 particles/mL in SM-NO3

media before being mixed at a volume ratio of 1:1 with 2.5 μ g/mL BODIPY^{505/515} and incubated in the dark for 0.5h. The PicoShells were washed three times with SM-NO₃ before being imaged in the FITC channel (ex: 488nm /em: 543nm) using a fluorescence microscope.

2.4.5. *Incubation and flow cytometric sorting of PicoShells*

Chlorella were encapsulated into 90 μ m diameter PicoShells following Poisson loading with $\lambda = 0.1$ for the initial sort and $\lambda = 0.05$ for the full selection and placed into SM-NO₃ medium at a particle to media volume ratio of 1:50. The particle-containing solution was then placed in a 250mL Erlenmeyer flask shaking at 120RPM and at room temperature under constant 150 μ E light for 48h to allow cells to divide.

Colony-containing PicoShells were screened and sorted using an On-Chip Sort (On Chip Biotechnologies, USA). The cytometer was equipped with both 488nm and 561nm excitation lasers and a PE-Cy5 (676/37nm) filter. Events were triggered based on particle absorbance from the 488nm laser. PicoShells were sorted based on their scatter readouts and thresholding desired intensity heights through the PE-Cy5 filter. PicoShell solutions were concentrated in fresh SM-NO₃ media at a 1:10 particle to media volume ratio for screening and sorting. PicoShells within the selection gates were dispensed in a single collection reservoir. The sorted particles were then imaged using an inverted microscope and the number of cells in each particle was counted using MATLAB code.

2.4.6. *Release of cells and re-culture of selected populations*

Post-selection, *Chlorella*-containing PicoShells were placed onto a 37 μ m cell strainer and placed over a 15mL conical tube containing fresh SM-NO₃ media supplemented with P/S. The

PicoShells were then ruptured by ‘grinding’ the particles with a pestle and washing with SM-NO₃ media for ~5min, causing released cells to fall through the pores of the cell strainer and into the fresh media. Despite being able to be ruptured by direct mechanical shearing pressure, PicoShells remain stable in adverse indirect mechanical shearing pressures such as mixing, vigorous pipetting, and vortexing. The solution containing released cells was then transferred into a 250mL Erlenmeyer flask and put in standard bulk *Chlorella* culture conditions for 7 days to allow released cells re-grow to a concentration of 15-20 million cells/mL.

To test for maintenance of an enhanced growth phenotypes in the selected population, we seeded the selected population and an un-selected population into separate 250mL Erlenmeyer flasks with SM-NO₃ media supplemented with P/S at a concentration of 500,000 cells/mL. The flasks were placed side-by-side under standard *Chlorella* culturing conditions for 4 days. The cell concentration was measured using a hemocytometer every 12h. At 48h of growth, we also measured growth by aliquoting several fractions from the selected and un-selected sample into a well plate and measured the chlorophyll density (ex: 620nm, em: 676nm) using a well plate reader at this time point.

2.4.7. *Chemically-induced degradation of PicoShells*

To chemically degrade the various types of PicoShells, we first diluted or concentrated PicoShells to a concentration of 1×10^6 particles/mL and added the following reagents at the indicated final concentration to degrade each PicoShell type: 10 μ g/mL sodium periodate (NaIO₄, Fisher Scientific, P120504) for particles crosslinked with 4-arm PEG-MAL and DTT, 10mg/mL DTT or 3mg/mL Tris(2-carboxyethyl)phosphine (TCEP, Sigma-Aldrich, 646547) for particles

crosslinked with 4-arm PEG-OPSS and DTT, and 0.0025% Trypsin with EDTA (Thermo Fisher Scientific, 25300120) for particles crosslinked with 4-arm PEG-MAL and di-cysteine modified MMP degradable peptide.

2.4.8. *Environmental effects studies*

To test the effects of the presence of leucine in the external solution on encapsulated cell behavior, we first encapsulated *cdc3-mcherry::leu2 S. cerevisiae* strains with an average loading lambda of 0.1 into PEG-MAL PicoShells using methods previously detailed. Half the sample was then placed into yeast media without any leucine at a concentration of 50,000 PicoShells/mL and the other half of the sample was placed into yeast media supplemented with 76 mg/L leucine. The samples were allowed to incubate in their respective medias within 5mL Eppendorf tubes at 30°C for 12h. After the incubation period, each sample was imaged and the number of cells within each PicoShell were counted visually.

To test the effects of the presence of cells in the external solution on encapsulated cell behavior, we first encapsulated *cdc3-mcherry::leu2 S. cerevisiae* strains with an average loading lambda of 0.1 into PEG-MAL PicoShells using methods previously detailed. Half the sample was then placed into yeast media without any cells at a concentration of 50,000 PicoShells/mL and the other half of the sample was placed into yeast media containing *cdc3-mcherry::leu2 S. cerevisiae* at a concentration of 100 million cells/mL in stationary phase. The cell-containing media was prepared by pelleting a culture of cells and re-suspending into fresh media within 5 minutes of mixing with PicoShells to make sure that the nutrients were fully replenished. The samples were allowed to incubate in their respective medias within 5mL Eppendorf tubes at 30°C for 12h. After the incubation period, PicoShells incubated in the media with external cells were isolated from this

external population by running the sample through a CellTrichs® 20 µm cell strainer (Fisher Scientific). Once PicoShells were isolated, the samples were imaged and the number of cells within each PicoShell were counted visually.

To test the possibility of PicoShells being incubated in a bioreactor, we made a custom chamber with an autoclaved 100mL glass beaker sealed with a rubber stopper with 2 holes (United States Plastic Corp). Two 6 in long 3 mm I.D. x 5 mm O.D. x 1 mm Wall excelon laboratory metric tubing (United States Plastic Corp) were inserted into the two holes to allow gas to be exchanged with the external environment. The ends of the tubes outside of the beaker were sealed with sterile Kimwipes™ so that the environment can remain sterile while still allowing for gas exchange. The beaker was placed onto a hot plate set at 30°C and contained a magnetic stir bar that rotated at 50 RPM. The beaker also contained 80mL of yeast broth containing *cdc3-mcherry::leu2 S. cerevisiae* at a concentration of 2 million cells/mL at the start of the PicoShell incubation. *cdc3-mcherry::leu2 S. cerevisiae* yeast were encapsulated into PEG-MAL PicoShells with an average loading lambda of 0.1 using previously detailed methods and placed into the homemade bioreactor at a concentration of 50,000 PicoShells/mL for 12h. PicoShells were isolated from the un-encapsulated cells by running the entire solution through a pluriSelect® 20 µm cell strainer 3 times. The isolated PicoShells were imaged and the cells in each PicoShell were visually counted.

2.5 References

1. Hood E. Plant-based biofuels. *F1000 Research* **185**, (2016).
2. Chisti Y. Biodiesel from microalgae. *Biotechnol Adv.* **25**, 294-306 (2008).
3. Sheehan J., Dunahay T., Benemann J., & Roessler P. Look Back at US Department of Energy's Aquatic Species Program – Biodisel from Algae (1998).
4. Dismukes, G. C. et al. Aquatic phototrophs: efficient alternatives to land-based crops for biofuels. *Curr. Opin. Biotechnol.* **19**, 235–240 (2008).
5. Radakovits R. et al. Genetic Engineering of Algae for Enhanced Biofuel Production. *Amer. Society For Microbio.* **9**, 486-501 (2010).
6. Khan M., Shin J., & Kim J. The promising future of microalgae: current status, challenges, and optimization of a sustainable and renewable industry for biofuels, feed, and other products. *Microb Cell Fact.* **17**, (2018).
7. Chen M., Mertiri T., Holland T., & Basu A. Optical microplates for high-throughput screening of photosynthesis in lipid-producing algae. *Lab on a Chip.* **20**, (2012).
8. Lindstrom S. & Andersson-Svahn H. Single cell culture in microwells. *Methods Mol Biol.* **853**, 41-52 (2012).
9. Chen B. et al. High-throughput analysis and protein engineering using microcapillary arrays. *Nat Chem Biol.* **12**, 76-81 (2016).
10. Lu H. et al. High-throughput of single cell counting in droplet-based microfluidics. *Sci Rep.* **7**, 1366 (2017).
11. Kim H., et al. High-throughput droplet microfluidics screening platform for fast-growing and high lipid-producing microalgae from a mutant library. *Plant Direct.* **27**, (2017).

12. Li M., et al. A Gelatin Microdroplet Platform for High-Throughput Sorting of Hyperproducing Single-Cell-Derived Microalgal Clones. *Small*. **14**, (2018).
13. Eun Y. et al. Encapsulating Bacteria in Agarose Microparticles Using Microfluidics for High-Throughput Cell Analysis and Isolation. *ACS Chem. Biol.* **6**, 260-266 (2011).
14. Nakagawa Y., et al. Are droplets really suitable for single-cell analysis? A case study on yeast in droplets. *Lab on a Chip*. (2021).
15. Mocciano A., et al. Light-activated cell identification and sorting (LACIS) for selection of edited clones on a nanofluidic device. *Commun Biol.* **3**, (2018).
16. Munoz H, et al. Fractal LAMP: Label-free analysis of fractal precipitate for digital loop-mediated isothermal nucleic acid amplification. *ACS Sensors*. **5**, 385-394 (2020).
17. de Rutte J., Koh J. & Di Carlo D. Scalable high-throughput production of modular microgels for in situ assembly of microporous tissue scaffolds. *Adv. Funct. Mat.* (2019).
18. Kahkeshani S. & Di Carlo D. Drop formation using ferrofluids driven magnetically in a step emulsification device. *Lab on a Chip*. **13**, (2016).
19. Hatti-Kaul R. Aqueous two-phase systems. *Mol. Biotech.* **19**, 269-277 (2001).
20. Asenjo tJ. & Andrews B. Aqueous two-phase systems for protein separation: Phase separation and applications. *Jour. Of Chroma.* **123**, 1-10 (2012).
21. Griffin D., Weaver W., Scumpia P., and Di Carlo D. Accelerated wound healing by injectable microporous gel scaffolds assembled from annealed building blocks. *Nat. Mater.* **14**, 737-744 (2015).
22. Vijawakumar K., Gulati S., deMello A., and Edel J. Rapid cell extraction in aqueous two-phase microdroplet systems. *Chem. Sci.* **4**, (2010).

23. Yasukawa M., Kamio E., & Ono T. Monodisperse water-in-water-in-oil emulsion droplets, Yasukawa. *Chem. Phys. Chem.* **12**, (2011).
24. Ma S., et al. Fabrication of microgel particles with complex shape via selective polymerization of aqueous two-phase systems. *Small* **8**, (2012).
25. Liu Q. et al. Self-orienting hydrogel micro-buckets as novel cell carriers. *Angew. Chem. Intern. Edit.* **58**, (2018).
26. Watanabe T. Motohiro I. & Ono T. Microfluidic Formation of Hydrogel Microcapsules with a Single Aqueous Core by Spontaneous Cross-Linking in Aqueous Two-Phase System Droplets. *Langmuir* **35**, 2358-2367 (2019).
27. Leonaviciene G. Leonavicius K., Meskys R., & Mazutis L. Multi-step processing of single cells using semi-permeable capsules. *Lab on a Chip.* **21**, (2020).
28. de Rutte J., Dimatteo R., van Zee M., & Di Carlo D. Massively parallel encapsulation of single cells with structured microparticles and section-based flow sorting. *bioRxiv* (2020).
29. McMillan T., Leatherman E., Ridley A., Shorrocks J., Tobi S.E., & Whiteside J.R. Cellular effects of long wavelength UV light (UVA) in mammalian cells. *J. Pharma. and Pharmaco.* **60**, (2010).
30. Phelps E., et al. Maleimide Cross-Linked Bioactive PEG Hydrogel Exhibits Improved Reaction Kinetics and Cross-Linking for Cell Encapsulation and In Situ Delivery. *Adv. Mat.* **24**, (2011).
31. Sprague Jr. G. & Winans S. Eukaryotes learn how to count: quorum sensing by yeast. *Genes and Dev.* **20**, 1045-1049 (2006).

32. Periyannan Rajeswari P.K., Joensson H.N., & Andersson-Svahn H. Droplet size influences division of mammalian cell factories in droplet microfluidic cultivation. *Electrophoresis*. **38**(2), 305-310 (2017)
33. Dean J. & Reddy P. Metabolic analysis of antibody producing CHO cells in fed-batch production. *Biotech. And Bioeng.* **110**(6), 1735-1747 (2013).
34. Casey G., Magnus C., & Ingledew W.M. High-Gravity Brewing: Effects of Nutrition on Yeast Composition, Fermentative Ability, and Alcohol Production. *Appl. and Environ. Microbio.* **48**(3), 639-646 (1984).
35. Ye W., Hao J., Chen Y., Zhu M., Pan Z., & Hou F. Difference Analysis of Gas Molecules Diffusion Behavior in Natural Ester and Mineral Oil Based on Molecular Dynamic Simulation. *Molecules*. **24**(24). 4463 (2019).
36. Carruthers D., Chang B. Cardinale B., & Lin X. Demonstration of transgressive overyielding of algal mixed cultures in microdroplets. *Integrative Biology* **9**, 687-694 (2017).
37. Best R., et al. Label-Free Analysis and Sorting of Microalgae and Cyanobacteria in Microdroplets by Intrinsic Chlorophyll Fluorescence for the Identification of Fast Growing Strains. *Anal. Chem.* **88**, 10445-10451 (2016).
38. Barahoei M., Hatamipour S., & Afsharzadeh S. CO₂ capturing by *chlorella vulgaris* in a bubble column photo-bioreactor; Effect of bubble size on CO₂ removal and growth rate. *J. of CO₂ Utiliz.* **37**, 9-19 (2020).
39. Gruner P., et al. Stabilisers for water-in-fluorinated oil dispersions: Key properties for microfluidic applications. *Curr. Opin. In Colloid & Inter. Sci.* **20**, 183-191 (2015).

40. Hamza M., Serratrice G., Stebe M., and Delpuech J. Solute-solvent interactions in perfluorocarbon solutions of oxygen. An NMR study. *J. Am. Chem. Soc.* **103**, 3733-3738 (1981).
41. Lent E., Crouse L., & Eck W. Acute and subacute oral toxicity of periodate salts in rats. *Reg. Toxic. and Pharm.* **83**, 23-27 (2017).
42. Luxmi R. et al. Proteases Shape the *Chlamydomonas* Secretome: Comparison to Classical Neuropeptide Processing Machinery. *Proteomes* **6**, 36 (2018).
43. Wang C. & Lan C. Effects of shear stress on microalgae. *Biotechnol. Adv.* **36**(4), 986-1002 (2018).
44. Stafford R.A. Yeast Physical (Shear) Stress: The Engineering Perspective. *Brew. Yeast Ferm. Perform.* **4** (2003).
45. Keane J., Ryan D., & Gray P. Effect of shear stress on expression of a recombinant protein by Chinese hamster ovary cells. *Biotechnol. Bioeng.* **81**(2), 2011-220 (2003).
46. Morimoto Y., Tan W.H., & Takeuchi S. Three-dimensional axisymmetric flow-focusing device using stereolithography. *Biomedical Microdevices.* **11**, 369-377 (2009).
47. Destgeer G., Ouyang M., Wu C.Y., Di Carlo D. Fabrication of 3D concentric amphiphilic microparticles to form uniform nanoliter reaction volumes for amplified affinity assays. *Lab on a Chip.* **19**, (2020).
48. Wu C.Y., et al. Monodisperse drops templated by 3D-structured microparticles. **6**, (2020).
49. Lee S., de Rutte J., Dimatteo R., Koo D., & Di Carlo D. Scalable Fabrication of 3D Structured Microparticles Using Induced Phase Separation. *bioRxiv* (2021).
50. Di Carlo D. Technologies for the Directed Evolution of Cell Therapies. *SLAS Tech.* (2019).

51. Zhou Y., et al. Production of fatty-acid derived oleochemicals and biofuels by synthetic yeast cell factories. *Nat. Commun.* **7**, (2016).
52. Petrovic U. Next-generation biofuels: a new challenge for yeast. *Yeast* (2015).
53. Lu W., et al. Biosynthesis of Monomers for Plastics from Renewable Oils. *J. Am. Chem. Soc.* **132**, 15451-15455 (2010).
54. Shen W., et al. Yeast-based microporous carbon materials for carbon dioxide capture. *Chem. Sus. Shem.* **5**, (2012).
55. Lodolo E., Kock J., Axcell B., & Brooks M. The yeast *Saccharomyces cerevisiae* – the main character in beer brewing. *FEMS Yeast Res.* **8**, 1018-1036 (2008).
56. Gorman, D.S. & R.P. Levine, Cytochrome f and plastocyanin: their sequence in the photosynthetic electron transport chain of *Chlamydomonas reinhardi*. *PNAS* **54**, 1665-1669 (1965).
57. Luo Y., Yang F., Li C., Wang F., Zhu H., & Guo Y. Effect of the molecular weight of polymer and diluent on the performance of hydrophilic poly(vinyl butyral) porous heddle via thermally induced phase separation. *Mat. Chem. and Phys.* **261** (2021).
58. Pregibon D. and Doyle P. Optimization of Encoded Hydrogel Particles for Nucleic Acid Quantification. *Analytical Chemistry* **81** 4873-4881 (2009).
59. Witte R., Blake A., Palmer C., and Kao W. Analysis of poly(ethylene glycol)-diacrylate macromer polymerization within a multicomponent semi-interpenetrating polymer network system. *Journal of Biomedical Materials Research* **71** 508-518 (2004).
60. Broguiere N., Husch A., Palazzolo G., Bradke F., Madduri S., and Zenobi-Wong M. Macroporous hydrogels derived from aqueous dynamic phase separation. *Biomaterials* **200** 56-65 (2019).

61. Verruto J., et al. Unrestrained markerless trait stacking in *Nannochloropsis gaditana* through combined gene editing and marker recycling technologies. *PNAS* **115**, 7015-7022 (2017).
62. Koren L.E. High-yield media for photosynthesizing *Euglena gracilis*. *J. Eukar. Microbio.* **14**, 17 (1967).
63. Qin, D., Xia, Y. & Whitesides, G.M. Soft lithography for micro- and nanoscale patterning. *Nat. Protocols.* **5**, 491-502 (2010).
64. Isozaki A., et al. Sequentially addressable dielectrophoretic array for high-throughput sorting of large-volume biological compartments. *Sci. Adv.* **6**(22), (2020).
65. Langer K. & Joesnsson H. Rapid production and recovery of cell spheroids by automated droplet microfluidics. *bioRxiv.* (2019).

Chapter 3. Retention of released cell materials and future directions

3.1 Optimizing PicoShell pore size to retain protein and genetic material

Many cells used in fermentation during scale up of biomaterials are designed to secrete the desired bioproduct, therefore it is necessary to optimize the PicoShell workflow to enable selection based on cell secretions. Since the outer shell is composed of PEG, it is possible to conjugate capture groups to the outer shell matrix using commonly used methods¹. Unfortunately, ~80% of the possible conjugation sites are taken up by crosslinker. So, while conjugating capture sites to the outer shell matrix may work for short term secretion studies (<12h), it will be difficult to use this method for production studies where the cells are expected to multiply over a multi-day period.

So, we thought the best strategy to try and retain secretions it to optimize the pore size such that the secretion of interest can be retained within the PicoShell while also large enough such that fluorescent labels can diffuse into the inner cavity. To accomplish this, we can change the molecular weight and the number of arms on the PEG used to make the outer shell (Figure 3-1). We tested this by encapsulating *Escherichia coli* protein lysate into PicoShells fabricated with various types of PEG-maleimide, allowing protein to leak out of the shells overnight, washing, breaking down the shells to release the retained proteins, and running the released proteins on an SDS-PAGE gel. We found that all proteins under 200kDa leaked out of PicoShells fabricated with 20kDa and 10kDa 4-arm PEG-MAL. PicoShells fabricated with 5kDa 4-arm and 10kDa 8-arm PEG-MAL had a protein molecular weight cutoff (MWCO) between 15 and 20kDa. PicoShells fabricated with 5kDa 8-arm PEG-MAL had a MWCO below 10kDa.

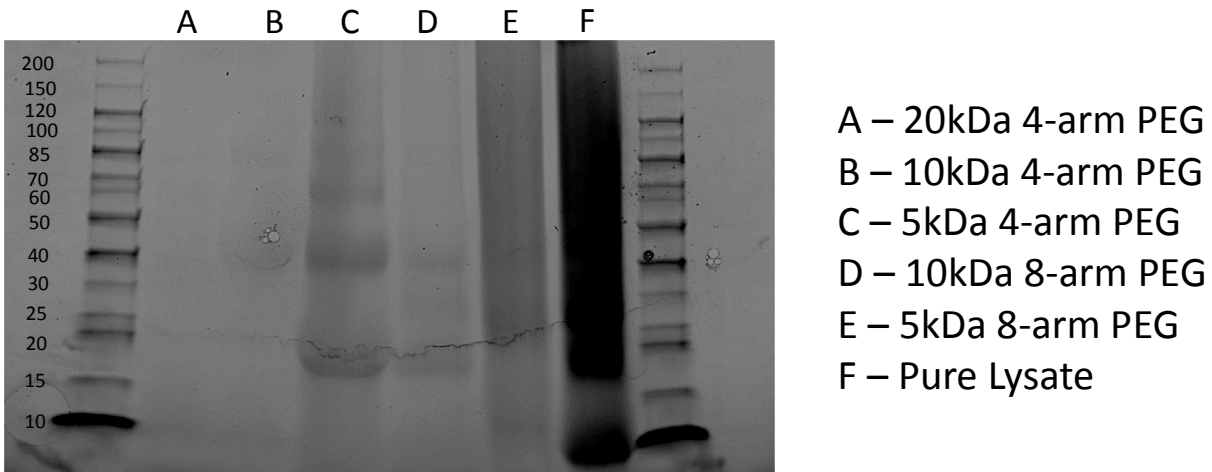


Figure 3-1. Protein MWCO of PicoShells. We were able to obtain a protein MWCO above 200kDa when using 20kDa 4-arm PEG to fabricate PicoShells. We were also able to obtain a protein MWCO as low as 10kDa when using 5kDa 8-arm PEG.

The discovered range of MWCO's is well suited to retain many relevant proteins as they tend to range between 40 and 150kDa. However, it may be challenging to have larger fluorescent labels diffuse into the cavity of the PicoShell if needed. Previous research has shown that the pore size can be fine-tuned by including porogens in the PEG phase^{2,3,4}. Additionally, the size of the secreted proteins can be increased by attaching large, non-functional protein groups to the protein of interest such that we obtain a size difference between the target protein and the fluorescent label that makes it compatible with the system.

We also characterized the DNA MWCO of PicoShells fabricated with varying types of PEG-MAL (Figure 3-2). This may be useful if an engineer wishes to lyse encapsulated cells post-sort and perform PCR or other genetic manipulation within the PicoShell. This may also be useful for protein directed evolution approaches where colonies of transformed bacteria or yeast producing a protein of interest are lysed within the PicoShell, exposed to a fluorescent label or stimulus, and sorted based on the protein's fluorescence and/or response. To test this, we encapsulated DNA ladder into PicoShells with varying types of PEG-MAL, allowed DNA to leak

out of the PicoShells for 24h, washed, broke down the PicoShells to release retained DNA, and ran the retained DNA through gel electrophoresis. We found that the DNA MWCO of PicoShells made with 20kDa 4-arm PEG was 300bp, 10kDa and 5kDa 4-arm PEG was 200bp, and 10kDa 8-arm and 5kDa 8-arm PEG was below 100bp.

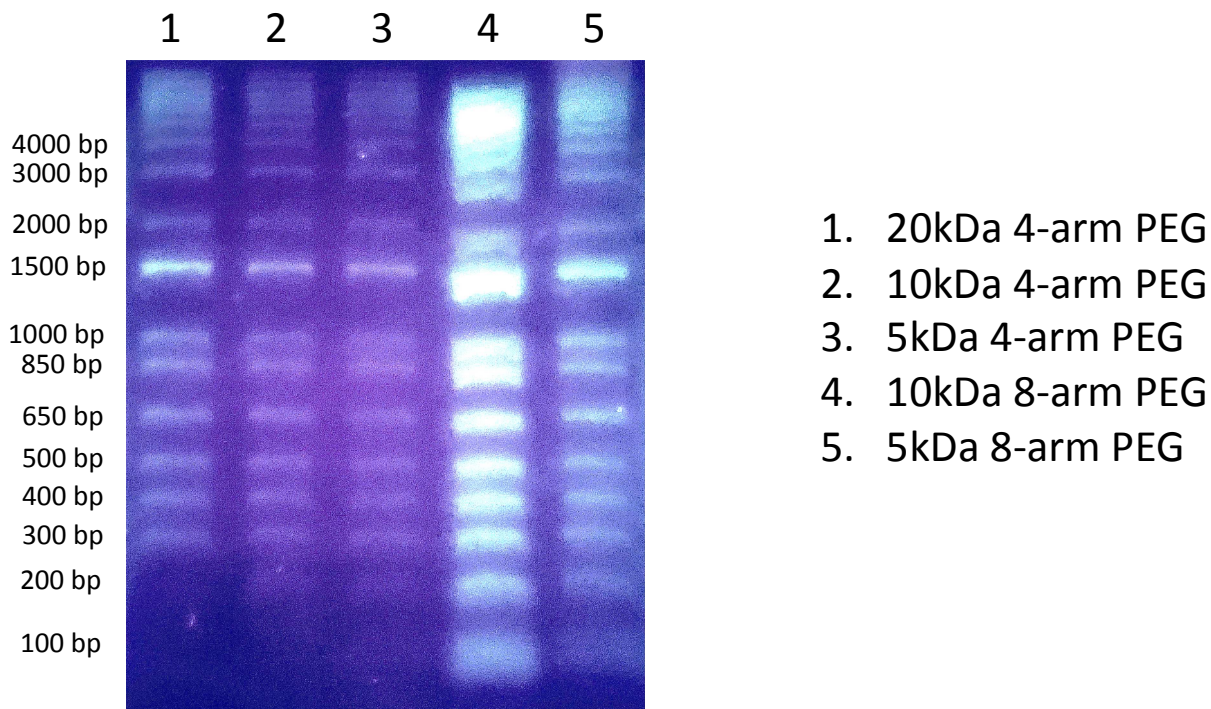


Figure 3-2. DNA MWCO of PicoShells. We were able to obtain a cutoff between 200 and 300 bp when using 20kDa 4-arm PEG to fabricate PicoShells. We were also able to obtain a cutoff as low as 100 bp when using 5kDa 8-arm PEG.

3.2. Protein engineering using PicoShells

3.2.1. Introduction

Various types of proteins (antibodies, enzymes, etc) have recently demonstrated many demonstrated and potential use cases such as therapeutic applications⁵, sustainable infrastructure development⁶, and biosensor use cases⁷. Over the past couple decades, scientists have developed

tools that enable our understanding and manipulation of proteins for desired applications. This includes sequencing and gene editing technologies that allow us to make targeted changes to amino acid sequences⁸. This also include computational methods that allow us to understand how these proteins fold and interact with other molecules⁹. Typically, functionality (i.e. enzymatic activity, binding, reactivity) is improved by directed evolution workflows¹⁰. In these workflows, random mutations are introduced into the protein sequences of a protein library, which is placed under selection pressures and screening processes that result in the isolation of variants with desired phenotypes¹¹. These isolated variants are then sequenced such that scientists can understand the changes that resulted in improved functionality and/or run through the mutagenesis/selection workflow in aim to further improve functionality.

While current directed evolution workflows have been widely successful and have resulted in many industrially-used proteins¹², the current screening techniques have several limitations that need to be improved upon. Traditionally, cell libraries that have been transformed or transfected with gene variants of the desired protein are placed into microtiter plates, grown into clonal colonies, and lysed to release proteins that either bind to a surface or induce some catalytic activity that can be recognized (e.g. ELISA)¹³. DNA within the wells of the clonal colonies of interest is then amplified (typically via PCR) and sequenced for further downstream processing. While relatively effective, this method has a very low throughput even when sped up with robotic liquid handling systems (~10,000 variants per screen)¹⁴. This is non-ideal because researchers cannot explore the full sequence space (typically 10-100 million variants), making it unlikely for scientists to pick out the variant that produces the best possible results. To increase the total number of variants that can be screened in a single assay, researchers can have the desired proteins retained within the cell and labeled with or result in the presence of a fluorescent marker such that the

variants can be sorted via high-throughput fluorescent activated cell sorters (FACS) [ref]. While such methods can achieve very high throughputs (>1 million cells per screen), applications where the fluorescent marker can pass through the cell membrane are very limited. More recently, scientists have developed mechanisms to have the desired proteins displayed on the outer surface of a yeast^{15, 16}, bacteria¹⁷ or mammalian cell¹⁸. As a result, fluorescent markers can directly interact to the extracellularly via binding or catalytic activity and the cell library can be sorted via FACS. The desired protein can also be displayed on the surface of a phage¹⁹ or ribosome²⁰ and washed over a surface that results in the selective binding of desired variants. Such methods have throughputs of >10 million variants per screen and can be used for a large number of protein evolution applications. Unfortunately, the protein folding and/or structure are oftentimes different than when the proteins are free floating in solution²¹. There are also often different charge and steric interactions that occur with display techniques²². As a result, selected phenotype is often not maintained when translated to its final product.

To the issues with protein directed evolution, we propose a novel protein screening workflow involving PicoShells (Figure 3-3). These microparticles are 40-60 μm in diameter, have a hollow inner cavity where cells can be encapsulated, and a porous outer shell that can be modulated to retain proteins via size exclusion. We propose that individual cells transformed or transfected with a gene encoding for a protein of interest are encapsulated into PicoShells, incubated to form clonal colonies, lysed to release proteins and DNA that are retained within the PicoShells, exposed to fluorescent markers or catalytic substrates, sorted via FACS, and released by breaking down the PicoShell for PCR and additional downstream processing. Since cells can be encapsulated at a rate of 200-300 cell/s and sorted at a rate of 10-100 cells/s, the PicoShell workflow enables a throughput of >1 million variants per screen. In addition, the protein variants

are selected based on their phenotypic properties in a free-floating environment and natural morphology. A similar workflow using water-in-oil droplet emulsions are limited in scope since fluorescent markers cannot pass through the aqueous-oil barrier²³. Therefore, assays are limited to selecting based on catalytic activity²⁴ or those involving FRET mechanisms²⁵. Another similar workflow where cells are encapsulated into agarose²⁶, alginate²⁷, or gelatin²⁸ hydrogels are also limiting because the pore size cannot be made small enough to retain released proteins and DNA. While it is possible to include capture sites to the hydrogel matrix^{29, 30, 31}, it is challenging to find capture proteins specific to every target and such a mechanism to retain proteins will result in the localization of signal, negatively affecting fluorescent readouts. Additionally, the hydrogel matrix presents a non-natural environment that may affect protein behavior properties via material- or charge-interactions³². Poly-ethylene glycol (PEG) can be used to obtain pore sizes as small as 10kDa (Figure 3-1). Therefore, PicoShells with a shell composed of PEG are capable of retaining the majority of proteins via size exclusion, eliminating the need to add capture sites. Solid, non-hollow PEG particles are capable of such a protein retention mechanism. However, such PEG particles are often too stiff for cells to grow and a single cell (particularly *E. coli*) is unlikely to release enough protein that can be recognized via FACS. Also, the signal is likely to be highly localized, affecting readouts. The hollow-inner cavity of PicoShells allows for cell growth, a volume where the released protein can be evenly distributed, and an environment where there are no un-desired interactions with the hydrogel material.

Therefore, we propose that PicoShells can be used as a novel protein evolution platform that has unique advantages over previously developed workflows. To test this, we applied the workflow to evolve calcium-specific protein biosensors (GCaMP) that are a synthetic fusion of green fluorescent protein (GFP), calmodulin (CaM), and M13 and produces an GFP fluorescence

when exposed to Ca^{2+} . In particular, we formed a clonal population of *E. coli* transformed with pBAD-GCaMP8f, encapsulated individual cells into PicoShells, lysed to release proteins that are retained within the PicoShell via size exclusion, and exposed to Ca^{2+} . We propose that the GCaMP-containing PicoShells that produce the highest fluorescent readouts are sorted and broken down to release DNA that can be amplified via PCR and sequenced.

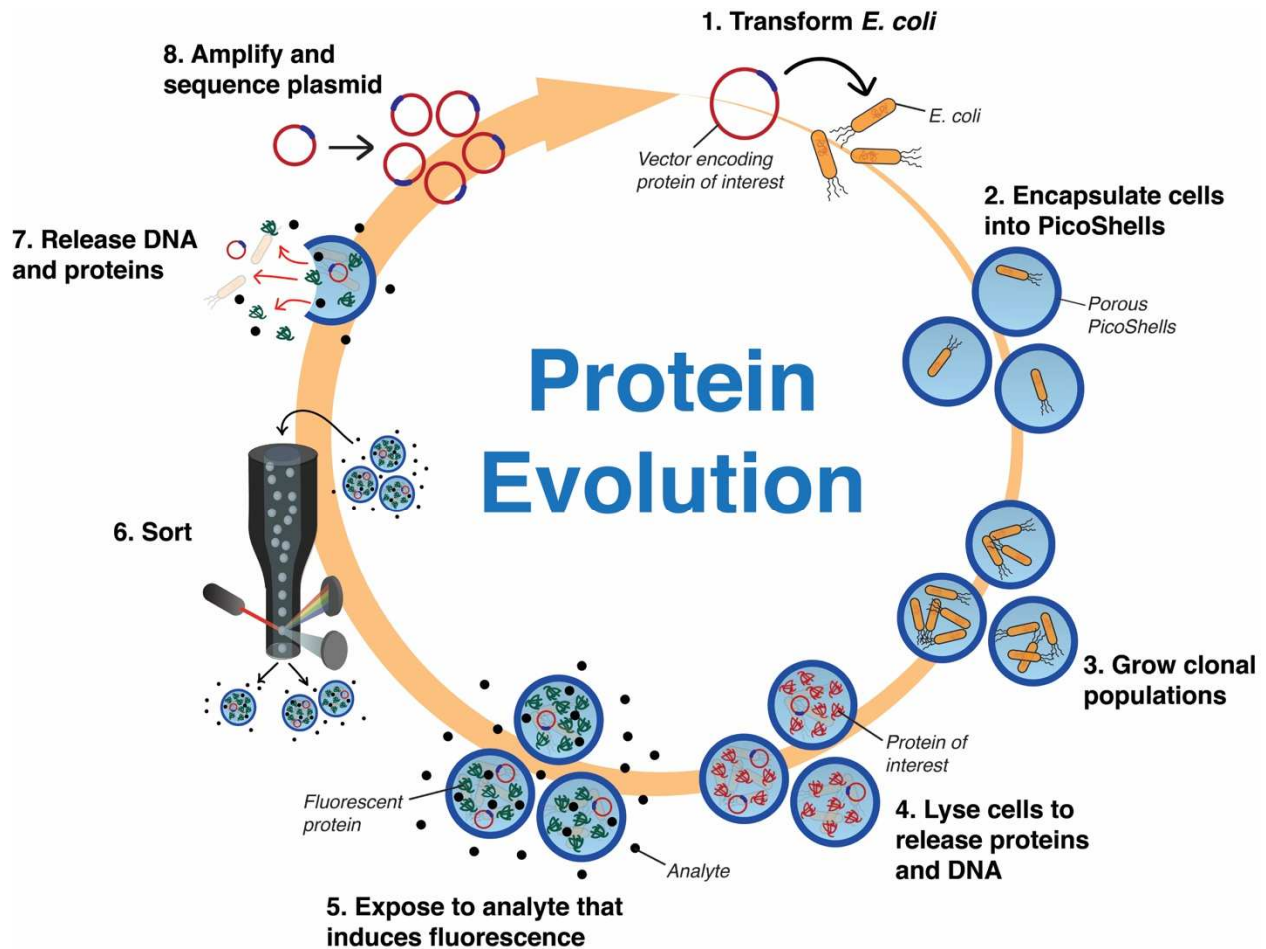


Figure 3-3. Protein Engineering Workflow with PicoShells. (1) A library of *E. coli* is generated by transforming the cells with a library of plasmids encoding for different variants of the gene of interest. (2) Individual *E. coli* cells are encapsulated into PicoShells. (3) These cells are then grown up into clonal colonies. (4) These colonies are lysed, causing the proteins and plasmids of interest to be released. These elements stay within the PicoShells because the pore size of the outer shell is smaller than the proteins and plasmids of interest. (5) The protein-containing PicoShells are exposed to an analyte that induces a localized fluorescence. This could be an ion that induces a FRET interaction, an antigen that binds to an antibody, or various other protein-analyte interactions that induce fluorescence. (6) PicoShells are sorted via FACS to select out PicoShells containing proteins with desired phenotypic properties. (7) Selected PicoShells are then broken down to release the plasmids encoding for the protein of interest. (8) The released plasmids are amplified via PCR and sequenced for further processing.

3.2.2 Results

We explored the different pore sizes that can be achieved with PicoShells by changing the type of PEG that is used to form the outer shell. In particular, we were able to change the pore size

by using PEG-malimide (PEG-MAL) with varying number of arms (4 vs 8) on the PEG and molecular weights. To estimate the protein molecular weight cutoff (MWCO), we encapsulated *E. coli* protein lysate into PicoShells fabricated with varying types of PEG, allowed the any proteins smaller than the cutoff to leak out, washed and broke down the PicoShells to release retained proteins, and ran these proteins on an SDS-PAGE gel. We found that the MWCO decreased with an increasing number of arms and decreasing molecular weight (MW). In particular, we were able to obtain a MWCO that ranged from >200kDa to <10kDa (Figure 3-1). We were able to explore the range of achievable DNA base-pair cutoff by performing the same experiment with DNA ladder rather than protein lysate. We found similar trends with the base-pair cutoff and obtained a range of 300bp to <100bp (Figure 3-2). Given that GCaMP8f has a molecular weight of 54kDa and the pBAD plasmid used to transform GCaMP is 3198bp in length, the desired proteins and DNA are capable of being retained within PicoShells composed of 5kDa 4-arm PEG-MAL.

To verify the protein MWCO, we formed clonal colonies of *E. coli* transformed with pBAD-EGFP (MW of 28kDa) in PicoShells fabricated with 8-arm 5kDa PEG-MAL, lysed the colonies, imaged under the FITC channel, and compared to images in the FITC channel to an un-lysed sample. We found that the FITC channel were highly localized at the location of the cells in the un-lysed samples but distributed throughout the inner cavity of the PicoShell with lysed sample (Figure 3-4). This indicates that lysis buffer can pass through the outer shell matrix and induce cell lysis to release EGFP. This also shows that the pore size is small enough to retain EGFP within the inner cavity.

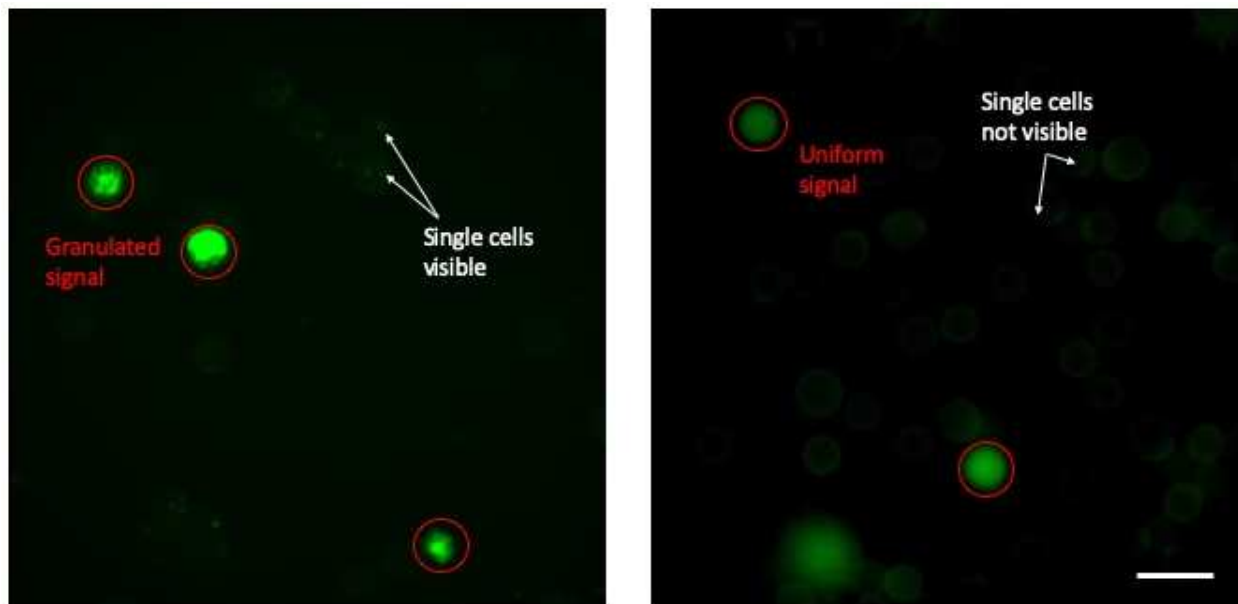


Figure 3-3. Lysis in PicoShells. *E. coli* expressing EGFP were grown in PicoShells and lysed. Before lysis, the EGFP signal is highly localized at individual cells. After lysis, the EGFP signal was evenly distributed throughout the PicoShell cavity. Scale bar = 100 μm .

To verify that proteins retained within the PicoShells can respond to external stimuli, we encapsulated *E. coli* transformed with GCaMP into PicoShells, allowed cells to grow for 24h, lysed cells, exposed separate fractions to Ca^{2+} -free buffer, Ca^{2+} -containing buffer, and Ca^{2+} -containing buffer with EGTA, and imaged under the FITC channel. We found that the fluorescence from GCaMP-containing PicoShells exposed to Ca^{2+} -containing buffer produced a visibly higher fluorescence in the FITC channel than both the Ca^{2+} -free buffer and Ca^{2+} -containing buffer with EGTA (Figure 3-5). We compared these samples to PicoShells containing EGFP exposed to the same conditions and found that the EGFP samples maintained a similarly high fluorescence when exposed to each of the conditions. This indicates that GCaMP can respond to varying calcium conditions in the external environment of the PicoShells.

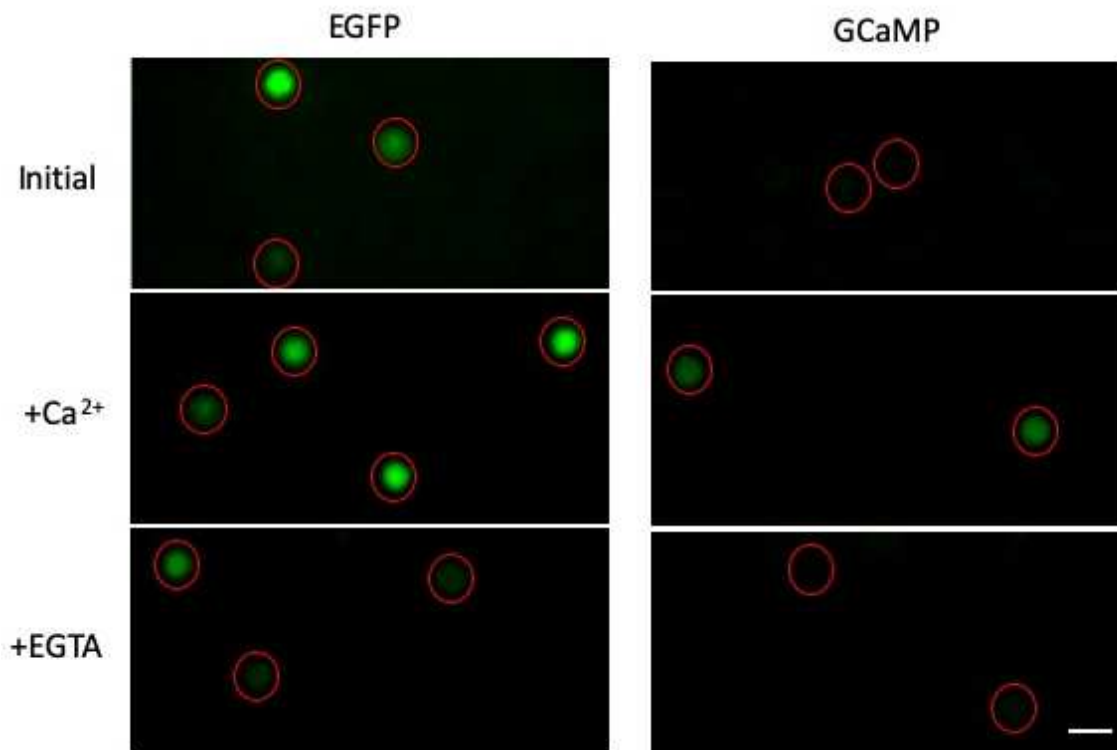


Figure 3-4. GCaMP responsiveness in PicoShells. *E. coli* expressing GCaMP and EGFP were grown up into separate samples of PicoShells and lysed. The PicoShells were then imaged under the FITC channel in calcium free medium (Initial). 100 μ M of CaCl_2 was then added to the sample and re-imaged. Afterwards, 1 mM of EGTA was added to each sample and imaged. The fluorescence intensity from GCaMP was only visibly seen when exposed to just CaCl_2 while that from EGFP was seen in each condition. Scale bar = 50 μ m.

3. 2. 3 Discussion and future directions

We have successfully shown preliminary studies that indicate PicoShells may be used in protein evolution workflows. Specifically, we have demonstrated that cells producing a protein of interest can be lysed within PicoShells and that the PicoShell pore size can be optimized to retain the protein of interest via size exclusion. Additionally, we have demonstrated that the retained proteins can respond to stimuli from the external environment.

More studies need to be done in order to show a proof-of-concept workflow for protein evolution using PicoShells. First, we need to demonstrate that the response of the desired proteins

to external stimuli can be recognized by flow cytometry. We propose exposing separate samples of PicoShells with retained GCaMP to Ca^{2+} -free buffer, Ca^{2+} -containing buffer, and Ca^{2+} -containing buffer with EGTA and reading out 10,000+ PicoShells in the FITC channel via a flow cytometer. We also need to verify that PCR can be performed following flow sorting, so we propose that a fraction of GCaMP-containing PicoShells are sorted via a flow sorter, broken down, exposed to PCR conditions that amplify the GCaMP-producing plasmids, and run on an agarose gel to verify the amplification of the target plasmid. We also propose that a single protein evolution cycle using clonal colonies of GCaMP-producing in PicoShells is performed and the GCaMP sequence is analyzed post-sort.

Several challenges for the proposed workflow also need to be considered. First, differences fluorescent readouts from PicoShells may be the result of a greater amount of protein retained rather than better functionality. To consider this effect, we propose that the plasmids producing the same protein of interest also produce an analyte-insensitive fluorescent protein and that flow sorting occurs by measuring the radiometric readouts between the two proteins. It may also be possible to normalize the fluorescent readouts from the protein of interest to the scatter readouts from the lysed cells. However, this may not take into account the faster production from the individual cells within the clonal colony. Second, the workflow is limited to assays where the protein of interest is significantly larger in size relative to the analyte(s) inducing a stimulus. It may be possible to expand the possible assays by having the PicoShell pore size be large enough to allow all proteins to diffuse and including capture sites to the shell. Unfortunately, not all proteins have corresponding capture motifs and it may be challenging to have enough capture sites to have a reasonable dynamic range.

Overall, the PicoShell workflow has shown preliminary evidence that it could be used as a *novel* directed protein evolution platform. It may not only produce high throughputs (>1 million genetic variants per screen), but also ensure that the proteins are free floating and exposed to their native functional environments. More work needs to be done, but PicoShells has the potential to accelerate the protein design space moving forward.

3. 2. 4 Methods

To determine the possible protein MWCO's of PicoShells, separate samples of 300 μ L of PicoShells were fabricated using the conditions indicated in Table C1 and parameters previously described³³. 27 μ g of *E. coli* protein lysate (Bio-Rad) was placed into the dextran phase during the fabrication of each respective PicoShell sample. Following fabrication, the PicoShells were incubated in DPBS (Fisher Scientific) for 24 h to allow for the diffusion of proteins. The PicoShells were then washed via a series of centrifugation and solution replacement steps to remove diffused proteins. The PicoShells were then pelleted, had all supernatant removed, and were exposed to 1 mg/mL sodium periodate (NaIO_4) for 30 min in order to chemically degrade the particles. 15 μ L from each sample were then mixed with 2 μ L Sample Buffer (Sigma Aldrich) placed into separate wells of a 20% Mini-PROTEAN[®] TGX Stain-Free Protein Gel (Bio-Rad) for SDS-PAGE and imaging. The same workflow was used to determine the DNA cutoff by using 2.5 μ g 1 Kb Plus DNA Ladder instead of protein lysate and running the samples on an agarose gel with 1X SYBR Green I nucleic acid stain (Fisher Scientific) for gel electrophoresis.

Separate One Shot[®] TOP10 Competent *E. coli* populations were chemically transformed with pBAD vectors encoding for the expression of EGFP or GCaMP8f. For each vector, one 50 μ L vial was thawed on ice, had 5 μ L of each vector added to it, and was incubated on ice for 30 min. Each

vial was then placed into a 42°C water bath for 30 sec. 250 µL of S.O.C medium was added to each vial and placed at 37°C for 1 hour at 225 rpm. Each solution was then spread out onto separate Luria Broth (LB)-agar plates containing 100 µg/mL ampicillin that served as a selection marker and incubated overnight. Colonies were stored at 4°C for long-term storage. To start a transformed *E. coli* culture, a colony was picked off of the appropriate agar plate and placed into a sterile 250 µL Erlenmeyer flask containing Miller's LB broth. The broth was supplemented with 0.2% (w/v) L-arabinose to induce expression of the intended protein. Cultures were maintained at 37°C and 225 rpm.

For lysis experiments, *E. coli* expressing EGFP were first encapsulated into PicoShells fabricated with 5kDa 8-arm PEG-MAL at a concentration of 10 million cells/mL. The PicoShells were then placed into LB-broth supplemented with 100 µg/mL and 0.2% (w/v) arabinose and incubated at 37°C for 24 h to allow colonies to form. Half of the colony-containing PicoShells were then pelleted, had all supernatant removed, and placed into 100% B-PER™ (Thermo Scientific) for 30 min to lyse cells. Separate aliquots of un-lysed and lysed samples were placed into separate wells on a 96-well plate and imaged under the FITC-channel.

For GCaMP8f pilot experiments, separate *E. coli* populations expressing EGFP or GCaMP8f were encapsulated in PicoShells, incubated, and lysed using the same parameters for lysis experiments. Following lysis, fractions from each sample were pelleted, had all B-PER removed, and placed into one of the following solutions: calcium-free DPBS (Thermo Fisher), DPBS supplemented with 100 µM calcium chloride (CaCl₂, Sigma Aldrich), and DPBS supplemented with 100 µM CaCl₂ and 1 mM of ethylene glycol-bis(β-aminoethyl ether)-N, N, N', N'-tetraacetic acid (EGTA, Sigma-Aldrich). Each sample was then placed into separate wells on a 96-well plate and imaged under the FITC channel.

3.3 Future directions and conclusion

We have successfully created a proof-of-concept workflow that has the potential to improve yields of useful bioproducts. More specifically, we have created a model system that meets the following criteria:

1. Selection of single cells and clonal colonies so that researchers can directly select for desired phenotypic traits and remove any un-desired ones
2. Applies an evolutionary selection pressure on clonal colonies based on coupled growth and bioproduct production rates, where the bioproduct is either retained intracellularly or secreted
3. Can achieve throughputs of 1,000,000+ cells or clonal colonies per screen so that the full genetic diversity can be explored
4. Has cells incubated and characterized in environments that replicate the factors experienced in a production setting

Unfortunately, a lot of work still needs to be done to translate this proof-of-concept workflow into a fully functional workflow that produces real-world results. First, the idea that cells sorted using this workflow will retain the same desired phenotypic properties when placed into a production environment is still hypothetical and not proven. It is unclear how offline effects (i.e. during cell sorting or encapsulation process) will change the genetics of the cells. It is also unclear if selected phenotypes will remain stable for multiple generations post-sort and if there needs to be an additional process to select out stable cell lines. Future work in this area will need to be done to fully validate this workflow for such applications. Second, the workflow still needs to be further

optimized to be compatible with secretion workflows. The current system is only set up for applications where the secreted protein is significantly larger than the target metabolite, fluorescent label, or antigen. Also, the current developed workflows are not well suited for developing cell lines that produce metabolites, vitamins, synthetic pharmaceuticals, and other small bioproducts. This significantly limits the total number of applications that the system can be used for. Therefore, it is necessary to develop new ways to capture and/or retain released bioproducts from cells.

However, we have discovered that the PicoShell can be used for different applications outside of enhancing bioproduct yields. In particular, PicoShells can be used as a general colony-picker with several advantages over current workflows. In these current workflows, colonies are plated onto agar plates and selected either by hand or via robotic handling systems. These systems are limited to only a few hundred to a few thousand colonies per hour, limiting the total genetic diversity that can be explored. In addition, colonies that grow the fastest are preferentially selected since slower growing colonies are unlikely to be visible. By using PicoShells, we could increase the throughput from thousands of colonies per hour to hundreds of thousands of colonies per hour. In addition, we will get much better resolution since the slower growing colonies that wouldn't be recognized using traditional workflows will be recognized using the PicoShell workflow.

PicoShells may also be used as a new protein directed evolution tool. In current workflows, protein engineers are required to select or develop targets that can enter cells to reach intracellular proteins³⁴, have proteins secreted and be characterized via low throughput methods such as ELISA³⁵, or have proteins displayed on the cell surface which may alter the properties of the desired protein³⁶. With PicoShells, we can grow up transformed bacteria or yeast colonies within the particles, lyse the cells to release protein and genetic material that is retained within the PicoShells, exposed to a target metabolite or antigen, sorted based on the protein response, and

broken down to have the genetic material sequenced for further analysis. This will significantly increase throughput over ELISA-based methods without needing to find stains that can pass through the cell membrane or alter protein morphology for display techniques.

Overall, we have developed a completely novel cell screening and sorting tool that has unique advantages over previous techniques. PicoShells can encapsulate individual cells and clonal colonies while uniquely enabling continuous solution exchange with the external environment. Additionally, PicoShells are fully suspendable and can be placed directly into environments that were not possible before such as a bioreactor. Lastly, cell/colony-containing PicoShells can be sorted using FACS, enabling highest throughput for cell selection workflows. The PicoShell workflow opens up a wide variety of assays that were not previously possible and has the potential to have a significant impact on many fields within biotechnology.

3.4 References

1. de Rutte J., Dimatteo R., Archang M. A., van Zee M., Koo D., Lee S., Sharrow A. C., Krohl P. J., Mellody M. P., Zhu S., Eichenbaum J., Kizerwetter M., Udani S., Ha K., Bertozzi A. L., Spangler J. B., Damoiseaux R., and Di Carlo D. Massively parallel encapsulation of single cells with structured microparticles and secretion-based flow sorting. *bioRxiv* (2020).
2. Pregibon D. and Doyle P. Optimization of Encoded Hydrogel Particles for Nucleic Acid Quantification. *Analytical Chemistry* 81(12), 4873-4881 (2009).
3. Witte R., Blake A., Palmer C., and Kao W. Analysis of poly(ethylene glycol)-diacrylate macromer polymerization within a multicomponent semi-interpenetrating polymer network system. *Journal of Biomedical Materials Research* 71(3) 508-518 (2004).
4. Broguiere N., Husch A., Palazzolo G., Bradke F., MAdduri S., and Zenobi-Wong M. Macroporous hydrogels derived from aqueous dynamic phase separation. *Biomaterials* 200, 56-65 (2019).
5. Benjamin L., Baca W., and Golan D. Protein therapeutics: a summary and pharmacological classification. *Nature Reviews Drug Discovery* 7(1), 21-39 (2008).
6. Zhu B., Wang D., and Wei N. Enzyme discovery and engineering for sustainable plastic recycling. *Trends Biotechnology* 40(1), 22-37 (2022).
7. Li I.T., Pham E., and Truong K. Protein biosensors based on the principle of fluorescence resonance energy transfer for monitoring cellular dynamics. *Biotechnology Letters* 28(24), 1971-1982 (2006).
8. Khalil A. The genome editing revolution: review. *Journal of Genetic Engineering and Biotechnology* 28(68) (2020).

9. Jumper J., Evans R., Pritzel A., Green T., Figurnov M., Ronneberger O., Tunyasuvunakool K., Bates R., Zidek A., Potapenko A., Bridgland A., Meyer C., Kohl S., Ballard A., Cowie A., Romera-Paredes B., Nikolov S., Jain R., Adler J., Back T., Peterson S., Reiman D., Clancy E., Zielinski M., Steinegger M., Packolska M., Berghammer T., Bodenstein S., Silver D., Vinyals O., Senior A., Kavukcuoglu K., Kohli P., and Hassabis D. Highly accurate protein structure prediction with AlphaFold. *Nature* 596, 583-589 (2021).
10. Yuan L., Kurek I., English J., and Keenan R. Laboratory-Directed Protein Evolution. *Microbiology and Molecular Biology Reviews* (2005).
11. Shivange A., Marienhagen J., Mandhada H., Schenck A., and Schwaneberg U. Advances in generating functional diversity for directed protein evolution. *Current Opinion in Chemical Biology* 13(1), 19-25 (2009).
12. Puetz J. and Wurm F. Recombinant Proteins for Industrial versus Pharmaceutical Purposes: A Review of Process and Pricing. *Processes* 7(8), 476 (2019).
13. Ueda H., Tsumoto K., Kuboata K., Suzuki E., Nagamune T., Nishimura H., Schueler P., Winter G., Kumagai I., and Mahoney W. Open sandwich ELISA: A novel immunoassay based on the interchain interaction of antibody variable region. *Nature Biotechnology* 14, 1714-1718 (1996).
14. Mendoza L., McQuary P., Mongan A., Gangadharan R., Brignac S., and Eggers M. High-Throughput Microarray-Based Enzyme-Linked Immunosorbent Assay (ELISA). *Biotechniques* 27(4) (2018).
15. Boder E., Raeeszadeh M., and Price J. Engineering antibodies by yeast display. *Archives of Biochemistry and Biophysics* 526(2), 99-106 (2012).

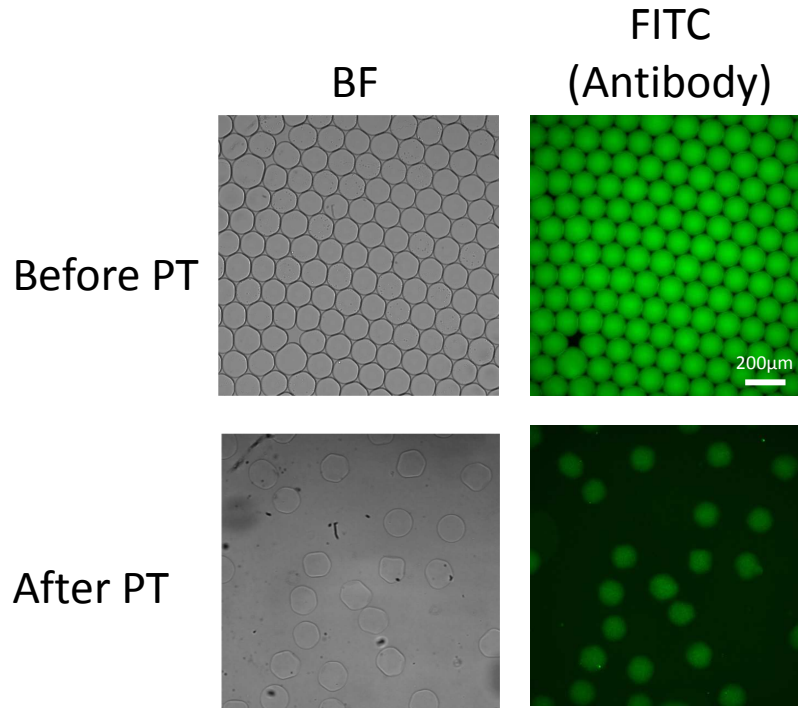
16. Chen I., Dorr B., and Liu D. A general strategy for the evolution of bond-forming enzymes using yeast display. *Proceedings of the National Academy of Sciences* 108(28), 11399-11404 (2011).
17. Daugherty P. Protein engineering with bacterial display. *Current Opinion in Structural Biology* 17(4), 474-480 (2007).
18. Mason D., Webner C., Parola C., Meng S., Greiff V., Kelton W., and Reddy S. High-throughput antibody engineering in mammalian cells by CRISPR/Cas9-mediated homology-directed mutagenesis. *Nucleic Acids Research* 46(14), 7436-7449 (2018).
19. Smith G. and Petrenko V. Phage Display. *ACS Publications* 97(2), 391-410 (1997).
20. Plucktun A. Ribosome Display: A Perspective. *Ribosome Display and Related Technologies* 805 (2012).
21. Hoess R. Protein Design and Phage Display. *ACS Publications* 101(10), 3205-3218 (2001).
22. Bendahmane M., Koo M., Karrer E., and Beachy R. Display of epitopes on the surface of tobacco mosaic virus: impact of charge and isoelectric point of the epitope on virus-host interactions. *Journal of Molecular Biology* 290(1), 9-20 (1999).
23. Kim H., Guzman A., Thapa H., Devarenne T., and Han A. A droplet microfluidics platform for rapid microalgal growth and oil production analysis. *Biotechnology and Bioengineering* 113(8), 1691-1701 (2016).
24. Cela-Abalde S., Gould A., Liu X., Kazamia E., Smith A., and Abell C. High-throughput detection of ethanol-producing cyanobacteria in a microdroplet platform. *The Royal Society* 12(106), (2015).

25. Srisa-Art M., Kang D., Hong J., Park H., Leatherbarrow R., Edel J., Chang S., and deMello A. Analysis of Protein-Protein Interactions by Using Droplet-Based Microfluidics. *ChemBioChem* 10(10), 1605-1611 (2009).
26. Gift E., Park H., Paradis G., Demain A., and Weaver J. FACS-based isolation of slowly growing cells: Double encapsulation of yeast in gel microdrops. *Nature biotechnology* 14, 884-887 (1996).
27. Wu L., Chen P., Dong Y., Feng X., and Liu B.F. Encapsulation of single cells on a microfluidic device integrating droplet generation with fluorescence-activated droplet sorting. *Biomedical Microdevices* 15, 553-560 (2013).
28. Li M., van Zee M., Riche C.T., Tofig B., Gallaher S., Merchant S., Damoiseaux R., Goda K., and Di Carlo D. A Gelatin Microdroplet Platform for High-Throughput Sorting of Hyperproducing Single-Cell Derived Microalgal Clones. *Small* 14(44), (2018).
29. Weaver J., McGrath R., and Adams S. Gel microdrop technology for rapid isolation of rare and high producers. *Nature Medicine* 3(5), 583-585 (1997).
30. Hammill L., Welles J., and Carson G. The gel microdrop secretion assay: Identification of a low productivity subpopulation arising during the production of human antibody in CHO cell. *Cytotechnology* 34, 27-37 (2000).
31. Fujitani H., Tsuda S., Ishii T., and Machida M. High-throughput screening of high producer budding yeast using gel microdrop technology. *bioRxiv* (2019).
32. Sutter M., Siepmann J., Hennink W., and Jiskoot W. Recombinant gelatin hydrogels for the sustained release of proteins. *Journal of Controlled Release* 119(3), 301-312 (2007).

33. van Zee M., de Rutte J., Rumyan R., Williamson C., Burnes T., Radakovits R., Sonico Eugenio A., Badih S., Lee S., Lee D.H., Archang M., and Di Carlo D. *Proceedings of the National Academy of Sciences* 119(4), (2022).
34. Hill B. D., Prabhu R., Rizvi S. M., and Wen F. Yeast Intracellular Staining (yICS): Enabling High-Throughput, Quantification Detection of Intracellular Proteins via Flow Cytometry for Pathway Engineering. *ACS Synthetic Biology* 9(8), 2119-2131 (2020).
35. Pluckthum A. and Pack P. New protein engineering approaches to multivalent and bispecific antibody fragments. *Immunotechnology* 3(2), 83-105 (1997).
36. Gai S. A. and Wttrup K. D. Yeast surface display for protein engineering and characterization. *Current Opinion in Structural Biology* 17(4), 467-473 (2007).

Appendix A

Supporting information for Chapter 1



PT = Phase transfer to water

Figure A1. Retention of FITC-IgG in gelatin gel microdroplets. Droplets were encapsulated with gelatin and FITC-IgG before being gelled and phase transferred from oil to aqueous solution. FITC-IgG remained localized at the gelatin hydrogels mostly likely due to charge-charge interactions between IgG and proteins within the gelatin matrix.

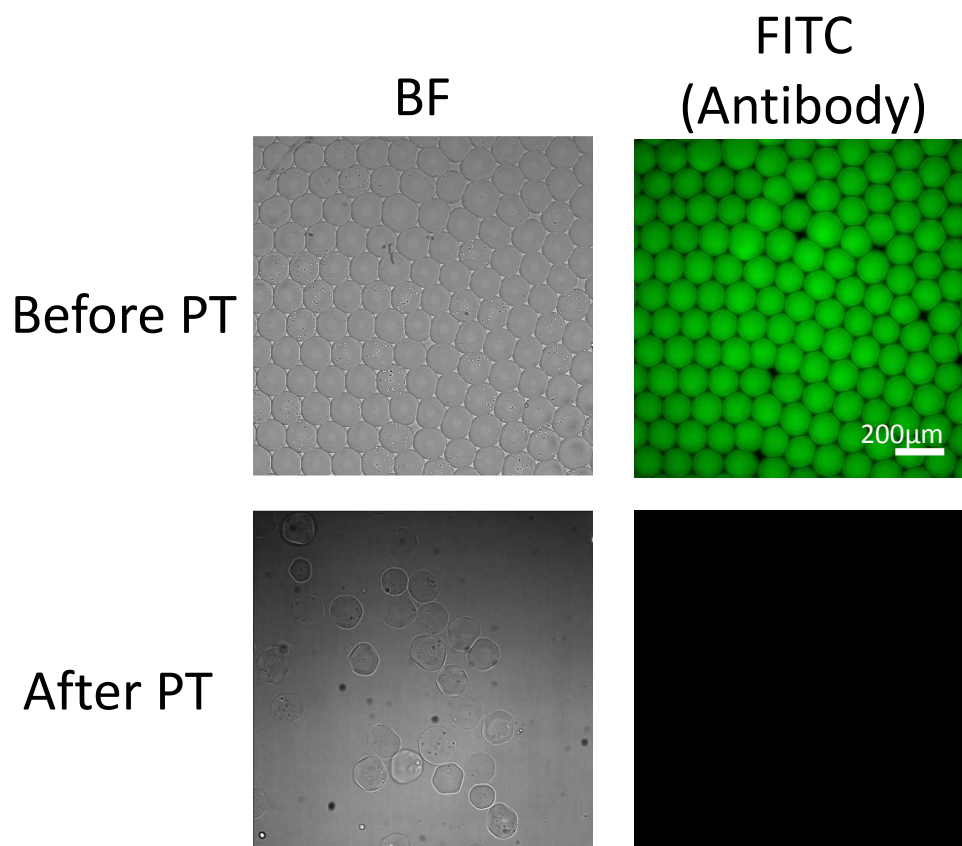


Figure A2. Leakage of FITC-IgG out of agarose gel microdroplets. Droplets were encapsulated with agarose and FITC-IgG before being gelled and phase transferred from oil to aqueous solution. Unlike with gelatin gel microdroplets, FITC-IgG completely leaks out of agarose gel microdroplets after phase transfer.

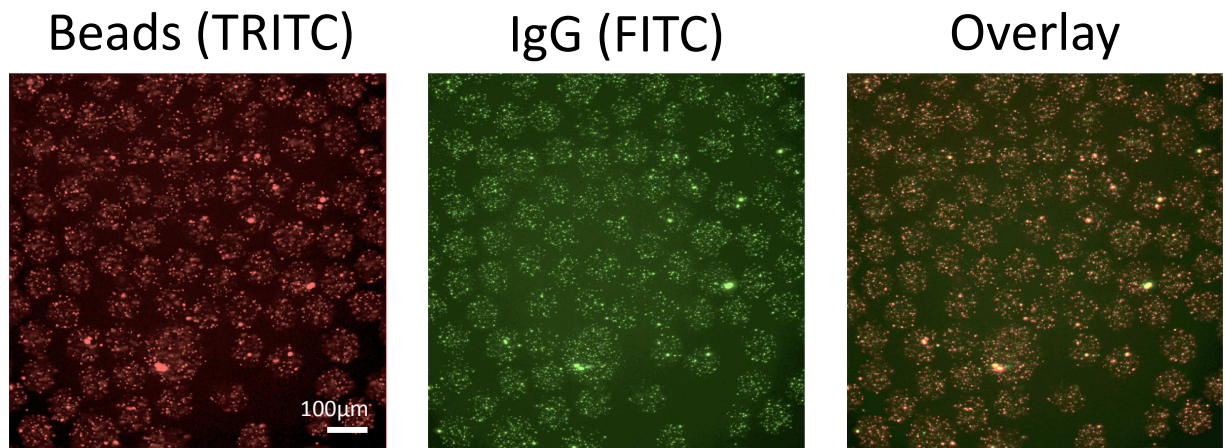


Figure A3. Localization of FITC-IgG at beads within agarose gel microdrops. Agarose gel microdrops were formed with protein A-coated beads (visible in the TRITC channel) and FITC-IgG. Images in the TRITC and FITC channels show that the protein A-coated beads and FITC-IgG stay retained in the agarose gel microdrops after phase transfer and that FITC-IgG localized at the protein A-coated beads.

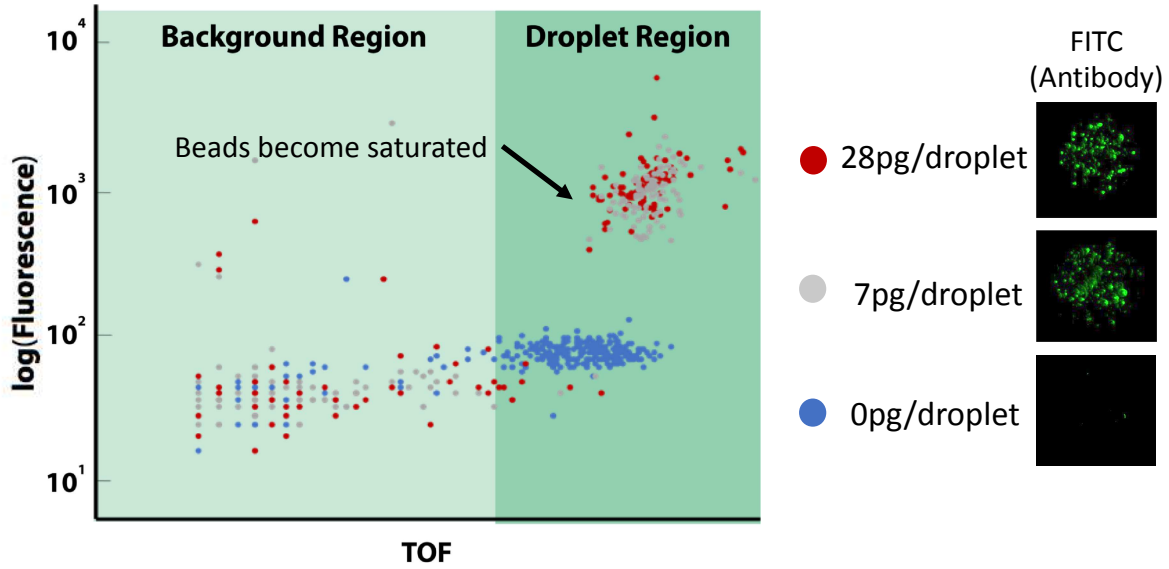


Figure A4. Saturation of protein A-coated beads. Agarose gel microdrops with protein A-coated beads and varying amounts of FITC-IgG (0 pg/droplet, 7 pg/droplet, 28 pg/droplet) were formed in water-in-oil emulsions before being gelled, phase transferred, washed, and screened using a flow cytometer. There was an order of magnitude difference in the fluorescent readout between the 0 pg/droplet and 7 pg/droplet samples. However, there was little to no difference between the 7 pg/droplet and 28 pg/droplet samples (the difference in concentrations that we would expect from low and high secretors after a couple hours of incubation). This indicates that the protein A beads become saturated after at least a 7 pg/droplet concentration.

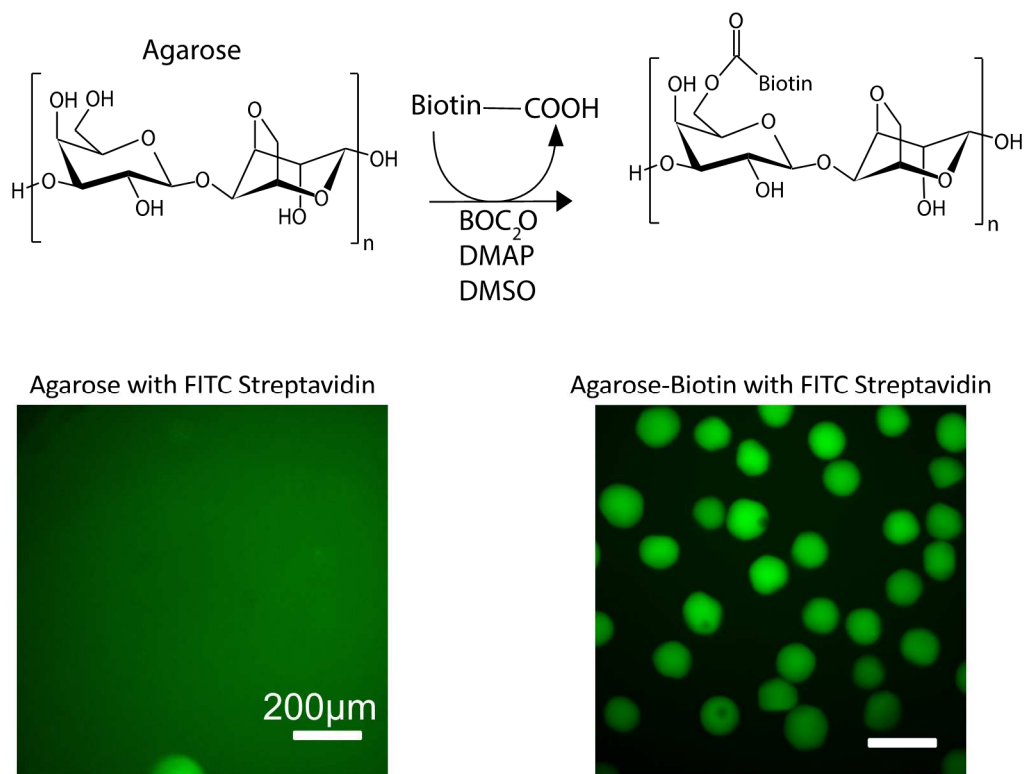


Figure A5. Conjugation of biotin groups to agarose. The hydroxyl group of agarose is activated using di-tert-butyl dicarbonate (BOC_2) and 4-dimethylaminopyridine (DMAP) within DMSO. The activated hydroxyl group allows for an ester to form with the carboxylic acid group in biotin, allowing biotin to be conjugated to the agarose matrix. We verified that presence of biotin within the agarose matrix by forming two separate gel microdrops samples, one with normal agarose and one with agarose-biotin, with FITC streptavidin and transferring to aqueous solution. We found that the agarose-biotin samples had FITC streptavidin still localized within the gel microdrops and the normal agarose samples did not.

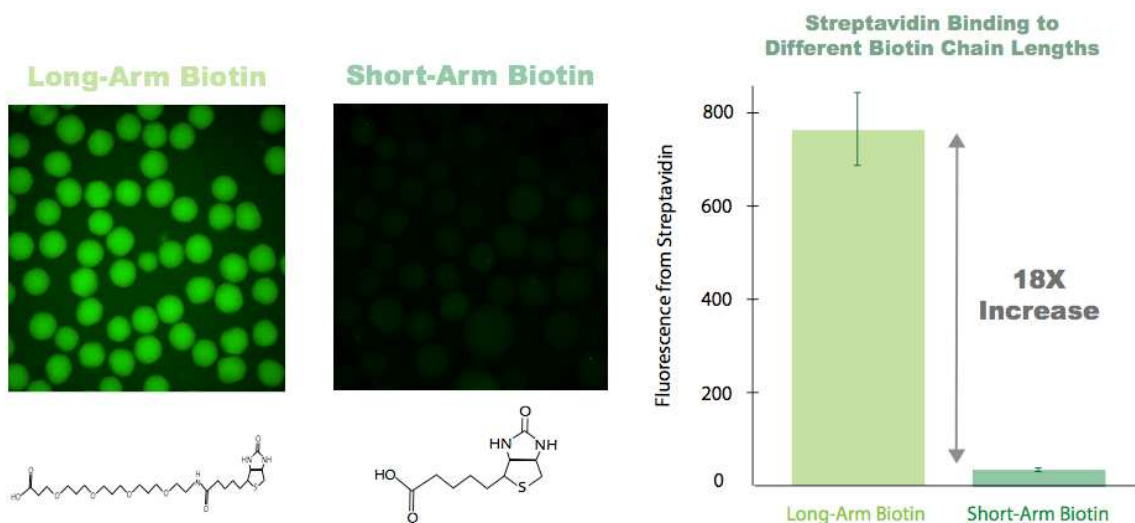


Figure A6. Differences in streptavidin binding with biotin containing different chain lengths. Biotin with different chain lengths with conjugated to two separate agarose samples and used to form gel microdrops with FITC streptavidin. We found that there was an 18X increase in the fluorescence intensity from FITC streptavidin in agarose conjugated with long-arm biotin, indicating that agarose with long-arm biotin is more efficient at binding to streptavidin.

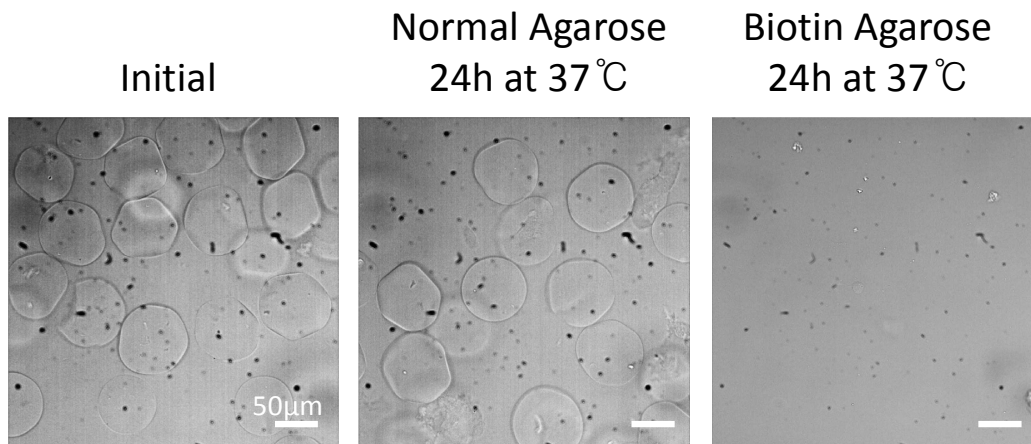


Figure A7. Effects of conjugating biotin to agarose on melting point. Separate gel microdrop samples were formed using normal agarose and biotin agarose and placed at 37°C for 24h. The gel microdrops made using biotin agarose melted over the incubation time while those made with normal agarose stayed intact.

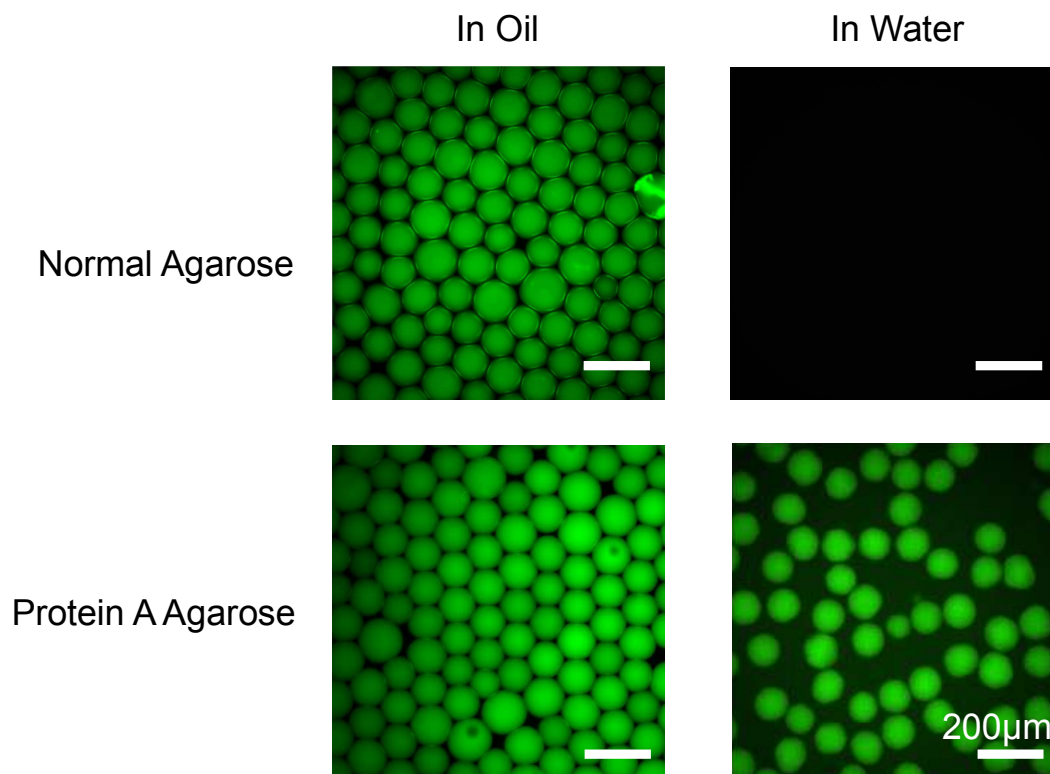


Figure A8. Binding of FITC-IgG to protein A agarose. Protein A was conjugated to biotin agarose via streptavidin-biotin affinity interactions, used to make gel microdrops with FITC-IgG, and compared to gel microdrops formed with normal agarose containing FITC-IgG. FITC-IgG was able to be retained with agarose containing protein A while FITC-IgG leaked out of samples made with normal agarose.

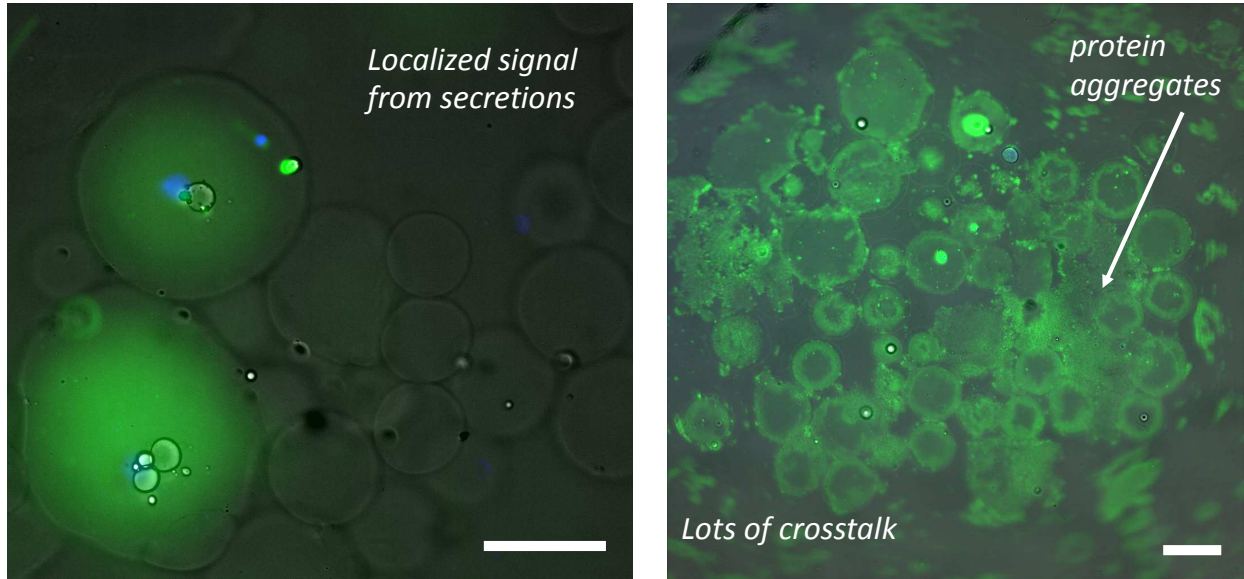
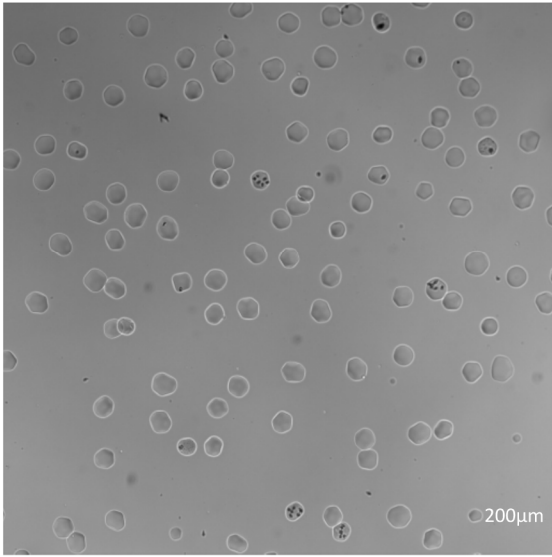


Figure A9. Capture of antibodies from secreting hybridomas. Hybridomas secreting anti-human IgG antibodies were placed into protein A agarose gel microdrops, stained with Hoescht (blue), and FITC human IgG antibodies (green). While there were some gel microdrops with a clear localization of FITC human IgG antibodies within gel microdrops containing cells (indicating that secretions were retained), there was a lot of crosstalk and protein aggregation within the sample.

~5% of the time



~95% of the time

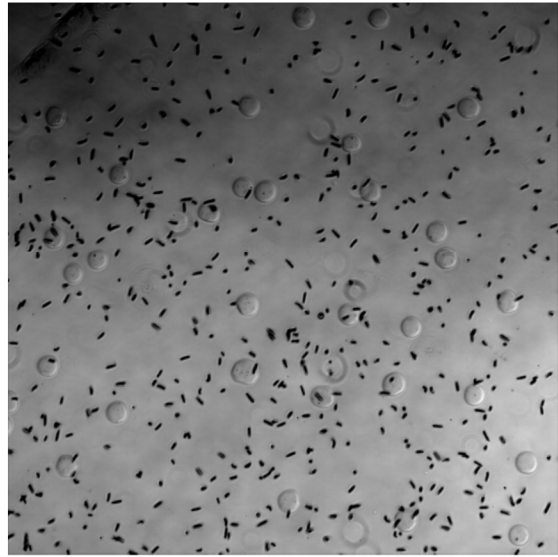


Figure A10. *Euglena* release from gelatin gel microdroplets. After a 24h incubation of *Euglena* (and other microalgae in gelatin gel microdroplets, there were sometimes when the gel microdroplets would stay intact and capable of being sorted via FACS. However, the gel microdroplets containing *Euglena* tended to fall apart during this time period, releasing the encapsulated microalgae into the external environment.

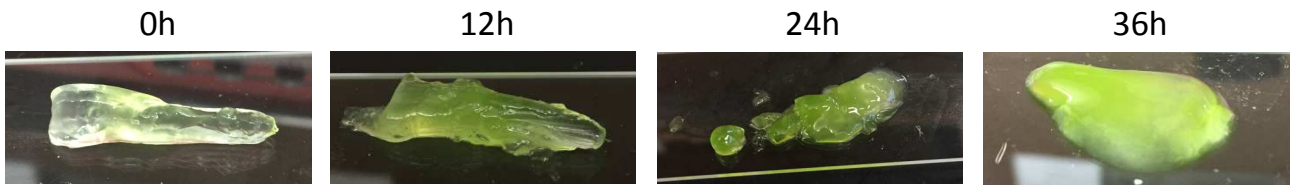


Figure A11. Microalgae degradation of gelatin. *Chlamydomonas reinhardtii* samples were placed into a microcentrifuge tube containing un-gelled gelatin, incubated for incremental amounts of time over a 36h period, placed at 4°C for 1h for gelling, and removed from the tube for imaging. While the gelatin was able to fully gel into a stable morphology when incubated <12h, very little gelling occurred at times points >12h and resulted into a “gooey” like substance without much stability. This indicated that the *C. reinhardtii* tended to degrade the gelatin over time.

Appendix B

Supporting information for Chapter 2

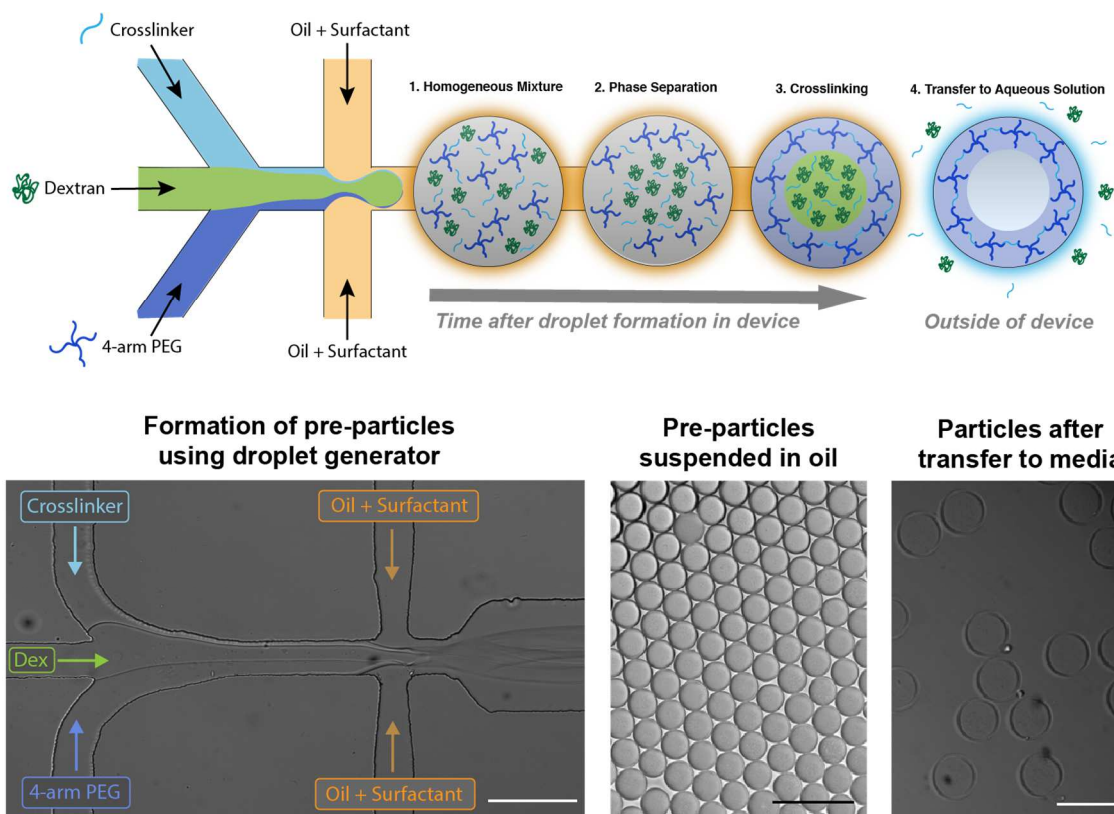


Figure B1. Microfluidic fabrication of PicoShells. PicoShells are formed by mixing together crosslinker, dextran, and 4-arm PEG to form a water-in-oil droplet emulsion. The reagents are mixed at the point of droplet formation to reduce premature gelation and phase separation. There is initially a homogeneous mixture of reagents, but the 4-arm PEG and dextran phases separate as the droplet travels down the channel. It is likely that the crosslinker remains uniformly distributed throughout the droplet. As 4-arm PEG and dextran separate, the crosslinker and 4-arm PEG react. Following gelation, the particles are phase transferred from oil to aqueous solution where dextran and un-reacted crosslinker leaks out of the particles via pores in the outer shell. The outer diameter of PicoShells is larger than that of pre-particles ($\sim 90 \mu\text{m}$ and $\sim 70 \mu\text{m}$ respectively) due to the expected swelling of the PEG hydrogel in aqueous solutions. Scale bars = $200 \mu\text{m}$.

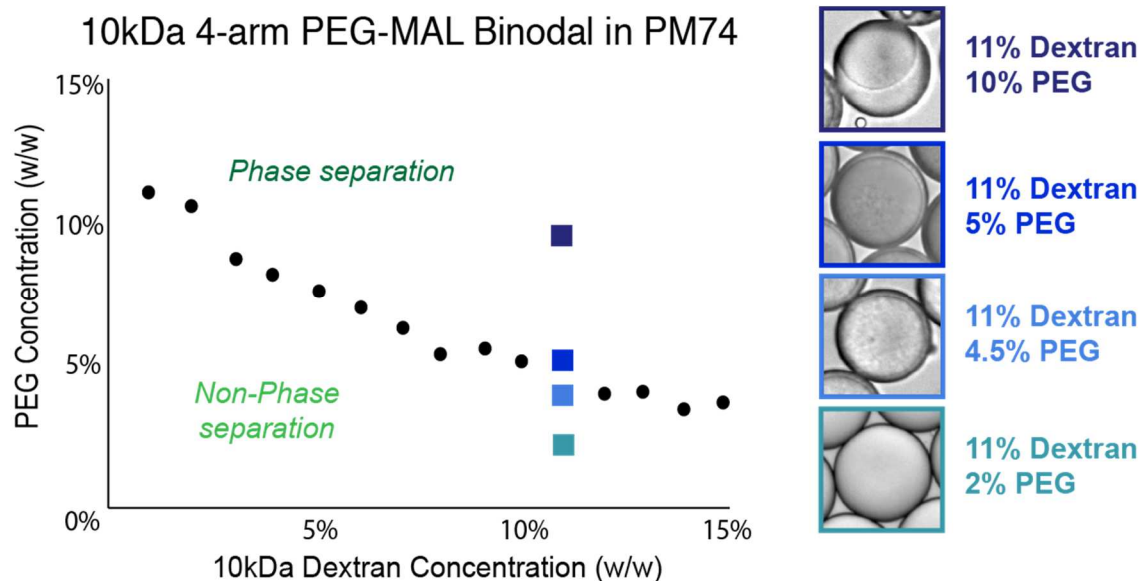


Figure. B2. Phase diagram of 10kDa 4-arm PEG-maleimide and 10 kDa dextran in PM74 seawater medium. Black dots represent concentrations we experimentally determined where the binodal is located through visual observation of droplets with varying concentrations of PEG and Dextran. PEG and dextran with concentrations below the binodal curve do not undergo phase separation, resulting in solid hydrogel particles. At PEG and dextran concentrations above the curve the droplets phase separate into PEG rich and dextran rich regions. The resulting morphology is dictated by the balance of interfacial tensions between the PEG, dextran and oil phases and the resulting particle shape is dictated by the cross-linkable PEG rich region. It was found that at higher PEG and Dextran concentrations (11% Dextran, 10% PEG) the Dextran rich region partially wets the oil interface resulting in bowl shaped particles. At lower concentrations the PEG rich region completely wets the oil interface resulting in fully enclosed Picoshells. In general it was found that PEG and dextran concentrations 0.5-2% above and to the right of the points of the binodal curve result in the desired Picoshell morphology.

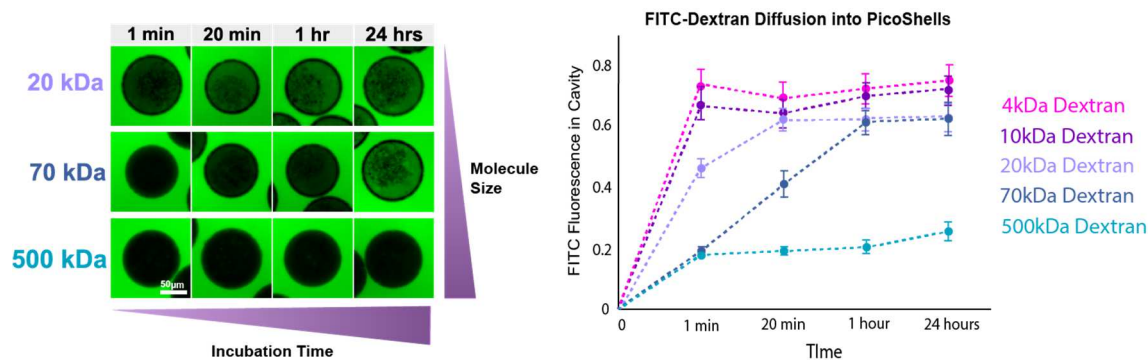


Figure B3. Characterization of diffusion through the outer hydrogel matrix of the PicoShells. The rate at which molecules diffuse through the PicoShell's outer matrix depends on the size of the molecules. PicoShells were placed into solutions containing FITC-dextran (green) of various molecular weights and the transport of those molecules into the PicoShell cavity was tracked over time. For FITC-dextran ≤ 20 kDa we observe rapid entry into the cavity (i.e. equilibrium within 20min). 70kDa FITC-dextran diffuses more slowly into the cavity, reaching equilibrium at between 1 and 24h. 500kDa FITC-dextran was not seen to enter into the PicoShell cavity even after 24h. Error bars represent standard deviation in the fluorescence measurements between PicoShells in each sample. 50 particles were measured for each sample. Scale bar = 50 μ m.

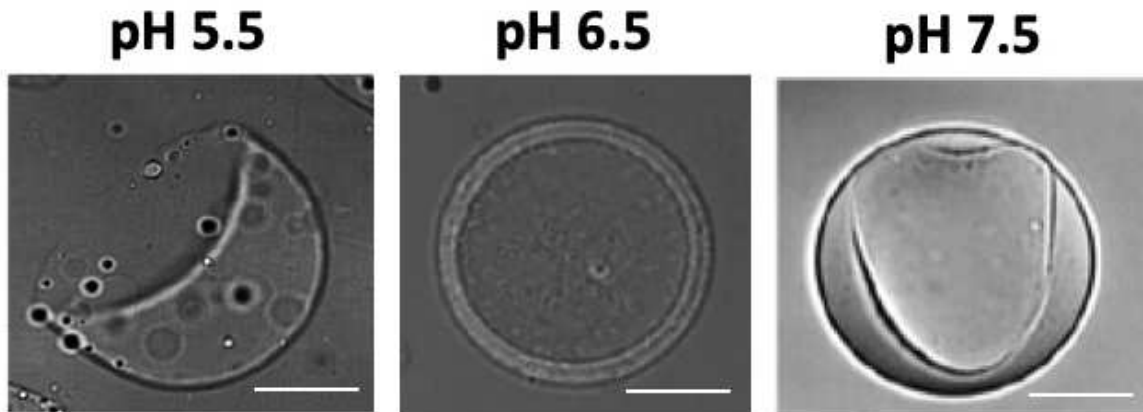


Figure S4. Sensitivity of particle shape to crosslinking rate. The rate of crosslinking was varied by adjusting the pH of the precursor solution from 5.5 – 7.5 for a fixed PEG and dextran concentration. At a pH of 7.5, the time between droplet formation and crosslinking occurs too quickly, resulting in polymerization before the PEG and dextran are able to phase separate completely and form a uniform hollow shell structure. At a pH of 5.5, crosslinking rate is reduced resulting in formation of janus particles. We theorize that in the initial phase of crosslinking the effective molecular weight of the PEG monomers increases as they link together leading to a shift in the binodal which changes the equilibrium morphology. At a pH of 6.5 we found that the crosslinking rate is slow enough to allow for complete phase separation and quick enough to preserve the ideal PicoShell morphology. Scale bar = 25 μ m.

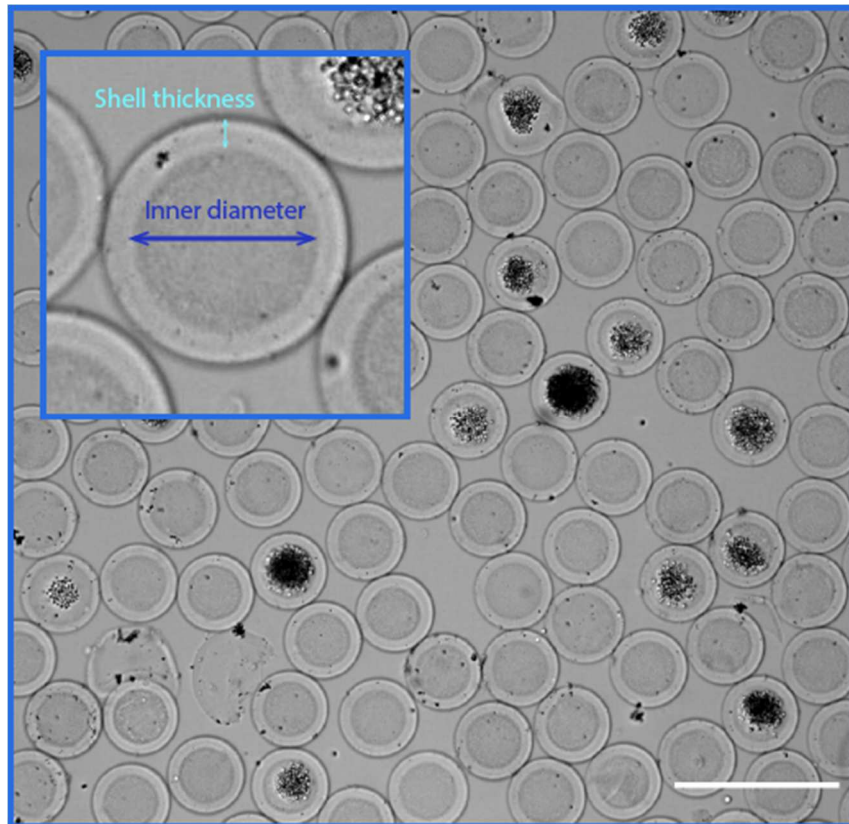


Figure B5. PicoShell uniformity. PicoShells fabricated with encapsulated *Chlorella* colonies are highly uniform in size and morphology. PicoShells have an average outer diameter of $90.7\mu\text{m}$ with a CV of 1.7%. The particles also have an average shell thickness of $12.7\mu\text{m}$ with a CV of 6.9%. Scale bar = $200\mu\text{m}$.

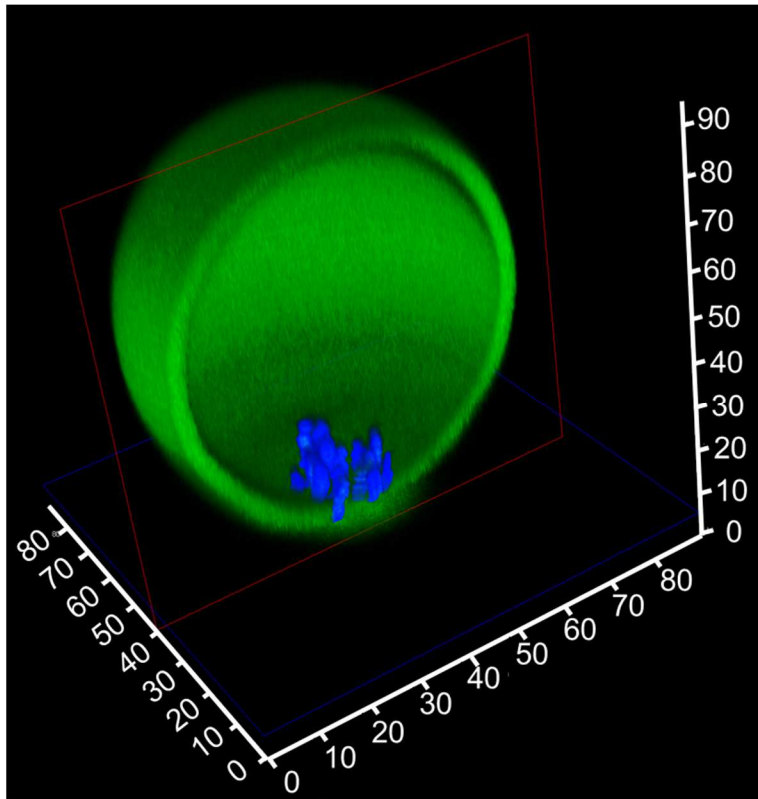


Figure B6. Confocal microscopy images of PicoShell. *S. cerevisiae* are stained with CellTracker™ Deep Red Dye (blue) and encapsulated into PicoShell stained with Alexa Fluor™ 488 Maleimide (green). Cells fall to the bottom of the PicoShell when at rest.

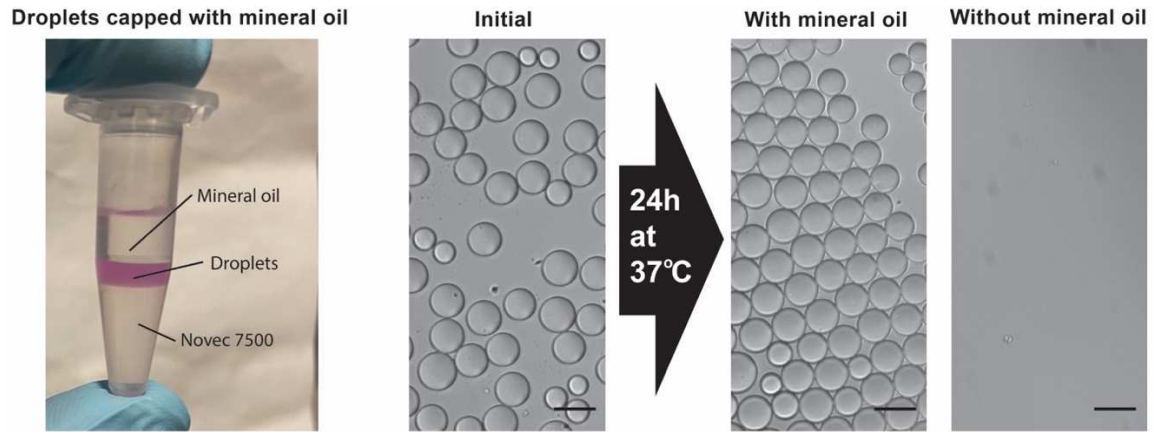


Figure B7. Effects of mineral oil cap on droplet stability. Droplets containing adherent CHODP12 media were formed using standard droplet generation techniques. One sample was capped with mineral oil the other was not capped. After 24h in the incubator at 37°C, droplets that were capped with mineral oil remained stable while droplets not capped with mineral oil de-stabilized. Scale bars = 100 μm .

Yeast Growth Comparison

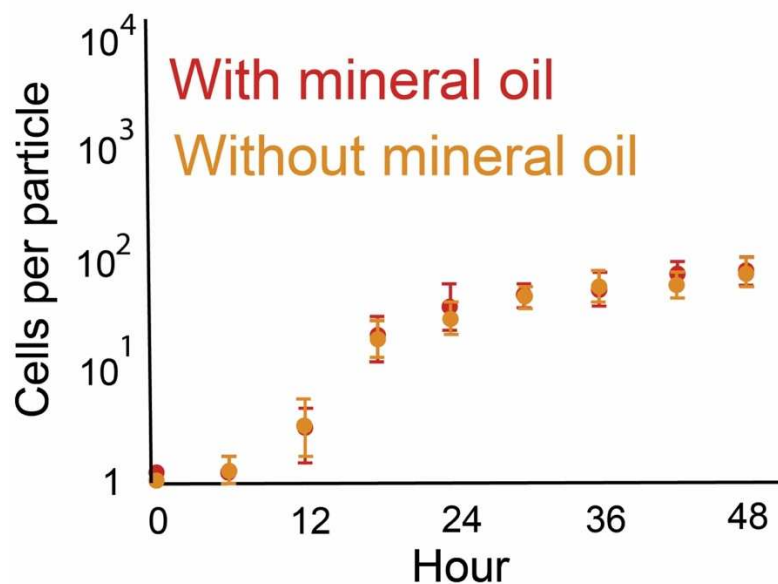


Figure B8. Mineral oil growth comparison. *S. cerevisiae* from the same respective culture was encapsulated into droplets. Half of the sample was placed separated from the other half and covered in mineral oil. Growth of cells over a 48h period was tracked. We found that there is no statistically significant difference ($P > 0.05$) of the growth of *S. cerevisiae* in droplets covered with mineral oil versus without mineral oil. 5000-6000 cell-containing droplets were counted for each sample.

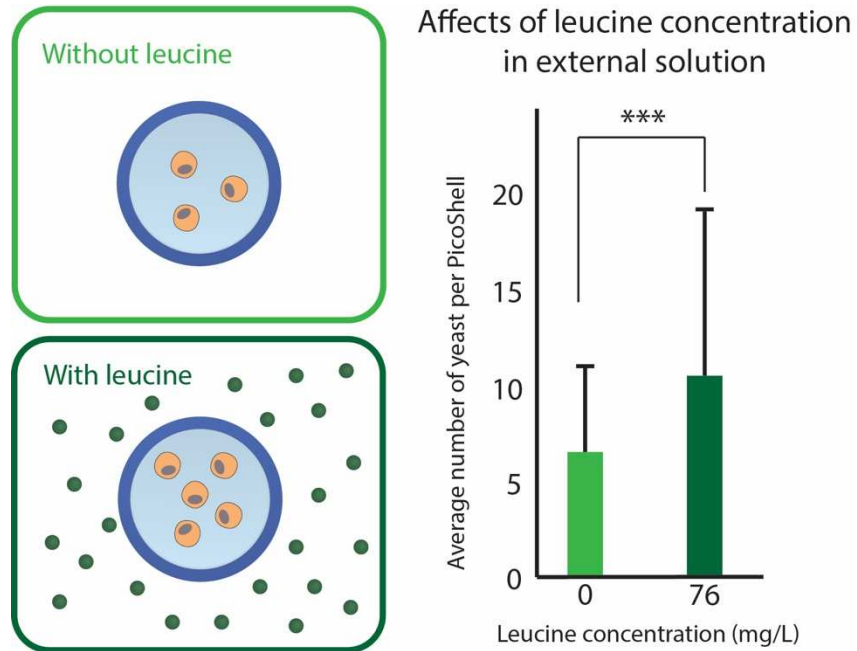


Figure B9. Leucine replenishment in PicoShells. *S. cerevisiae* shows a statistically significant growth increase ($P < 0.001$) over a 12h period when placed in a solution supplemented with 76mg/L leucine versus a solution without leucine. Error bars represent the standard deviation in the number of yeast cells per PicoShell. 300 cell-containing PicoShells were counted for each sample.

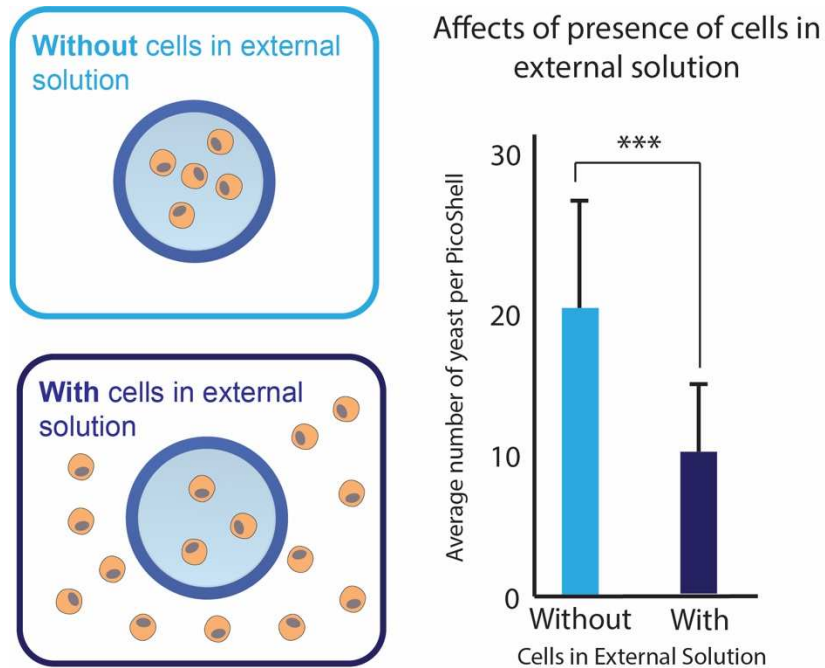


Figure B10. Effects of cells in external solution on growth in PicoShells. *S. cerevisiae* shows a statistically significant growth decrease ($P < 0.001$) over a 12h period when placed in a solution supplemented with 100 million cells/mL versus a solution without cells. Cells in external solution only grew 17% over the same period, presumably because of quorum sensing factors released due to the high density of cells. It is likely that these same factors diffused into the PicoShells and altered the growth and division properties of the enclosed cells. Error bars represent the standard deviation in the number of yeast cells per PicoShell. 300 cell-containing PicoShells were counted for each sample.

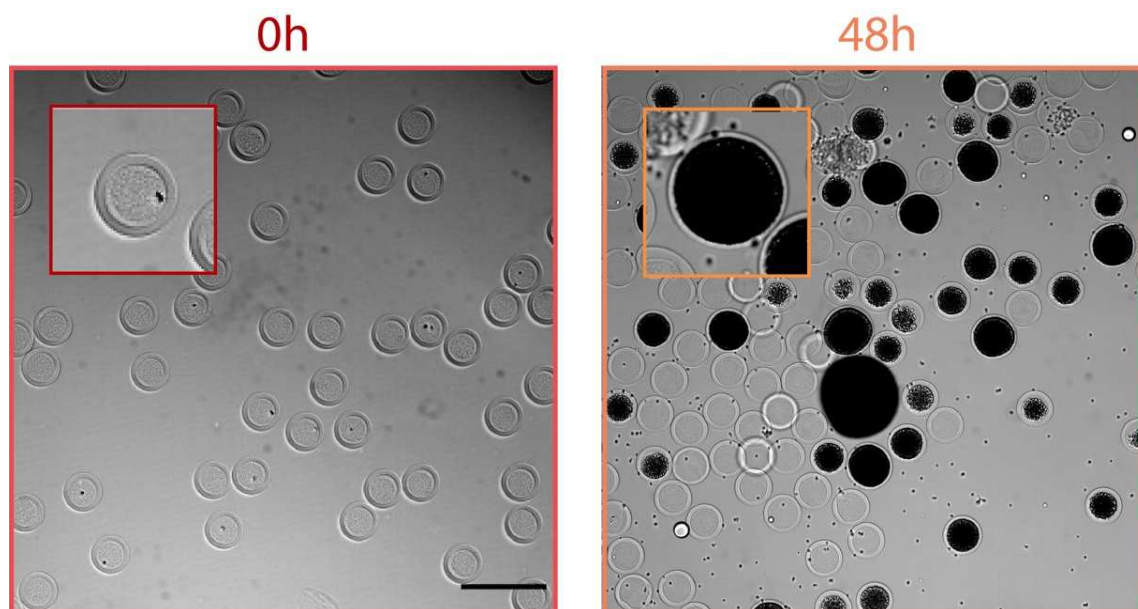


Figure B11. Expansion of PicoShells due to *S. cerevisiae* cell growth. (Left) PicoShells containing CHODP12 cells immediately after encapsulation have the same outer diameter as empty PicoShells (80 μ m OD, 2.1% CV). Inset shows PicoShell containing a single CHODP12 cell. (Right) As the CHODP12 cells grow the PicoShells were found to stretch and increase in diameter (122 μ m OD, 27.2% CV after 2 weeks). Inset shows a PicoShell containing >15000 cells that expanded from a single clone. Scale bar = 200 μ m.

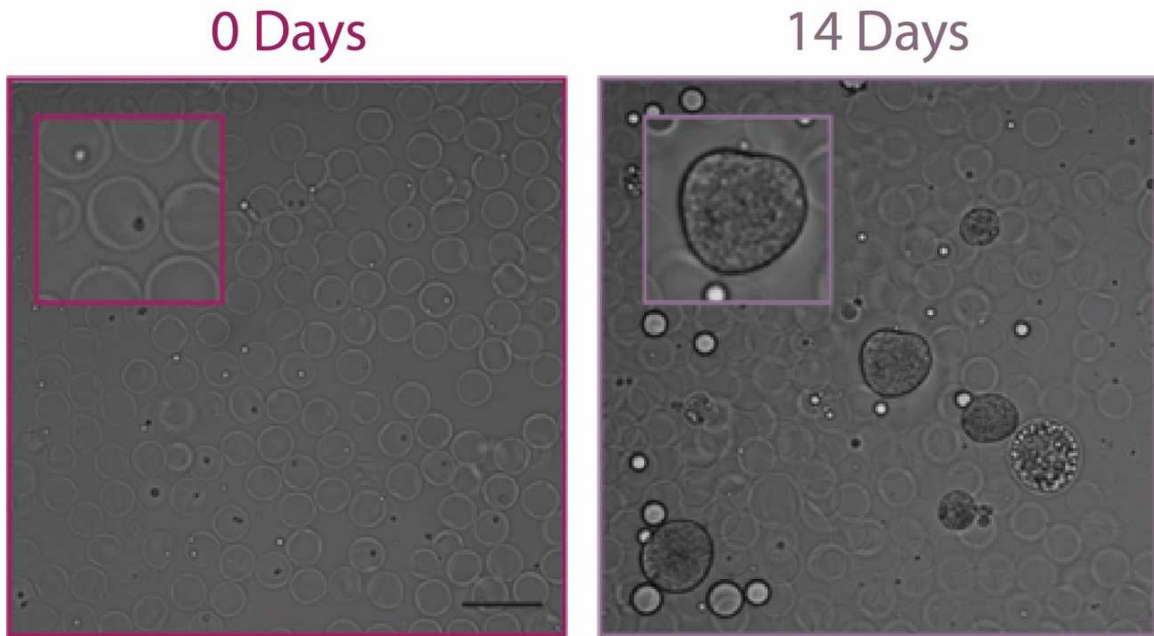


Figure B12. Expansion of PicoShells due to CHO cell growth. (Left) PicoShells containing CHODP12 cells immediately after encapsulation have the same outer diameter as empty PicoShells (80 μm OD, 2.1% CV). Inset shows PicoShell containing a single CHODP12 cell. (Right) As the CHODP12 cells grow the PicoShells were found to stretch and increase in diameter (122 μm OD, 27.2% CV after 2 weeks). Scale bar = 200 μm .

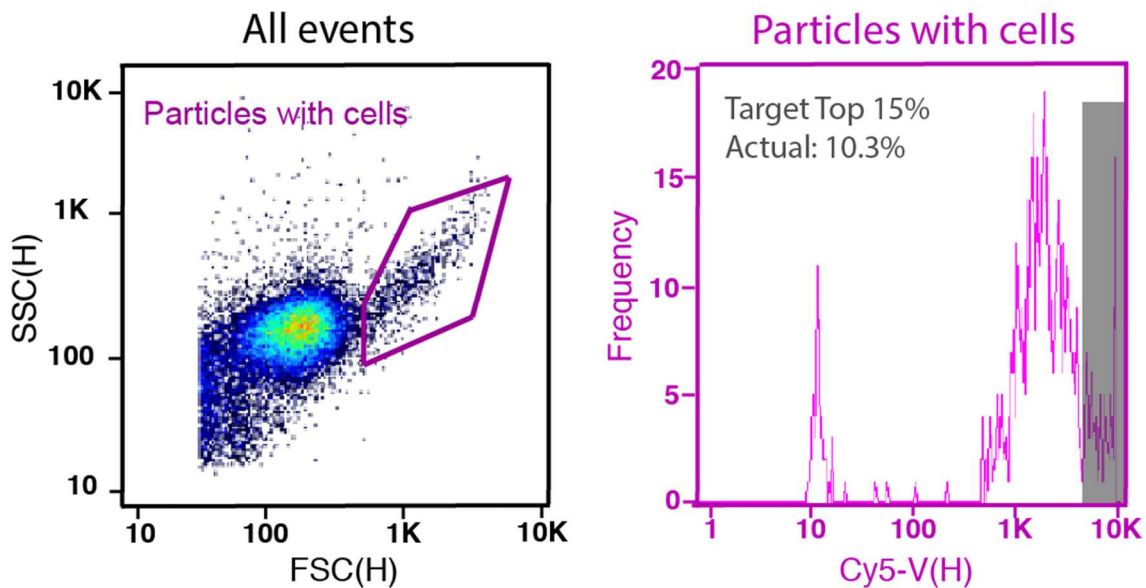


Figure B13. Full selection FACS data. For the full selection of hyperperforming *Chlorella* colonies, we first gated events that produced high scatter signal (purple gate) and sorted events that produced the highest 15% [Cy5-V(H)] signal. The data presented only shows 14,854 of the 121,213 PicoShells that were screened for the selection.

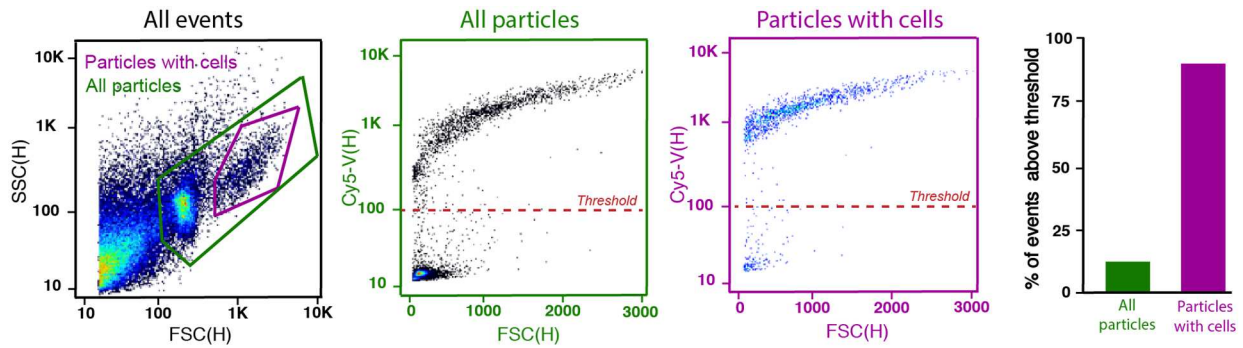


Figure B14. Additional *Chlorella*-containing PicoShell screening data. PicoShells containing *Chlorella* clonal colonies produce 3 distinct [FSC(H)] vs [SSC(H)] readout populations: one for particles containing colonies, one for empty particles, and one for debris. When all particles are gated, there are two distinct populations on a [FSC(H)] vs [Cy5-V(H)] plot, one population with a low [Cy5-V(H)] readout and another population with higher [Cy5-V(H)] readouts. When we gate the high scatter readouts from the [FSC(H)] vs [SSC(H)] plot, we find that this population corresponds to PicoShells that produce the highest [Cy5-V(H)] readouts. When all particles are gated, 14.1% of events are above a 100 [Cy5-V(H)] readout. When the high scatter population is gated, 89.9% of events are above a 100 [Cy5-V(H)] readout. Since we anticipate that colony-containing PicoShells will produce high scatter signal (as observed in an inverted microscope) and high Cy5 fluorescence signal due to a *Chlorella*'s chlorophyll autofluorescence, we infer that this high scatter, high Cy5 population corresponds to colony-containing PicoShells. When we gate for 'Particles with cells' on the [FSC(H)] vs [SSC(H)] plot, we obtain a 94.0% purity and 72.7% yield of colony-containing PicoShells.

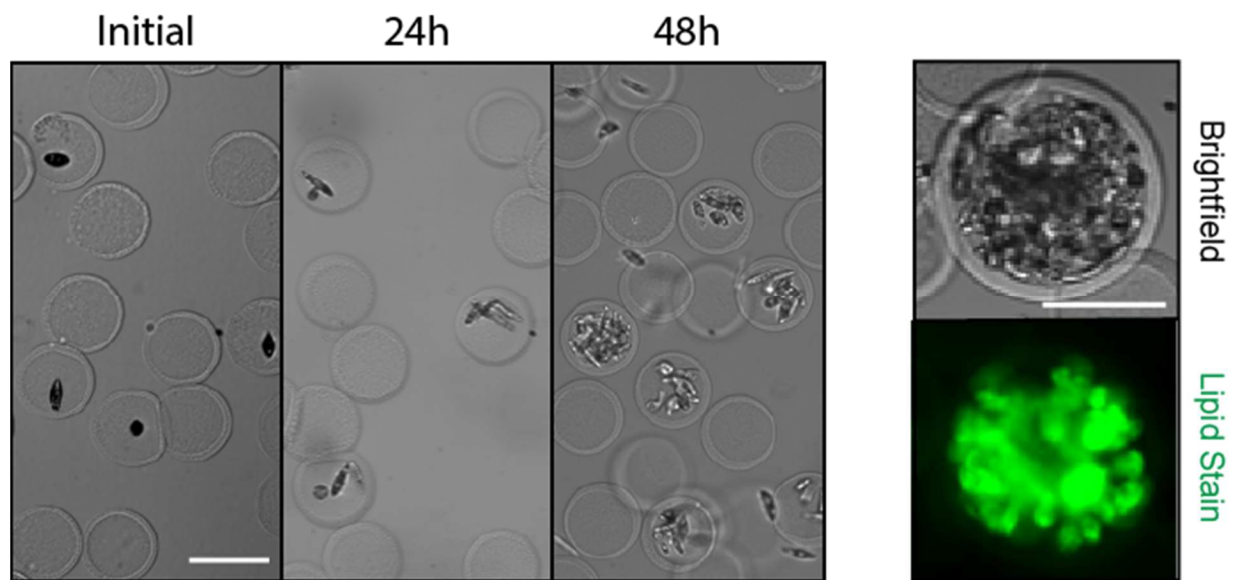


Figure B15. *Euglena gracilis* biomass and lipid accumulation within hollow shell particles. (a) *Euglena* cells were encapsulated into non-degradable hollow shell particles and allowed to grow over a 2-day period. We demonstrated that *Euglena* are viable and can accumulate biomass within hollow shell particles over this period. Particles were exchanged into a solution with BODIPY after the 2-day incubation to fluorescently label wax esters within the encapsulated microalgae. Stains were able to transport through the solid polymer matrix of the hollow particles and label cells without sticking a significant amount to the particle's PEG surface. Scale bars = 100 μ m.

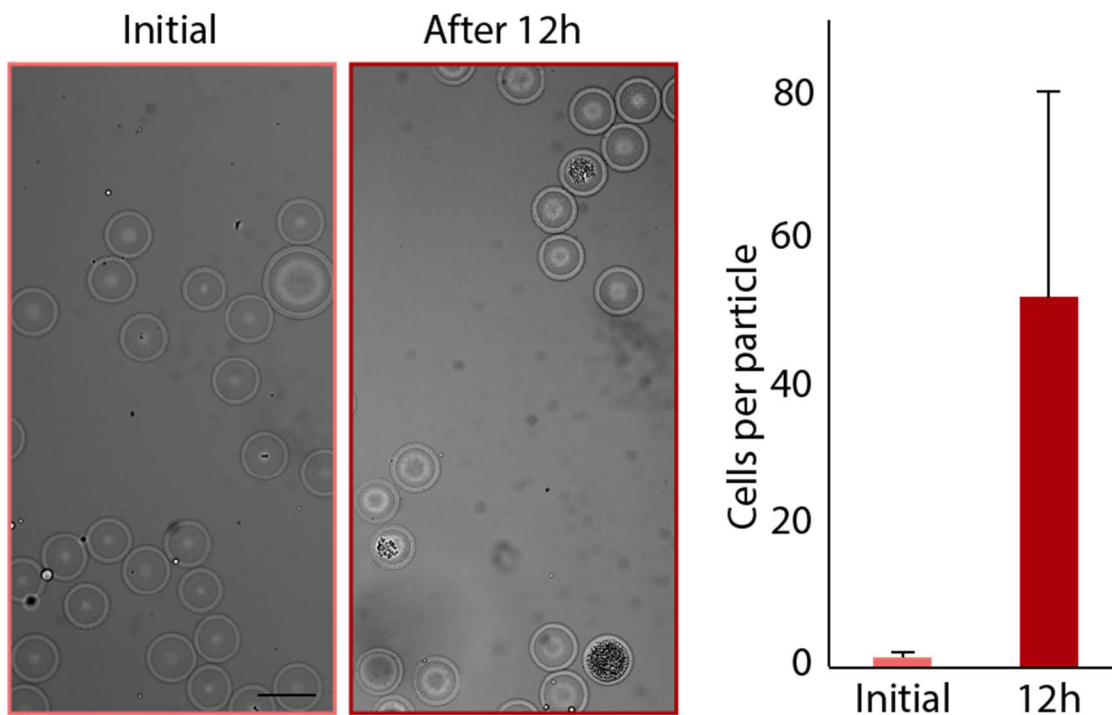


Figure B16. Growth of yeast in di-sulfide cross-linked particles. *S. cerevisiae* were encapsulated into PicoShells crosslinked with 20kDa PEG-OPSS and DTT, such that the particle's outer shell contains chemically degradable di-sulfide linkages. Yeast encapsulated into these particles were able to remain viable and multiply, increasing from an average 1.5 cells/PicoShell to 51.4 cell/PicoShell in 12h. Error bars represent the standard deviation in the number of cells between PicoShells in each sample. 150 cell-containing PicoShells were counted for each sample. Scale bar = 100 μ m.

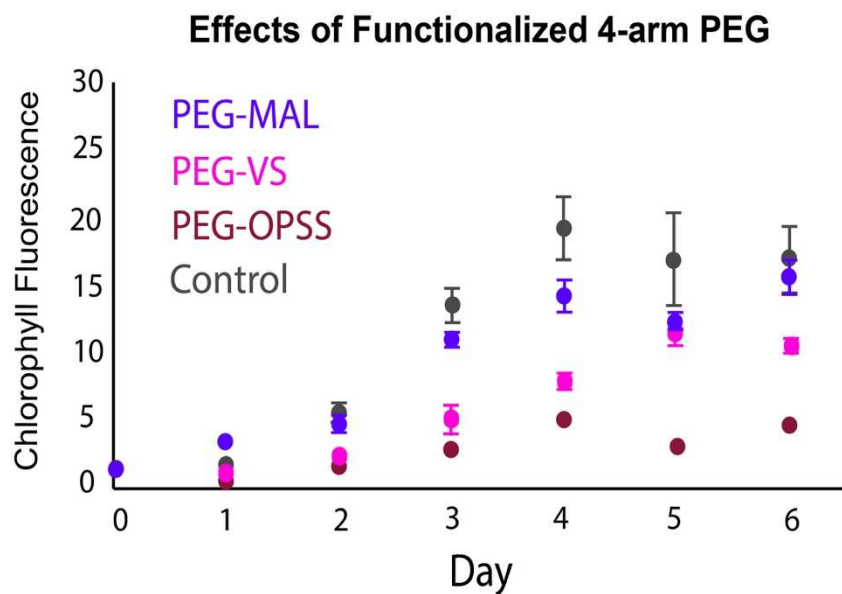


Figure B17. Effects of functionalized 4-arm PEG on *Chlorella* viability. *Chlorella* were incubated with 5% (w/w) 10kDa 4-arm PEG-maleimide (MAL), 10kDa 4-arm PEG-vinyl sulfone (VS), and 10kDa 4-arm PEG-Ortho-Pyridyldisulfide (OPSS) dissolved in PM74 medium for 2 hours before being transferred into fresh PM74 medium for tracking of biomass accumulation. 4-arm PEG MAL has slight effects on the growth ($P < 0.05$ at time = 3 days) but 4-arm PEG-VS and 4-arm PEG-OPSS has significant effects ($P < 0.001$) the overall of growth of *Chlorella*.

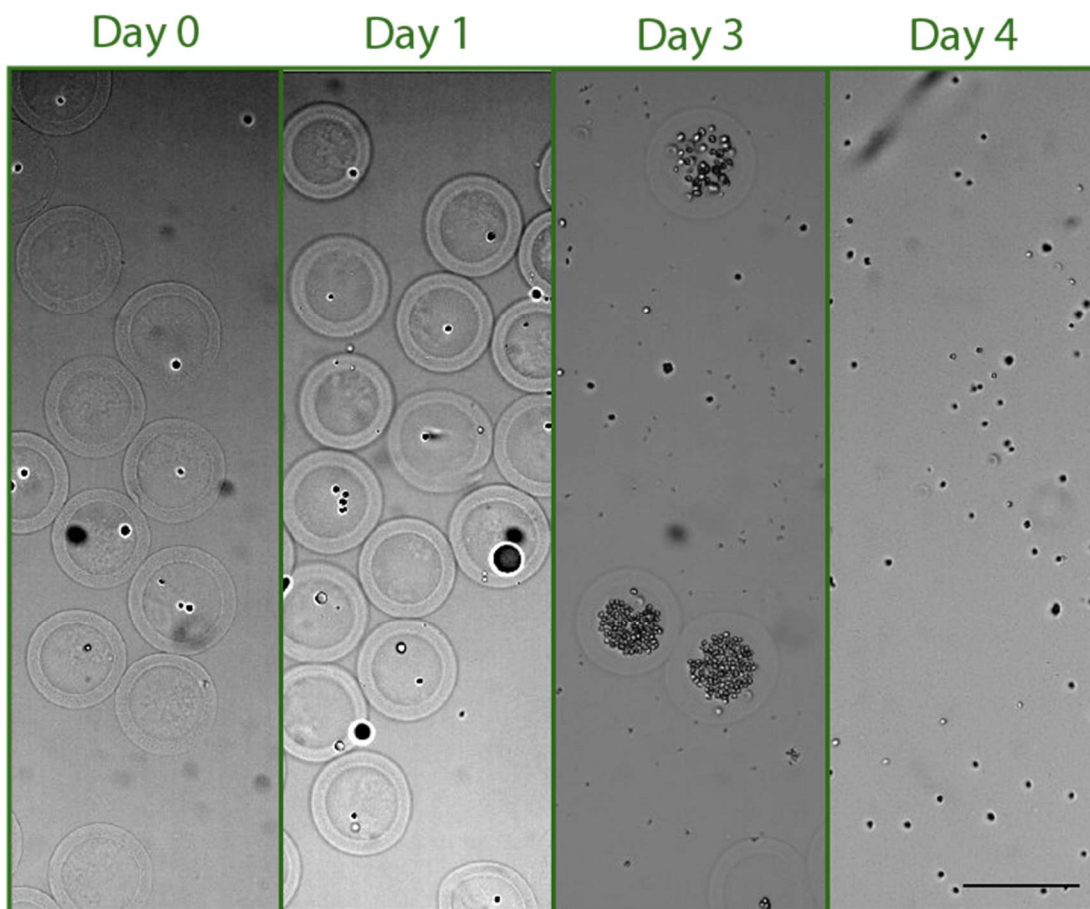


Figure B18. Growth of *Chlamydomonas reinhardtii* in MMP-degradable shells. *C. reinhardtii* are capable of growing in PicoShells crosslinked with MMP-degradable peptide crosslinker. However, cells pre-maturely induce the degradation of the PicoShells over time. This is likely due to natural MMPs secreted by *C. reinhardtii*. Scale bar = 100 μ m.

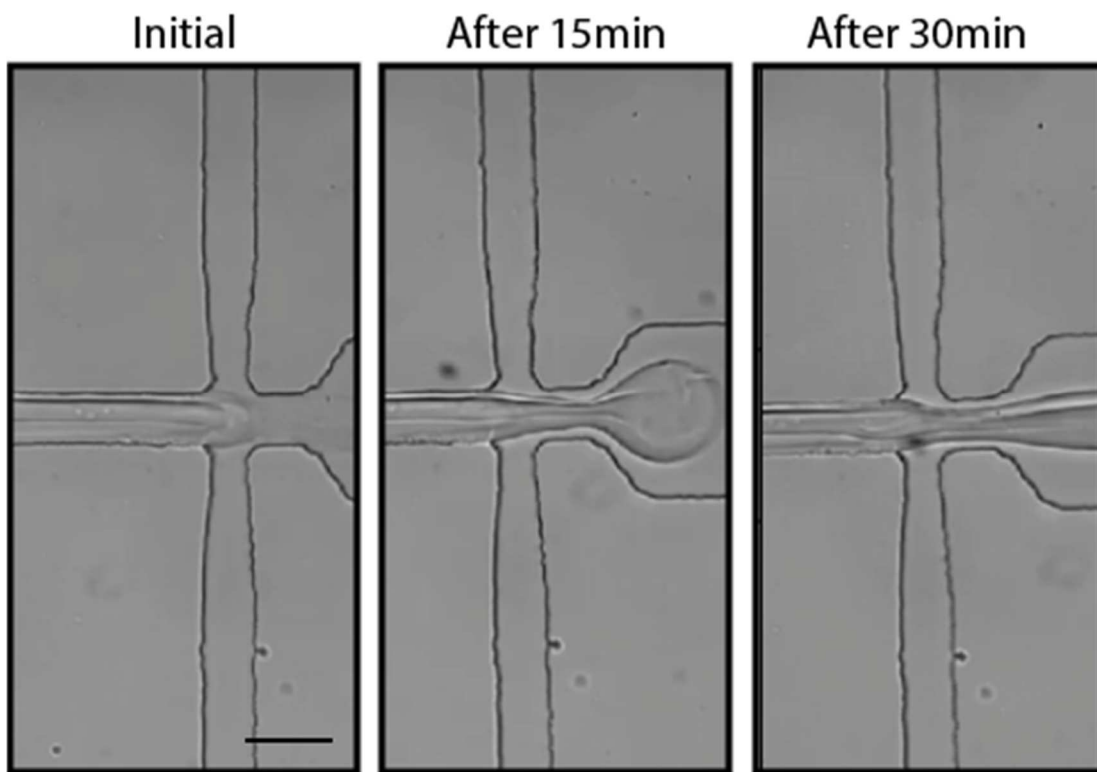


Figure B19. Disruption of PicoShell generation over time. Crosslinked material tends to form in the droplet generation junction over time, causing droplet formation to be disrupted. At a pH of 6.5, this usually starts to occur ~15 min after droplet generation is initiated when oversized droplets start to form. After ~30min, no droplets form. The time between initial mixing of reagents and jetting shortens as the pH of the solutions is increased. Scale bar = 100 μ m.

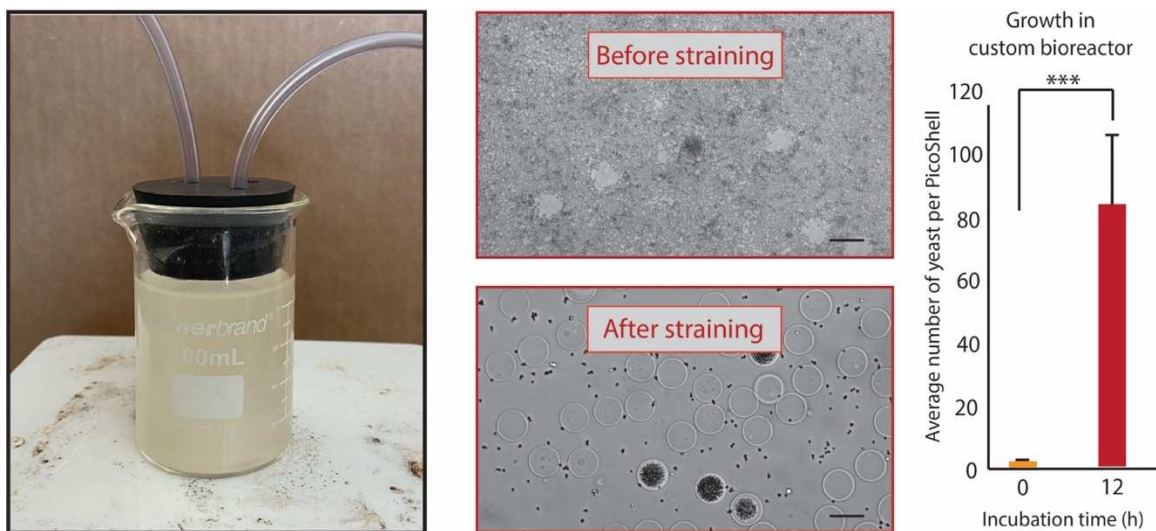


Figure B20. Incubation of PicoShells within custom bioreactor. Individual *S. cerevisiae* were placed into PicoShells and placed into a custom bioreactor. The custom bioreactor was composed of a 100 mL beaker that had been sterilized and sealed with a rubber stopper. Two tubes ran completely through the rubber stopper into the bioreactor to allow gas exchange. The bioreactor also contained a stir bar rotating at 300 RPM and sat on a hot plate set to 30°C. The PicoShells were placed into the bioreactor with un-encapsulated *S. cerevisiae* for 12h. After the incubation period, the un-encapsulated cells were removed by passing the sample through a 20 μm cell strainer. PicoShells were recovered by inverting the strainer and flushing. 200 PicoShells were counted manually before and after incubation. There was a statistically significant difference ($P < 0.001$) in the number of cells per PicoShell before and after incubation. The average number of cells per PicoShell before incubation was 1.1 cells/PicoShell and after incubation was 84.5 cells/PicoShell. Error bars represent the standard deviation in the number of cells per PicoShell. Scale bars = 100 μm .

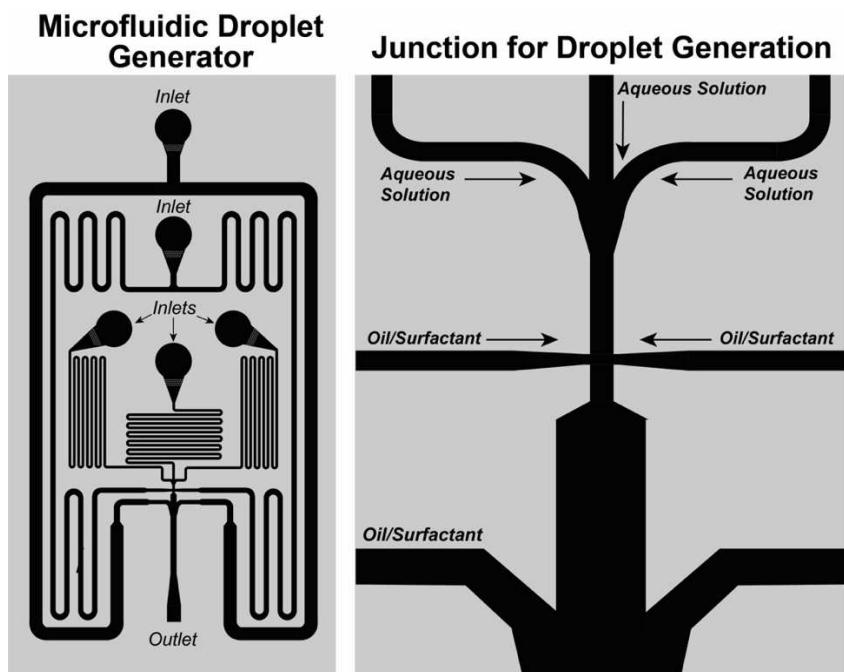


Figure B21. PicoShell and droplet generator schematic. Width of channel at the junction for droplet generation is $60\mu\text{m}$. Height of channel at junction is $70\mu\text{m}$.

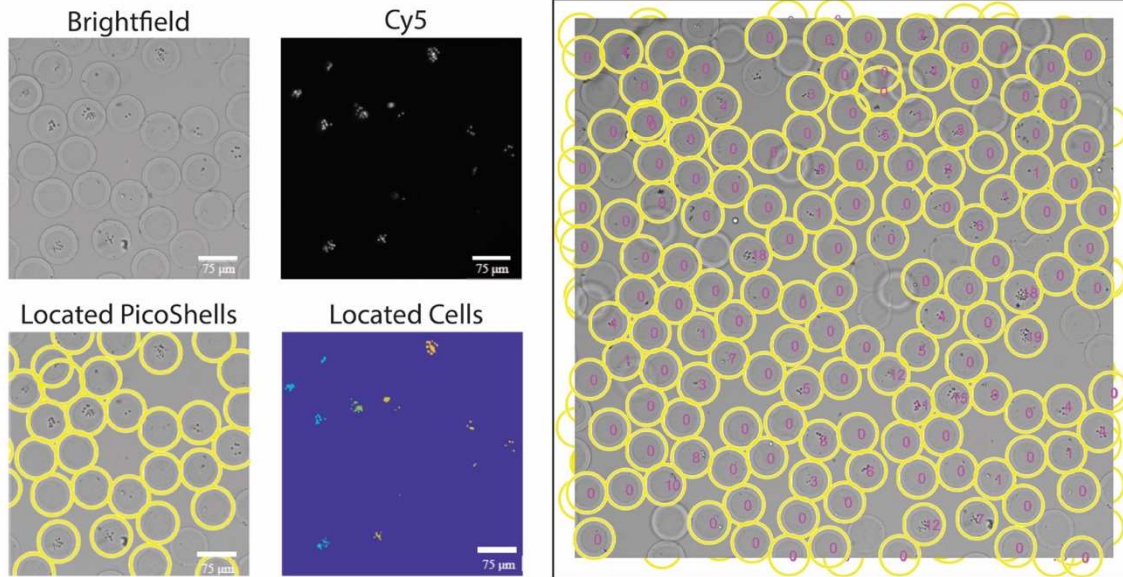


Figure B22. MATLAB code for cell counting. MATLAB code cell counting of *Chlorella sp.* in PicoShells. PicoShells were located using the FindCircles function in the brightfield channel. A fluorescence overlay was used to find the *Chlorella sp.* using the chlorophyll fluorescence in the Cy5 channel. The number of cells was calculated by taking the area of each blob and dividing it by the 2D area of each cell within the compartment region. Some of the cells in PicoShells were counted visually to verify the accuracy of the code. After counting the *Chlorella* in 200 cell-containing PicoShells, we found that the difference between the visual count and the count from the code is not statistically significant ($P > 0.05$).

Appendix C

Table C1. Parameters to fabricate PicoShells with different pore sizes. Concentrations indicated are the concentrations in-droplet.

# Arms	PEG Functional Group	PEG MW (kDa)	Dextran MW (kDa)	PEG Conc. (w/w %)	Dextran Conc. (w/w %)	DTT Conc. (mg/mL)	BP cutoff (bp)	MW Cutoff (kDa)
4	Maleimide	20	40	4	10	0.0625	300	>185
4	Maleimide	10	40	6	10	0.2	200	>185
4	Maleimide	5	10	8	15	0.5	200	15-20
8	Maleimide	10	10	8	17.5	0.5	< 100	15-20
8	Maleimide	5	10	10	18	0.8	< 100	<10
4	Orthopyridyl disulfide	20	10	3.25	10	0.8	300	>185